NASA CONTRACTOR REPORT

NASA CR-1497

THE DENSITY OF EIGENVALUES IN THIN CIRCULAR CONICAL SHELLS

by David K. Miller and Franklin D. Hart

Prepared by
NORTH CAROLINA STATE UNIVERSITY
Raleigh, N. C.
for Langley Research Center

NATIONAL AERONAUTICS AND SPACE ADMINISTRATION • WASHINGTON, D. C. • MARCH 1970

NASA CR-1497

DENSITY OF EIGENVALUES IN THIN CIRCULAR CONICAL SHELLS

By David K. Miller and Franklin D. Hart

Prepared under Grant No. NGR-34-002-035 by
NORTH CAROLINA STATE UNIVERSITY
Raleigh, N.C.

for Langley Research Center

NATIONAL AERONAUTICS AND SPACE ADMINISTRATION

For sale by the Clearinghouse for Federal Scientific and Technical Information
Springfield, Virginia 22151 – Price $3.00

TABLE OF CONTENTS

TABLE OF CONTENTS (continued)

LIST OF TABLES

LIST OF FIGURES

LIST OF FIGURES (continued)

LIST OF FIGURES (continued)

SUMMARY

A combined analytical and experimental study is made of the eigenvalue density and the cumulative number of eigenvalues of a thin circular conical shell. The investigation is directed toward the development of expressions that can be used easily in finding the eigenvalue density and number of eigenvalues of a conical shell which are applicable to a wide range of cone geometries, and which are valid over a frequency range sufficiently wide to be of engineering value. This is accomplished by applying wave number space integration techniques and numerical procedures to obtain expressions for the eigenvalue distribution function based on two separate frequency equations appropriate to thin conical shells. The expressions obtained are normalized with respect to cone geometry, and presented for the frequency range below the lower ring frequency and above the upper ring frequency of the cone.

The experimental arrangement used to determine the resonant frequencies of the conical shells examined is described, and the results of this investigation are presented in tabular and graphical form. The results of the analytical work are also presented along with the experimental data for easy comparison.

Excellent agreement is obtained between the analytic and the experimental results. It is concluded that the expressions presented for the cumulative number of eigenvalues and the eigenvalue density are applicable over a wide range of cone geometries, and frequency ranges of practical interest. The results represent computational procedures of considerable engineering value.

1. INTRODUCTION

The concept of the density of eigenvalues, or resonant frequencies as they are usually referred to in structures, arises from the fact that any continuous structure possesses an infinite number of natural modes of vibration. For this reason it is sometimes convenient to introduce the concept of modal or eigenvalue density. The eigenvalue density is essentially the density of resonant frequencies of natural vibration with respect to frequency. It is therefore an indication of the spacing of the resonant frequencies in the frequency domain.

When dealing with structures excited in a very complex, or random fashion, it is often not only useful but necessary to resort to statistical methods to determine the response of the structure to such loading. In order to effectively use the statistical energy method described in some detail by Ungar (1966) and Smith and Lyon (1965) it is necessary to know certain properties regarding the structural geometry being examined. One of these properties which must be known is the eigenvalue density. Therefore in order to apply a statistical type of analysis to a structural response problem it is necessary to know the eigenvalue density of the basic structural elements. Basic components such as beams, rectangular and circular plates, cylinders, and spheres have been handled successfully in the literature (Smith and Lyon, 1965; Bolotin, 1963; Miller and Hart, 1967). The problem of composite structures has also been examined[1]. However, the problem of

---

[1]Hart, F. D. and V. D. Desai. 1967. Additive properties of modal density for composite structures. Presented at the 74th Meeting of the Acoustical Society of America, Miami, Fla., Paper No. DD 11. Dept. of Mechanical and Aerospace Engineering, North Carolina State University at Raleigh, N. C.

the eigenvalue density of a conical shell is heretofore unresolved. Since the conical shell is a very common structural element it would seem that this problem deserves some attention. It is therefore the purpose of this paper to obtain an expression for the eigenvalue density of a thin circular conical shell.

Two separate but similar frequency equations for a conical shell are presented and used to obtain expressions for the cumulative number of eigenvalues and then the eigenvalue density. Both numerical counting and k-space integration techniques are used to obtain these expressions and then checked against each other. The results are normalized in such a manner as to be independent of the geometry of the conical shell. The frequency range over which the results of each frequency equation are valid is discussed in detail, and simple algebraic expressions are presented for the number of eigenvalues and the eigenvalue density.

An experimental program was conducted on two conical shells of different geometry, and the results are presented in some detail. The results of the experimental work are presented in graphical form and compared with the results of the two analytical expressions mentioned above.

The final expressions resulting from this investigation are then discussed and conclusions are drawn as to the correct expression for the modal density of a thin circular conical shell. The experimental results are also discussed in light of the analytical results.

Several appendices are included for more detailed explanation of equations and procedures employed in the main body of this report.

The first appendix presents in detail the derivation of the first frequency equation used beginning with the equilibrium equations on a shell element. The second appendix presents a comparison between the frequencies predicted by the first frequency equation and some of the experimental findings available in the literature. The third and fourth appendices present the details of the numerical computer programs used to obtain the expressions for the number of eigenvalues and the eigenvalue density.

2. REVIEW OF LITERATURE

The problem of determining the eigenvalue density of a shell may be broken down into what amounts to three distinct problems. First, the differential equation governing the motion of the shell in question must be obtained. Secondly, the differential equations for the shell must be solved in such a way as to obtain an equation for the eigenvalues. This is usually referred to as the frequency equation for the shell. Finally, the frequency equation must be used in some manner to obtain expressions for the cumulative number of eigenvalues. This expression is then differentiated with respect to frequency to obtain the eigenvalue density expression.

The first of these problems has been handled in some detail in the literature. Vlasov (1949) derived the general differential equations applicable to conical shells making use of equilibrium and compatibility relationships, as well as the fundamental elasticity relationships. A similar and somewhat less detailed development of basically the same equations is presented by Flugge (1966). Both authors make liberal use of all the standard elasticity relationships which are developed in depth by Wang (1953). Also, both of the above treatments consider extension of the middle surface as well as bending, transverse shear, and rotary inertia. The basic difference in the derivations is in the final form of the differential equations. Vlasov (1949) presents two simultaneous differential equations in terms of the normal displacement and the stress function. Flugge (1966) presents three simultaneous differential equations in terms of the three displacements of the shell surface.

The second part of the eigenvalue problem has also been presented in the literature. Federhofer (1962) used energy methods to obtain an approximate solution to the extensional vibration problem of conical shells. An explicit expression for the frequency equation was not obtained, however, and the calculation of the natural frequencies is somewhat involved. Seide (1964) employed a Rayleigh-Ritz type of solution to the conical shell problem. The order of the matrix type solution was increased and solved until it converged. It was found that a thirty by thirty matrix was necessary for convergence. A similar procedure was followed by Platus (1965) in which an eighteen by eighteen matrix was used corresponding to a six term approximation for each of the three displacements. Hu (1965) also used a similar technique along with the Galerkin method to obtain a matrix form solution in which both transverse shear and rotary inertia were included in the formulation. A five term series was used to describe the mode functions in the analysis. Other authors who have presented similar types of developments are Chao-tsin (1964) and Kol'man (1965) as well as Kogawa (1965) and Meyerovich (1966).

It should be noted that although all of these authors present solutions for the frequency equation problem, none of them present an explicit frequency equation applicable to a general cone. Many present approximate expressions for the minimum frequency of vibration, but no general frequency equation of reasonable simplicity has been obtained. It is also noted that Kol'man (1966) considered the effects of boundary conditions on the frequencies of natural vibration. He found that

with the exception of small mode numbers, the effect of boundary conditions are slight.

In addition to the analytical work discussed concerning the eigenvalues of a conical shell, there has been a fair amount of experimental work done along the same lines. Watkins and Clary (1964) conducted experiments with four different cones having different cone angles, and found the experimental frequencies to be in good agreement with the work of Platus (1965). Weingarten (1965) conducted extensive investigations with several different cones of different wall thickness and slant height, and found the results to be in good agreement with the work of Seide (1964). Hu and Lindholm (1966) conducted extensive experiments which they found substantiated his own work (Hu, 1965). Other experimental investigations along the same lines by Mixon (1967), Tang and Hong (1966), and Hu et al. (1967) have reached more or less the same conclusions. That is, the solutions of the differential equations for conical shells by energy methods, as long as enough terms are carried in the approximations, are in excellent agreement with experimental results, with respect to the frequencies of resonant modes.

In order to investigate analytically the problem of eigenvalue density, however, it is necessary to have an explicit expression for the natural frequencies of cones. Godzevich (1962) presented such an equation. The equation is based on the solution of the differential equations presented by Vlasov (1949) by the Galerkin method. The solution is only approximate, but it is an explicit expression, and

does compare with a fair degree of accuracy to experimental values. It will therefore be the frequency equation used in this paper.

The third part of the eigenvalue density problem, the use of the frequency equation to determine an expression for the eigenvalue density, will be the subject of this paper. A technique introduced by Courant and Hilbert (1953) will be used where possible to obtain the desired expressions. The k-space integration described in general in the proceeding reference was used by Bolotin (1963) and (1965) to obtain solutions to several eigenvalue density problems. The technique is also discussed in some detail by Miller and Hart (1967). There appears to be no specific information with regard to the cumulative number of eigenvalues or the eigenvalue density of conical shell available in the literature.

3. THEORETICAL DEVELOPMENT

3.1 Introduction

In this section the frequency equation which is developed in detail in Appendix 8.1 is used to obtain an expression for the cumulative number of eigenvalues contained in a specified frequency interval, as well as an expression for the model or eigenvalue density of the conical shell. The k-space geometry corresponding to the frequency equation developed in Appendix 8.1 (referred to as the first frequency equation in the work which follows) is obtained. Reasons prohibiting the use of k-space integration techniques are discussed and a purely numerical method is presented and used to obtain the desired expressions. Finally a second frequency equation is obtained from a simplification of the differential equations used in Appendix 8.1 to obtain the first frequency equation. The k-space geometry corresponding to the second frequency equation is obtained, and integrated to obtain the desired expressions. The results from both frequency equations are normalized with respect to cone geometry. The two results are then compared and their frequency range of application is discussed in detail.

3.2 Frequency Equation One

The frequency equation for a thin conical shell obtained at the conclusion of Appendix 8.1, and by Godzevich (1962) is as follows:

$$\omega^2 = \left[\frac{g_c E}{\gamma L^2}\right] \frac{\frac{D}{EL^2h}\left\{\frac{a_n^4}{10}(1-\alpha_1^5) + a_n\left(1 + \frac{2m^2}{\sin^2\psi}\right)\left[\frac{a_n}{6}(1+\alpha_1^3) - \frac{1}{2a_n}(1-\alpha_1)\right] + \right.}{\left\{\frac{a_n^4}{10}(1-\alpha_1^5) + a_n\left(1 + \frac{2m^2}{\sin^2\psi}\right)\left[\frac{a_n}{6}(1+\alpha_1^3) - \frac{1}{2a_n}(1-\alpha_1)\right] + \right.}$$

$$\frac{\left. + \left(\frac{m^4}{\sin^4\psi} - \frac{4m^2}{\sin^2\psi}\right)\frac{1}{2}(1-\alpha_1)\right\}^2 + \frac{a_n^4}{\tan^2\psi}\left\{\frac{1}{8}(1-\alpha_1^4) - \frac{3}{8a_n^2}(1-\alpha_1^2)\right\}^2}{\left. + \left(\frac{m^4}{\sin^4\psi} - \frac{4m^2}{\sin^2\psi}\right)\frac{1}{2}(1-\alpha_1)\right\}\left\{\frac{1}{10}(1-\alpha_1^5) - \frac{1}{2a_n^2}(1-\alpha_1^3) + \frac{3}{4a_n^4}(1-\alpha_1)\right\}} \qquad (3.1)$$

where $a_n = \frac{n\pi}{1-\alpha_1}$ and $\alpha_1 = \frac{L_t}{L}$.

The number of bending waves in the circumferential direction is given by m, and the number of half waves in the longitudinal direction is given by n. Equation (3.1) may be written in dimensionless form by defining a dimensionless frequency ratio and longitudinal and circumferential wave numbers in the following manner:

$$\lambda^2 = \omega^2 \frac{\gamma L^2}{g_c E} ; \qquad k_1 = a_n ; \qquad k_2 = \frac{m}{\sin\psi} . \qquad (3.2)$$

Substituting equations (3.2) into equation (3.1) and rearranging terms results in the following expression for the dimensionless frequency:

$$\lambda^2 = \frac{\frac{h^2}{12L^2(1-\nu^2)}\, k_1^4\{k_1^4\,\frac{1-\alpha_1^5}{10} + (1+2k_2^2)\,(k_1^2\,\frac{1-\alpha_1^3}{6} - \frac{1-\alpha_1}{2}) + (k_2^4 - 4k_2^2)\,\frac{1-\alpha_1}{2}\}^2 + \cot^2\psi[k_1^4\,\frac{1-\alpha_1^4}{8} - k_1^2\,\frac{3(1-\alpha_1^2)}{8}]^2}{\{k_1^4\,\frac{1-\alpha_1^5}{10} + (1+2k_2^2)\,(k_1^2\,\frac{1-\alpha_1^3}{6} - \frac{1-\alpha_1}{2}) + (k_2^4 - 4k_2^2)\,\frac{1-\alpha_1}{2}\}\ x\ x\ [k_1^4\,\frac{1-\alpha_1^5}{10} - k_1^2\,\frac{1-\alpha_1^3}{2} + \frac{3(1-\alpha_1)}{4}]} \tag{3.3}$$

3.2.1 Wave Number Space

In order to determine the k-space geometry corresponding to equation (3.3) it is necessary to obtain an explicit expression for either k_1 or k_2 in terms of the other and the dimensionless frequency λ. The algebraic manipulation necessary to accomplish this is fairly involved, but straightforward. It is found that the above equation (3.3) reduces to a quartic in terms of k_2^2, and may be expressed as a polynomial in the following form:

$$k_2^8 + Ak_2^6 + Bk_2^4 + Ck_2^2 + D = 0\ . \tag{3.4}$$

The coefficients A, B, C, and D are all multiple term expressions involving the variables k_1 and λ as well as the constants which describe the conical shell geometry. The coefficients indicated in equation (3.4) are as follows:

$$A = \frac{8}{1-\alpha_1}\left(k_1^2\,\frac{1-\alpha_1^3}{6} - \frac{1-\alpha_1}{2} - 1 + \alpha_1\right) \tag{3.5}$$

$$B = \frac{2}{1-\alpha_1}\left[\frac{8}{1-\alpha_1}\left(k_1^2\,\frac{1-\alpha_1^3}{6} - \frac{1-\alpha_1}{2} - 1 + \alpha_1\right)^2 + 2\left(k_1^4\,\frac{1-\alpha_1^5}{10} + k_1^2\,\frac{1-\alpha_1^3}{6} - \frac{1-\alpha_1}{2}\right) - \frac{12\lambda^2L^2(1-\nu^2)}{k_1^4h^2}\left(k_1^4\,\frac{1-\alpha_1^5}{10} - k_1^2\,\frac{1-\alpha_1^3}{2} + \frac{3(1-\alpha_1)}{4}\right)\right] \tag{3.6}$$

$$C = \frac{8}{(1-\alpha_1)^2}\left[2\left(k_1^2\,\frac{1-\alpha_1^3}{6} - \frac{1-\alpha_1}{2}\right)\left(k_1^4\,\frac{1-\alpha_1^5}{10} + k_1^2\,\frac{1-\alpha_1^3}{6} - \frac{1-\alpha_1}{2}\right) - 2(1-\alpha_1)\left(k_1^4\,\frac{1-\alpha_1^5}{10} + k_1^2\,\frac{1-\alpha_1^3}{6} - \frac{1-\alpha_1}{2}\right) + \frac{12\lambda^2L^2(1-\nu^2)}{k_1^4h^2}\left(1 - \alpha_1 - k_1^2\,\frac{1-\alpha_1^3}{6} + \frac{1-\alpha_1}{2}\right)\left(k_1^4\,\frac{1-\alpha_1^5}{10} - k_1^2\,\frac{1-\alpha_1^3}{2} + \frac{3(1-\alpha_1)}{4}\right)\right] \tag{3.7}$$

$$D = \frac{4}{(1-\alpha_1)^2}\left[\left(k_1^4\,\frac{1-\alpha_1^5}{10} + k_1^2\,\frac{1-\alpha_1^3}{6} - \frac{1-\alpha_1}{2}\right)^2 + \frac{12\,\cot^2\psi\,L^2(1-\nu^2)}{k_1^4h^2}\;x\;\left[k_1^4\,\frac{1-\alpha_1^4}{8} - k_1^2\,\frac{3(1-\alpha_1^2)}{8}\right]^2 - \frac{12\lambda^2L^2(1-\nu^2)}{k_1^4h^2}\;x\;\left(k_1^4\,\frac{1-\alpha_1^5}{10} + k_1^2\,\frac{1-\alpha_1^3}{6} - \frac{1-\alpha_1}{2}\right)\left(k_1^4\,\frac{1-\alpha_1^5}{10} - k_1^2\,\frac{1-\alpha_1^3}{2} + \frac{3(1-\alpha_1)}{4}\right)\right]. \tag{3.8}$$

Closed form expressions for the roots of a quartic equation are available; however, due to the complex nature of the constants involved the final expression for k_2 in terms of k_1 and λ is too involved to be of any real value. For this reason a numerical solution was used to obtain the roots of equation (3.4) on a computer, using several different cone geometries as well as a range of values for the independent variables k_1 and λ. In this way plots of k_1 versus k_2 with λ as a parameter were obtained for several different cone geometries. Samples of the results obtained in this manner are shown in Figures 3.1 and 3.2. Figure 3.1 illustrates a typical k-space for a truncated cone, and Figure 3.2 illustrates a typical k-space for a closed cone.

3.2.2 Cumulative Number of Eigenvalues

Study of Figures 3.1 and 3.2 indicate that it should be possible to obtain the number of eigenvalues within a frequency domain by the k-space integration technique (Courant and Hilbert, 1953; Bolotin, 1963 and 1965; Miller and Hart, 1967). Employing this method the cumulative number of eigenvalues is approximated by

$$N(\lambda) \approx \frac{1}{\Delta k_1 \Delta k_2} \int \int dk_1 dk_2 \tag{3.9}$$

where the integral is to be taken over that portion of the first quadrant where the k-space exists.

The integral in equation (3.9) may be written in iterated form by recognizing the fact that the region over which the integral is to be evaluated is bounded by an upper and lower value of k_1. The upper value will be referred to as b and the lower value as a. The region

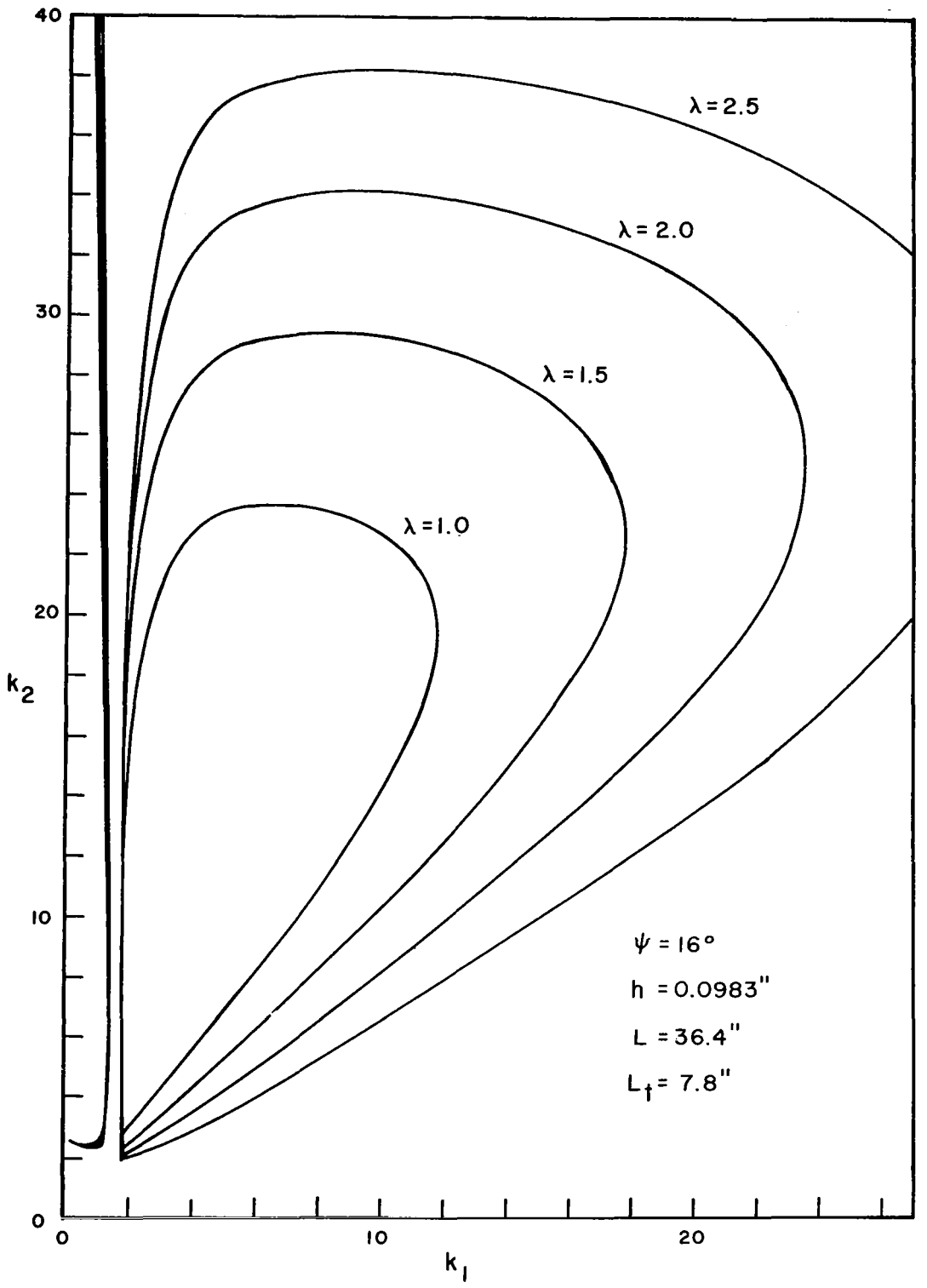

FIGURE 3.1 FREQUENCY EQUATION ONE K-SPACE FOR A TRUNCATED CONE

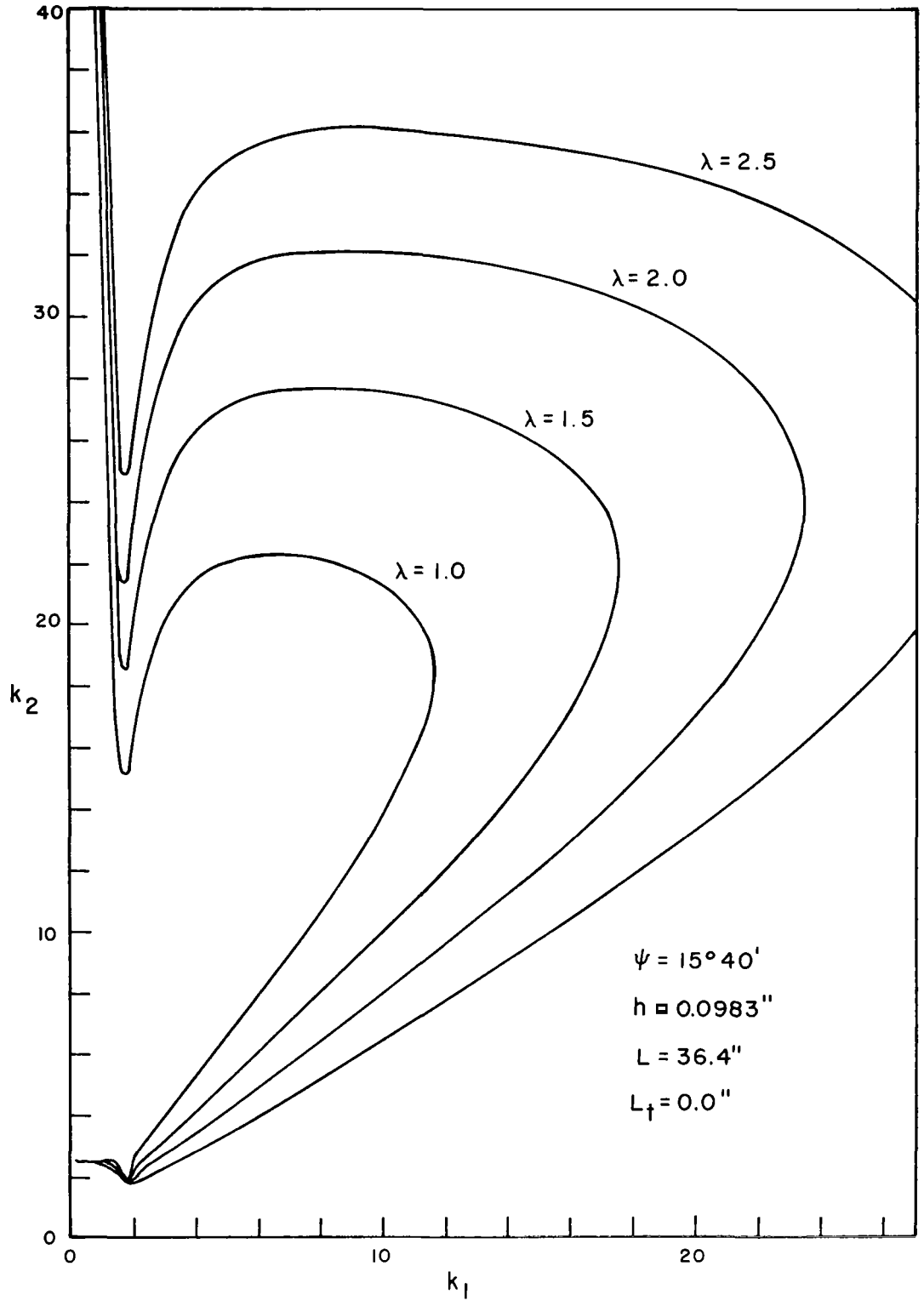

FIGURE 3.2 FREQUENCY EQUATION ONE K-SPACE FOR A CLOSED CONE

is also bounded by upper and lower curves which will be referred to as $[k_2]_u$ and $[k_2]_\ell$ respectively. Equation (3.9) therefore becomes

$$N(\lambda) \approx \frac{1}{\Delta k_1 \Delta k_2} \int_a^b ([k_2]_u - [k_2]_\ell) dk_1 \tag{3.10}$$

where $\underline{a}$ and $\underline{b}$ are functions of λ and the cone geometry, and $[k_2]_u$ and $[k_2]_\ell$ are functions of k_1, λ, and the cone geometry parameters. The expressions for $[k_2]_u$ and $[k_2]_\ell$ may be obtained from the solution of the quartic equation (3.4), however, the evaluation of $\underline{a}$ and $\underline{b}$ is somewhat more involved. Obviously, $\underline{a}$ and $\underline{b}$ must be the roots of the equation obtained by setting $[k_2]_u$ equal to $[k_2]_\ell$. Due to the extreme complexity of $[k_2]_u$ and $[k_2]_\ell$ it has not been possible to obtain expressions for $\underline{a}$ and $\underline{b}$. For this reason the integration of equation (3.10) to obtain an expression for the cumulative number of eigenvalues is a somewhat impractical approach to the problem.

Using a different approach, however, the number of eigenvalues below any selected frequency may still be obtained. Using equation (3.3) which is the frequency equation, the eigenvalues may be computed for different values of m and n, the circumferential and longitudinal wave numbers respectively. In this manner the number of eigenvalues occurring below certain dimensionless frequencies may be obtained. The values of m and n are increased until the count under each specified dimensionless frequency terminates. In order to obtain a sufficient number of calculations for different cone geometries an IBM 360 Model 75 digital computer was used. The details of the program used for these calculations may be found in Appendix 8.4. The results of

these calculations appear in graphical form in Figures 3.3 through 3.5. Examination of equation (3.3) reveals that there are three geometric parameters which will effect the dimensionless frequency, assuming that Poisson's ratio is constant and equal to 0.3. These are the cone angle (Ψ), the thickness over length ratio ($\frac{h}{L}$), and truncation ratio (α_1). Figure 3.3 shows the effect of changing the cone angle, Figure 3.4 shows the effect of changing the thickness, and Figure 3.5 shows the effect of changing the truncation ratio.

A study of Figures 3.3 through 3.5 indicates that the results obtained may be normalized. It will be of some value to first define what are known as the ring frequencies. The upper ring frequency is defined as the frequency at which the longitudinal wave length is equal to the circumference of the small end of the cone. In dimensionless form the upper ring frequency would be given by

$$\lambda \text{ (upper ring)} = \frac{1}{\alpha_1 \sin \Psi} \quad . \tag{3.11}$$

This is equivalent to ω times the small radius of the cone divided by the longitudinal wave velocity equal to unity.

Similarly the lower ring frequency is defined as the frequency at which the longitudinal wave length is equal to the circumference of the large end of the cone. In dimensionless form it is

$$\lambda \text{ (lower ring)} = \frac{1}{\sin \Psi} \quad . \tag{3.12}$$

This is equivalent to ω times the large radius of the cone divided by the longitudinal wave velocity equal to unity.

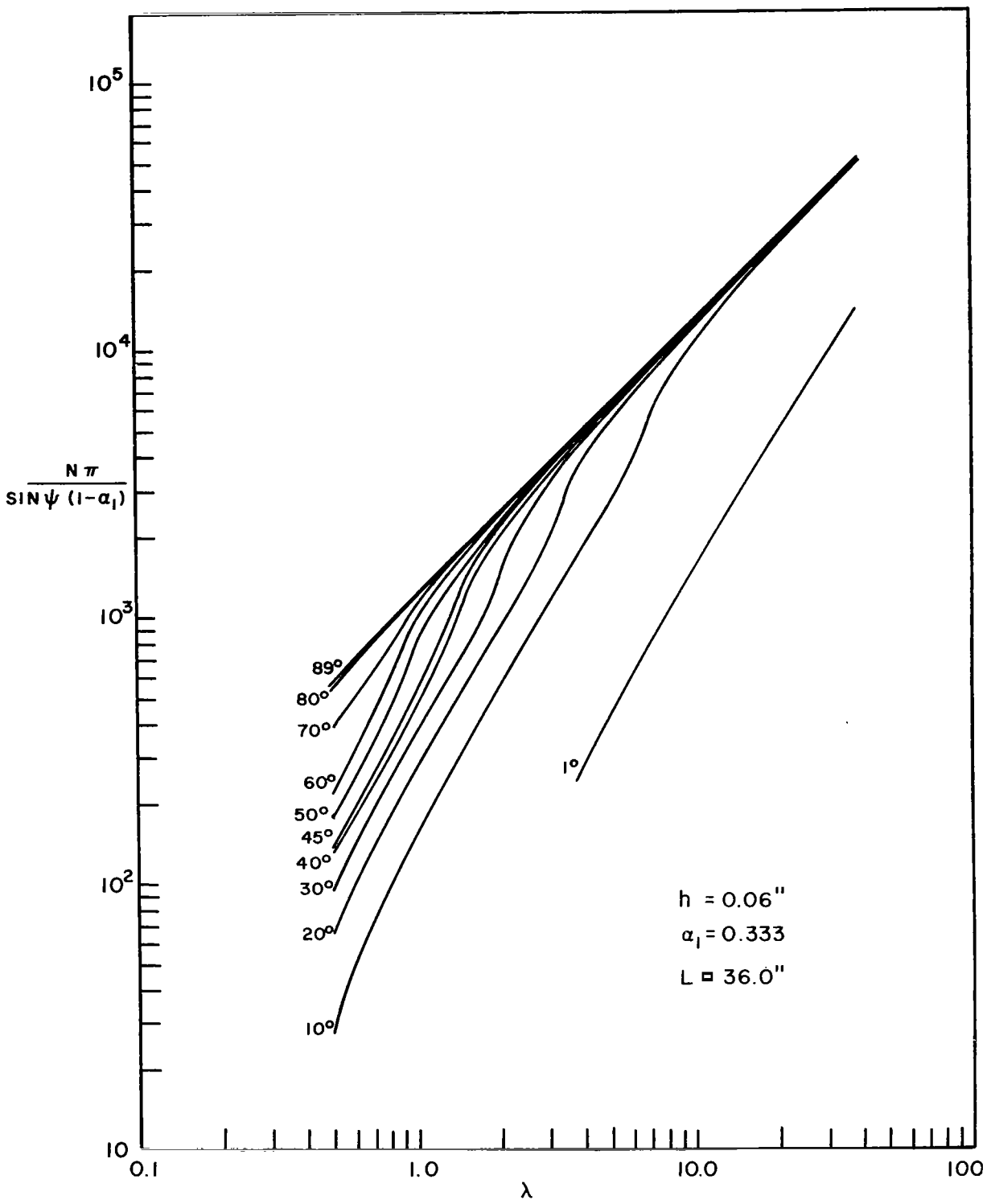

FIGURE 3.3 NUMBER OF MODES VERSUS λ WITH ψ AS THE PARAMETER FOR FREQUENCY EQUATION ONE

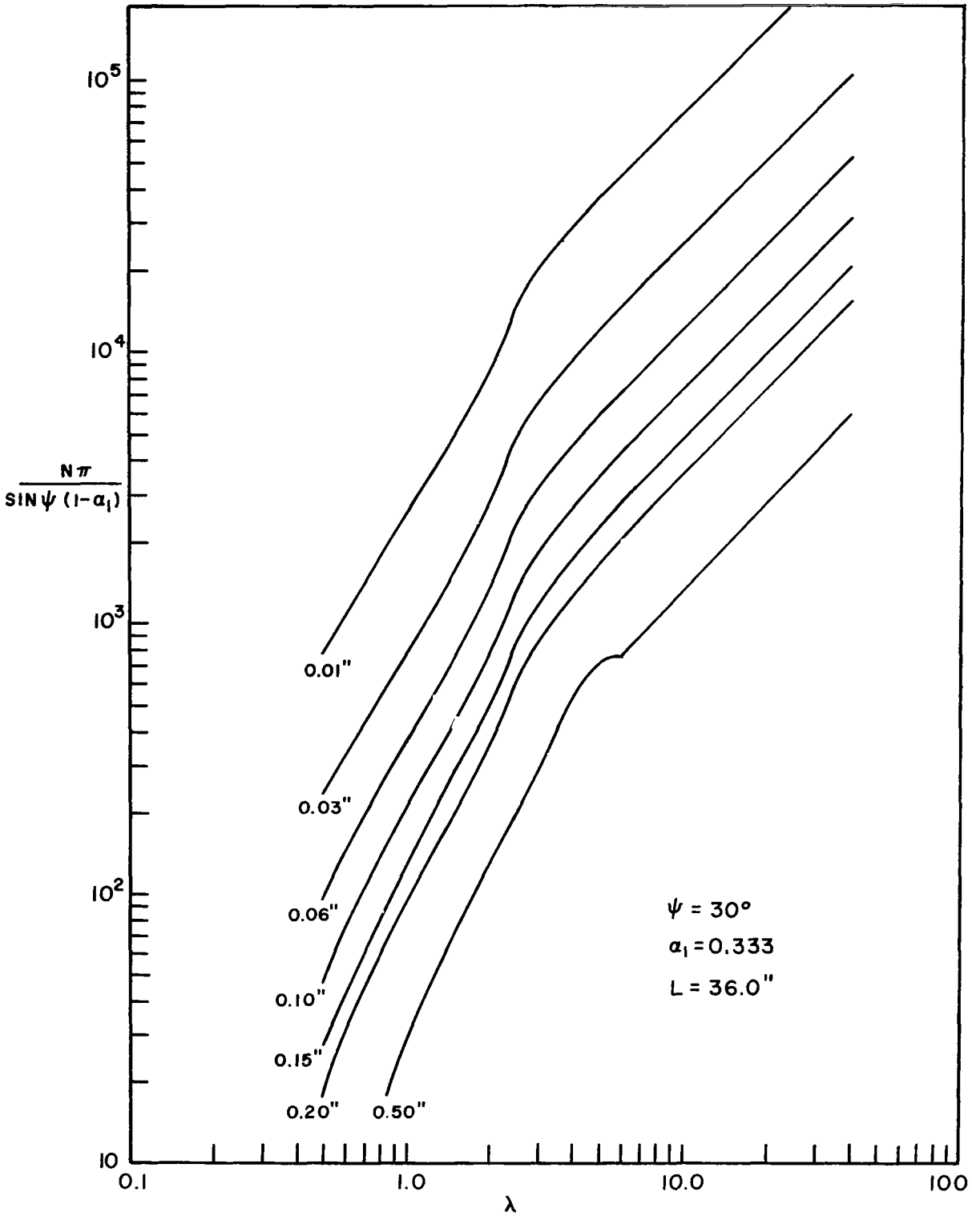

FIGURE 3.4 NUMBER OF MODES VERSUS λ WITH h AS THE PARAMETER FOR FREQUENCY EQUATION ONE

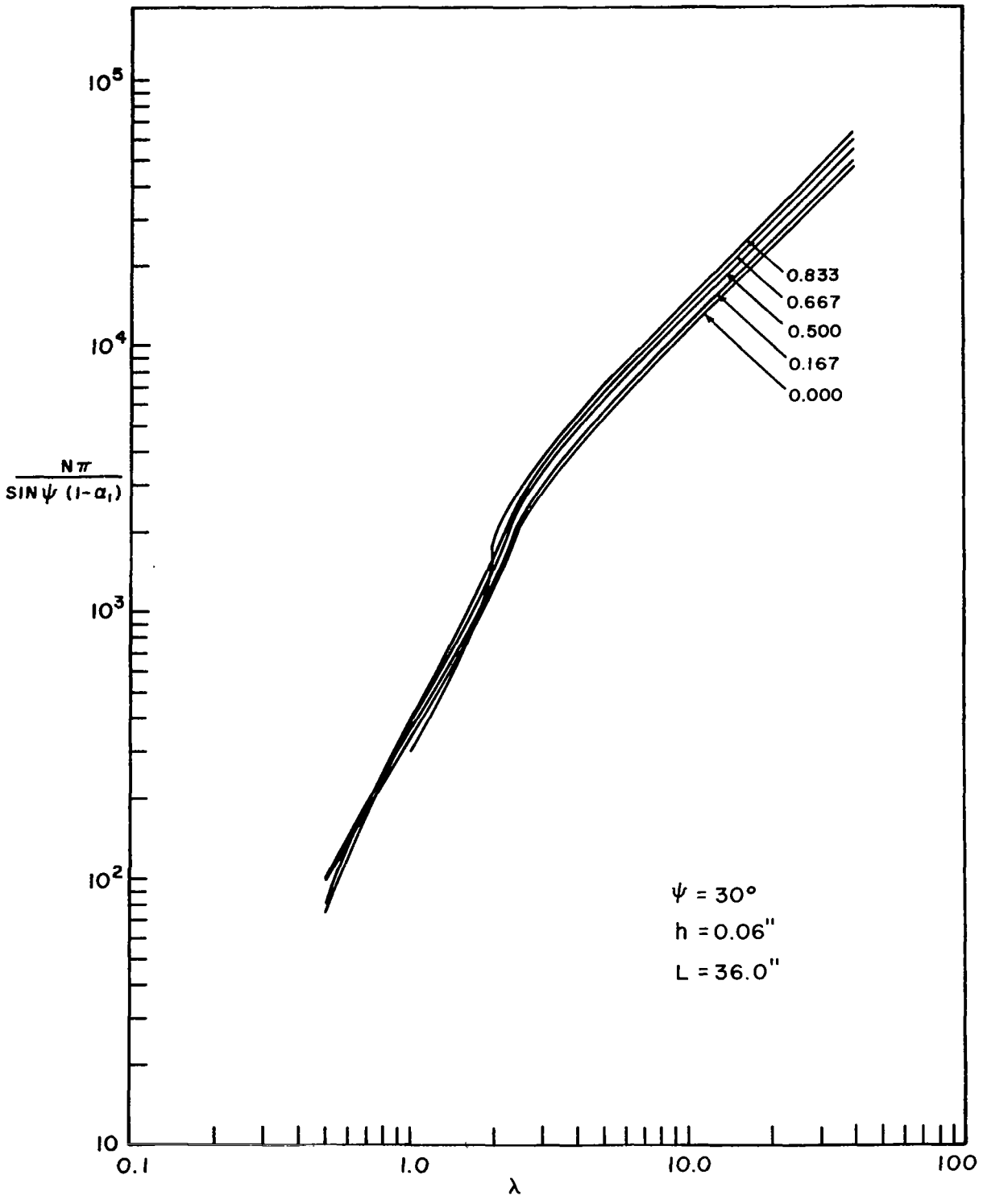

FIGURE 3.5 NUMBER OF MODES VERSUS λ WITH α_1 AS THE PARAMETER FOR FREQUENCY EQUATION ONE

The results given in Figures 3.3 through 3.5 will now be normalized in the frequency range above the upper ring frequency. Figure 3.3 indicates that the results are already normalized with respect to cone angle in this region. Figure 3.4 indicates a variation inversely proportional to h/L with variations in thickness, and Figure 3.5 indicates a variation inversely proportional to $(1-\alpha_1)^{1/5}$ due to variations in truncation ratio. Therefore the results obtained thus far may be normalized with respect to cone geometry by expressing them in the following form:

$$N(\lambda) \frac{\pi}{\sin\psi\,(1-\alpha_1)} \left[\frac{h}{L}\,(1-\alpha_1)^{1/5}\right] = F(\lambda) \quad . \tag{3.13}$$

The results of this normalization procedure are shown graphically in Figures 3.6 through 3.8. Figure 3.6 corresponds to the normalization of Figure 3.3 and so on. The figures indicate that above the upper ring frequency (3.11) the value of $F(\lambda)$ is independent of the geometry of the cone. The plot of $F(\lambda)$ in this region appears to be a straight line on log-log paper.

3.2.3 Numerical Approximations

Examination of Figures 3.6 through 3.8 yields the following numerically obtained expression for the number of eigenvalues above the upper ring frequency:

$$N(\lambda) \frac{\pi}{\sin\psi\,(1-\alpha_1)} \left[\frac{h(1-\alpha_1)^{1/5}}{L}\right] \approx 2.0\,\lambda \tag{3.14}$$

for $\lambda > \dfrac{1}{\alpha_1 \sin\psi}$.

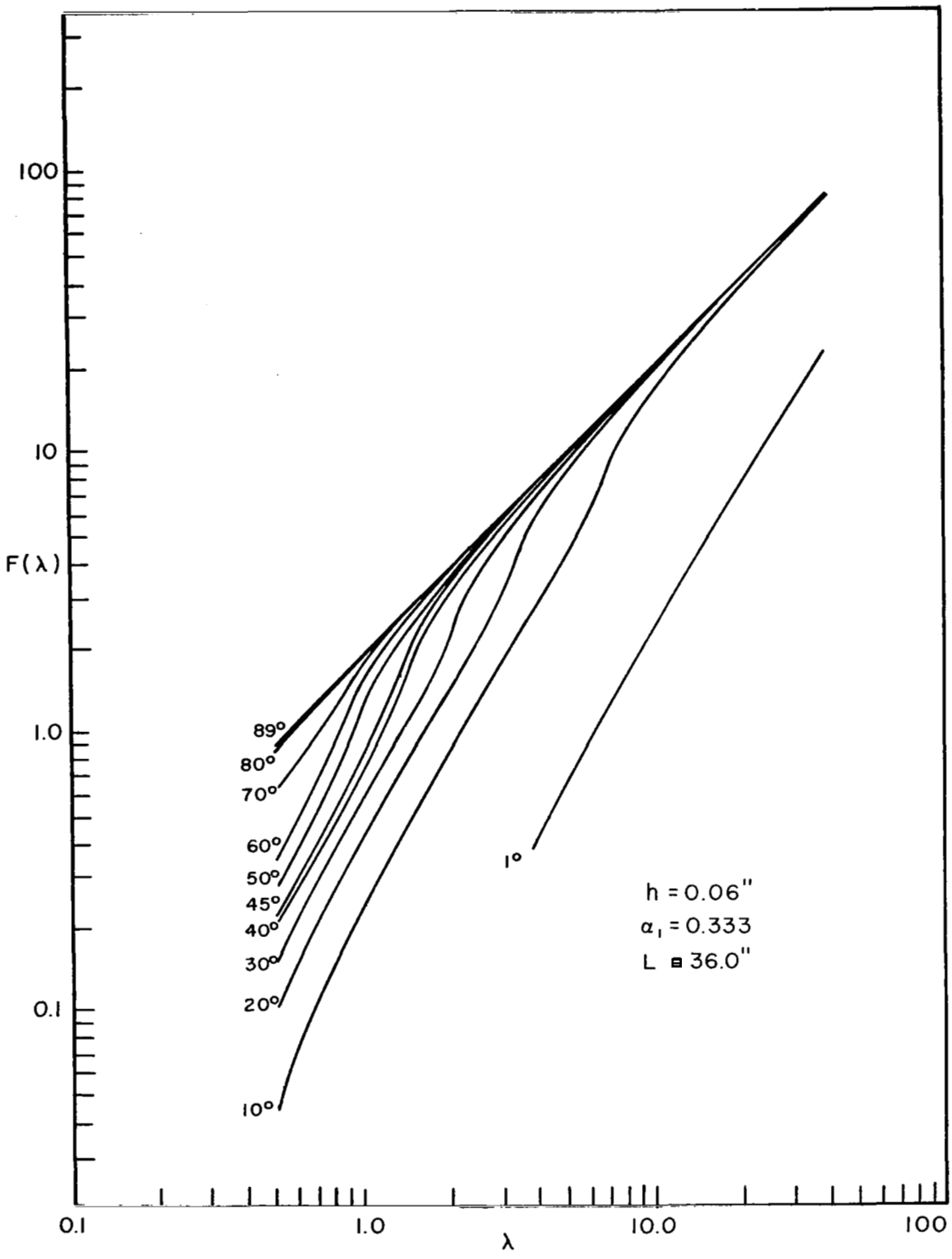

FIGURE 3.6 NORMALIZED NUMBER OF MODES VERSUS λ WITH ψ AS THE PARAMETER FOR EQUATION ONE

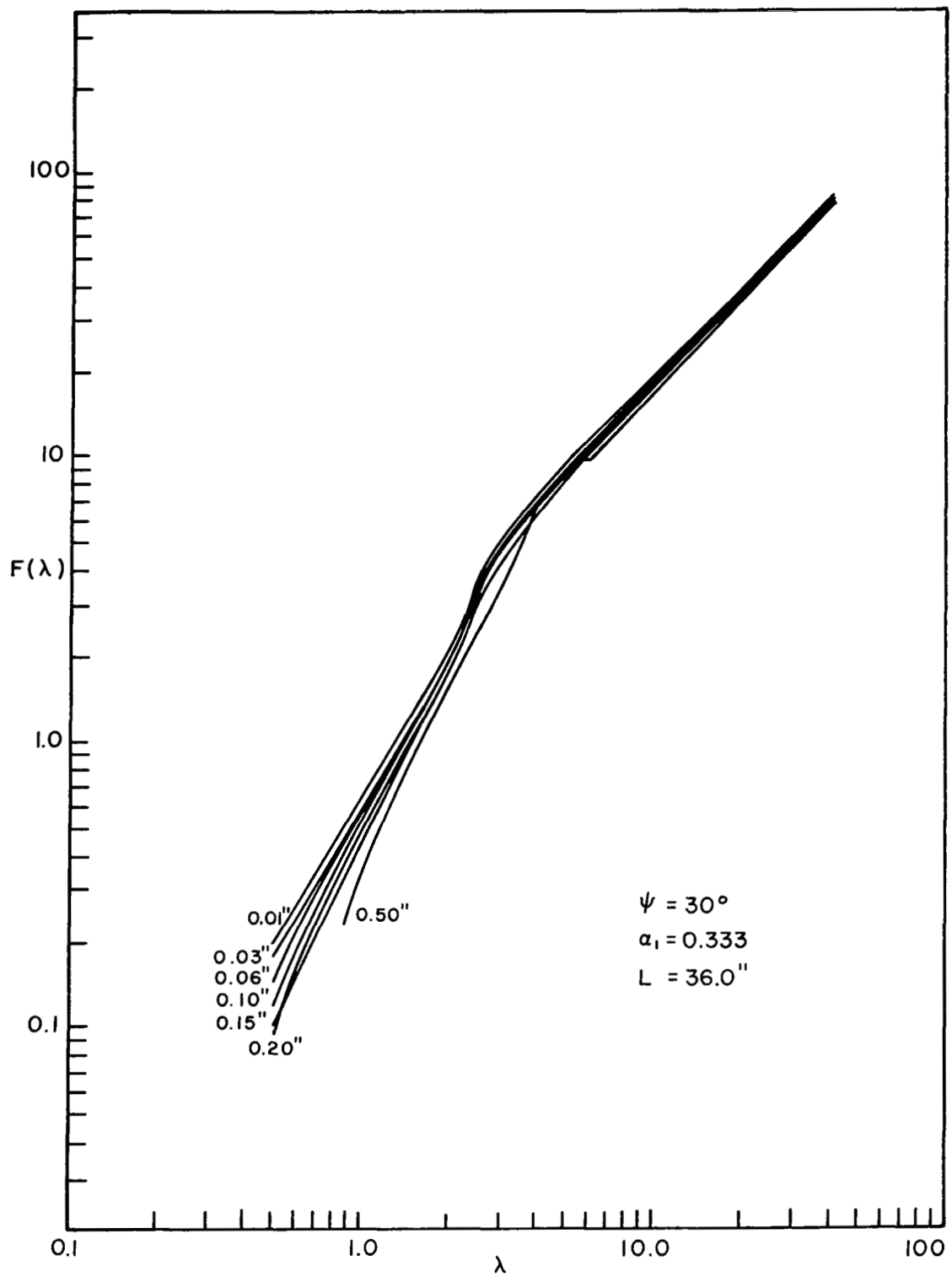

FIGURE 3.7 NORMALIZED NUMBER OF MODES VERSUS λ WITH h AS THE PARAMETER FOR EQUATION ONE

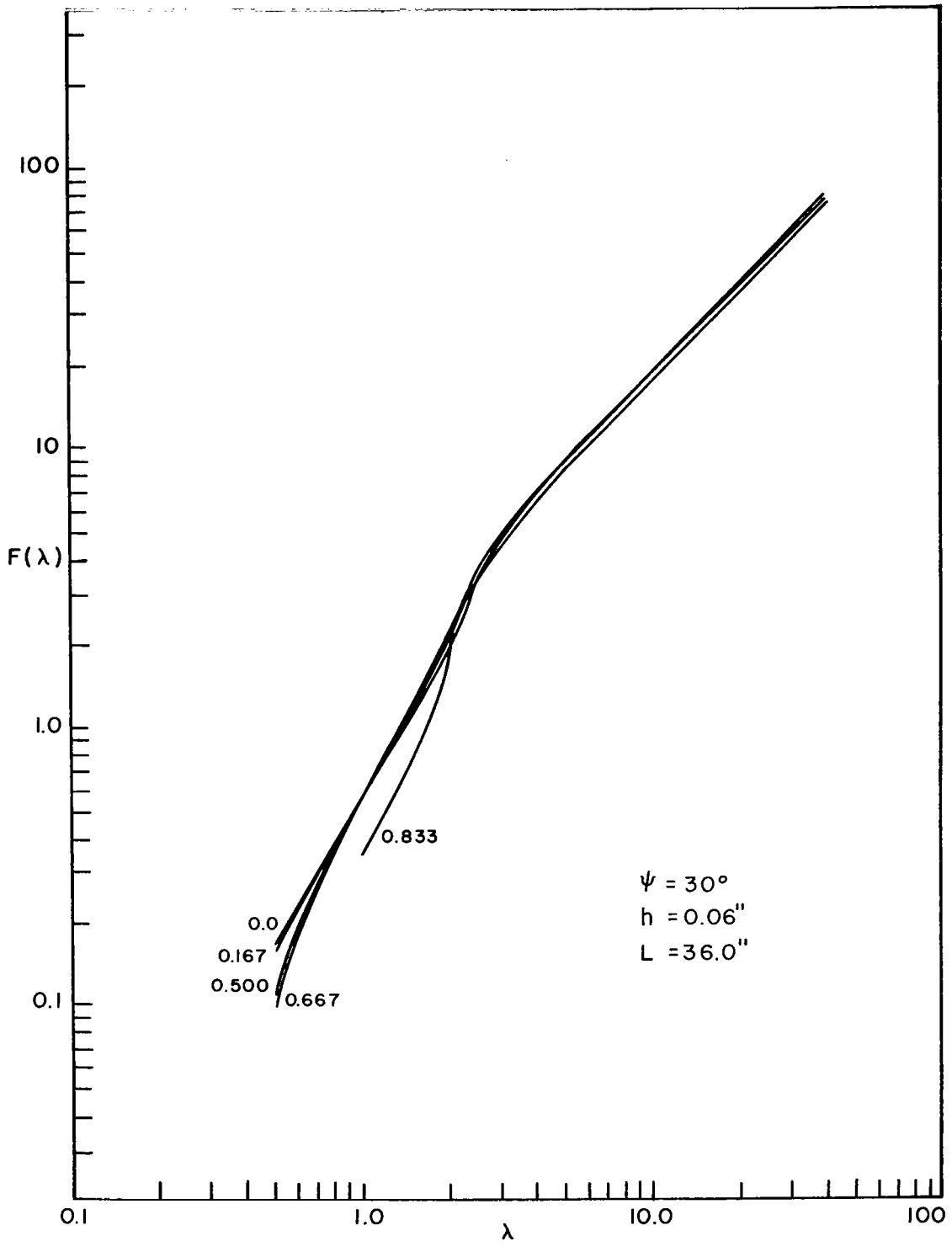

FIGURE 3.8 NORMALIZED NUMBER OF MODES VERSUS λ WITH α_1 AS THE PARAMETER FOR EQUATION ONE

Differentiating equation (3.14) with respect to λ the expression for the eigenvalue density is obtained where $n(\lambda) = \frac{dN(\lambda)}{d\lambda}$:

$$n(\lambda) \frac{\pi}{\sin\psi\,(1-\alpha_1)} \left[\frac{h(1-\alpha_1)}{L}\right]^{1/5} \approx 2.0 \quad . \tag{3.15}$$

As a form of limit check on the results it is of interest to adapt equation (3.14) to the case of a flat circular plate, since a solution to this problem is available in the literature (Miller and Hart, 1967). For the flat circular plate the cone angle becomes 90^{o}, the truncation ratio becomes zero, and the length of the cone becomes the radius of the circular plate (R). Hence for a circular plate equation (3.14) becomes:

$$N(\lambda) = \frac{2}{\pi}\frac{R}{h}\lambda = 0.637\,\frac{R}{h}\lambda \quad . \tag{3.16}$$

Replacing the dimensionless frequency by $\frac{\omega R}{C_L}$ where C_L is the velocity of the longitudinal waves in the shell material, and differentiating with respect to the circular frequency the following expression for the eigenvalue density of a circular plate is obtained:

$$n(\omega) = 0.637\,\frac{R^2}{hC_L} \quad . \tag{3.17}$$

The result cited above in the literature for the modal density of a flat circular plate is as follows, keeping in mind that the value given is one-half the actual value due to degeneracy of eigenvalue effects:

$$n(\omega) = 0.701\,\frac{R^2}{hC_L} \quad . \tag{3.18}$$

The difference between equation (3.17) and equation (3.18) is less than ten percent and considering the numerical nature of procedure used to obtain the equations on which equation (3.17) is based this is regarded as excellent agreement.

3.3 Frequency Equation Two

Using the differential equations presented in Appendix 8.1 (8.51) and (8.52) for a conical shell, and making the assumption that the bending contribution in the longitudinal direction is small when compared to the bending contribution in the circumferential direction, the equations reduce to the following:

$$\frac{1}{Eh} \nabla^2 \nabla^2 \phi - \frac{\cos \psi}{r} \frac{\partial^2}{\partial x^2} w = 0 \qquad (3.19)$$

$$\frac{\cos \psi}{r} \frac{\partial^2}{\partial x^2} \phi + D \nabla^2 \nabla^2 w - \frac{\gamma h \omega^2}{g_c} w = 0 \ , \qquad (3.20)$$

where $\nabla^2 = \frac{\sin \psi}{r} \frac{\partial}{\partial x} + \frac{1}{r^2} \frac{\partial^2}{\partial \theta^2}$.

Comparing equations (3.19) and (3.20) with equations (8.51) and (8.52) it is noted that the equations are identical except for the omission of the first tem in the ∇^2 operator. The solution of equations (3.19) and (3.20) is handled in the same manner as was the solution of equations (8.51) and (8.52). The procedure is described in Appendix 8.1, and will not be repeated here. The frequency equation

which is produced in this case is as follows:

$$\omega^2 = \left[\frac{g_c E}{\gamma L^2}\right] \frac{\frac{D}{EL^2h}\left(\frac{m^4}{\sin^4\psi}\frac{1-\alpha_1}{2}\right)^2 + \frac{a_n^4}{\tan^2\psi}\left[\frac{1-\alpha_1^4}{8} - \frac{3(1-\alpha_1)^2}{8a_n^2}\right]^2}{\left(\frac{m^4}{\sin^4\psi}\frac{1-\alpha_1}{2}\right)\left(\frac{1-\alpha_1^5}{10} - \frac{1-\alpha_1^3}{2a_n^2} + \frac{3(1-\alpha_1)}{4a_n^4}\right)} . \qquad (3.21)$$

Proceeding in the same manner as in section 3.2, the frequency equation is nondimensionalized by introducing the dimensionless frequency, the circumferential wave number, and the longitudinal wave number (see equation 3.2). Equation (3.21) therefore reduces to the following form:

$$\lambda = \frac{\frac{D}{EL^2h}\left(k_2^4\frac{1-\alpha_1}{2}\right)^2 + \cot^2\psi\, k_1^4\left[\frac{1-\alpha_1^4}{8} - \frac{3(1-\alpha_1^2)}{8k_1^2}\right]^2}{k_2^4\left(\frac{1-\alpha_1}{2}\right)\left(\frac{1-\alpha_1^5}{10} - \frac{1-\alpha_1^3}{2k_1^2} + \frac{3(1-\alpha_1)}{4k_1^4}\right)} . \qquad (3.22)$$

3.3.1 Wave Number Space

It is now necessary to solve for k_2 in terms of k_1 and λ in order to obtain the k-space geometry corresponding to frequency equation two (3.22). Rearranging terms and collecting powers of k_2 in the frequency equation it is found that the equation (3.22) reduces to a simple quadratic equation in powers of k_2^4. Therefore k_2 may be expressed explicitly as a function of k_1, λ, and the cone geometry parameters in the following form:

$$k_2 = \sqrt[4]{\frac{-B \pm \sqrt{B^2 - 4AC}}{2A}} \qquad (3.23)$$

where

$$A = \frac{D}{EhL^2} 80k_1^4$$

$$B = \lambda^2[-16k_1^4(1+\alpha_1+\alpha_1^2+\alpha_1^3+\alpha_1^4) + 8k_1^2(1+\alpha_1+\alpha_1^2)-120]$$

$$C = 5\cot^2\psi[k_1^4(1+\alpha_1+\alpha_1^2+\alpha_1^3) - 3k_1^2(1+\alpha_1)]^2 \quad .$$

Sufficient information is now available to describe the geometry of the k-space corresponding to frequency equation two. In equation (3.23) the positive and negative square roots indicate the upper and lower bounds of the space respectively. Figure 3.9 illustrates a typical k-space for a truncated cone, and Figure 3.10 illustrates a typical k-space for a closed one. Both figures are shown with dimensionless frequency as the parameter.

By equating the upper and lower bounds of the space given by equation (3.23) the k_1 limits of the space may be obtained as functions of the dimensionless frequency and the cone geometry parameters. The expression which results from this process is a cubic in powers of k_1^2 as follows:

$$k_1^6 + Sk_1^4 + Tk_1^2 + U = 0 \qquad (3.24)$$

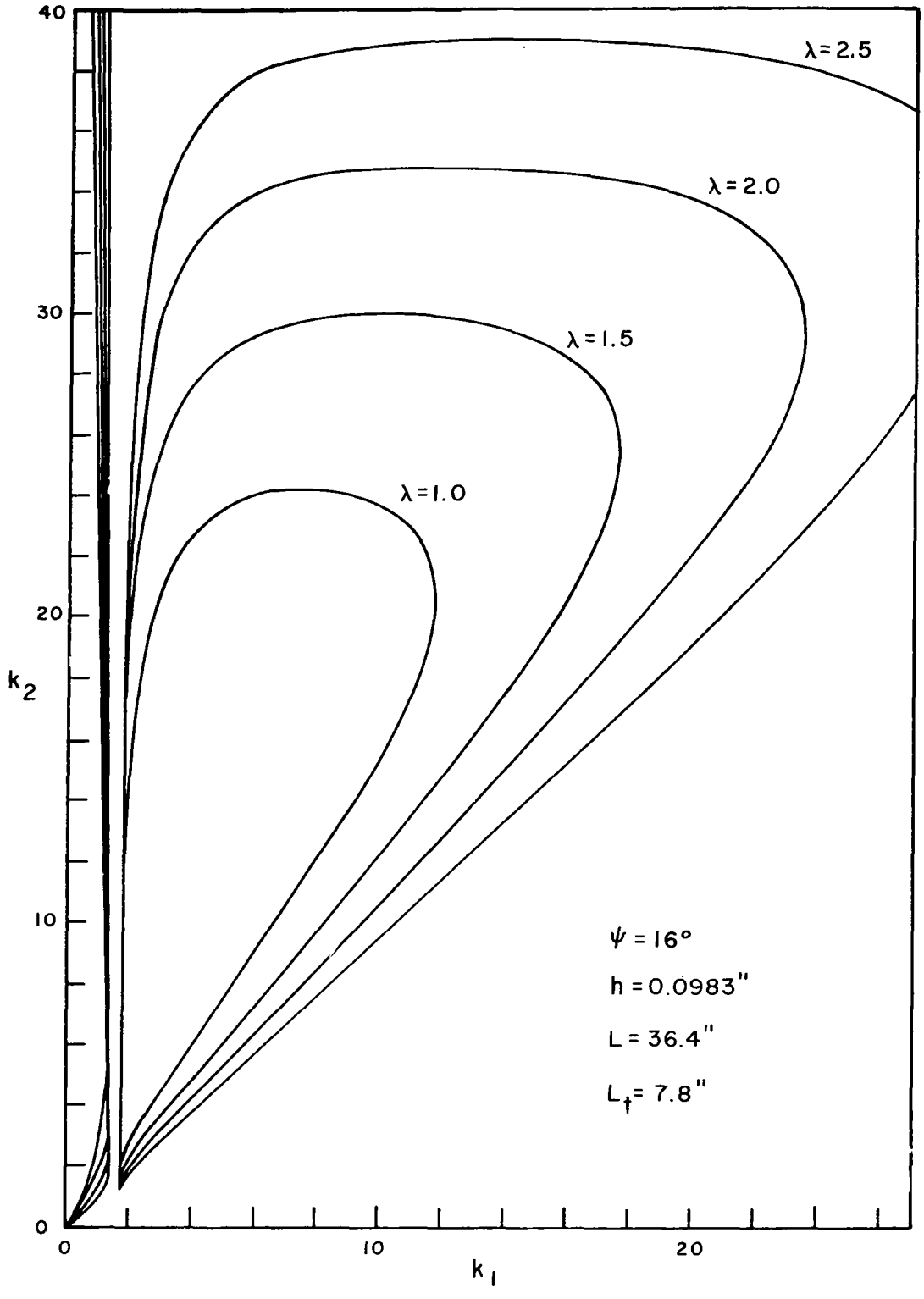

FIGURE 3.9 FREQUENCY EQUATION TWO K-SPACE FOR A TRUNCATED CONE

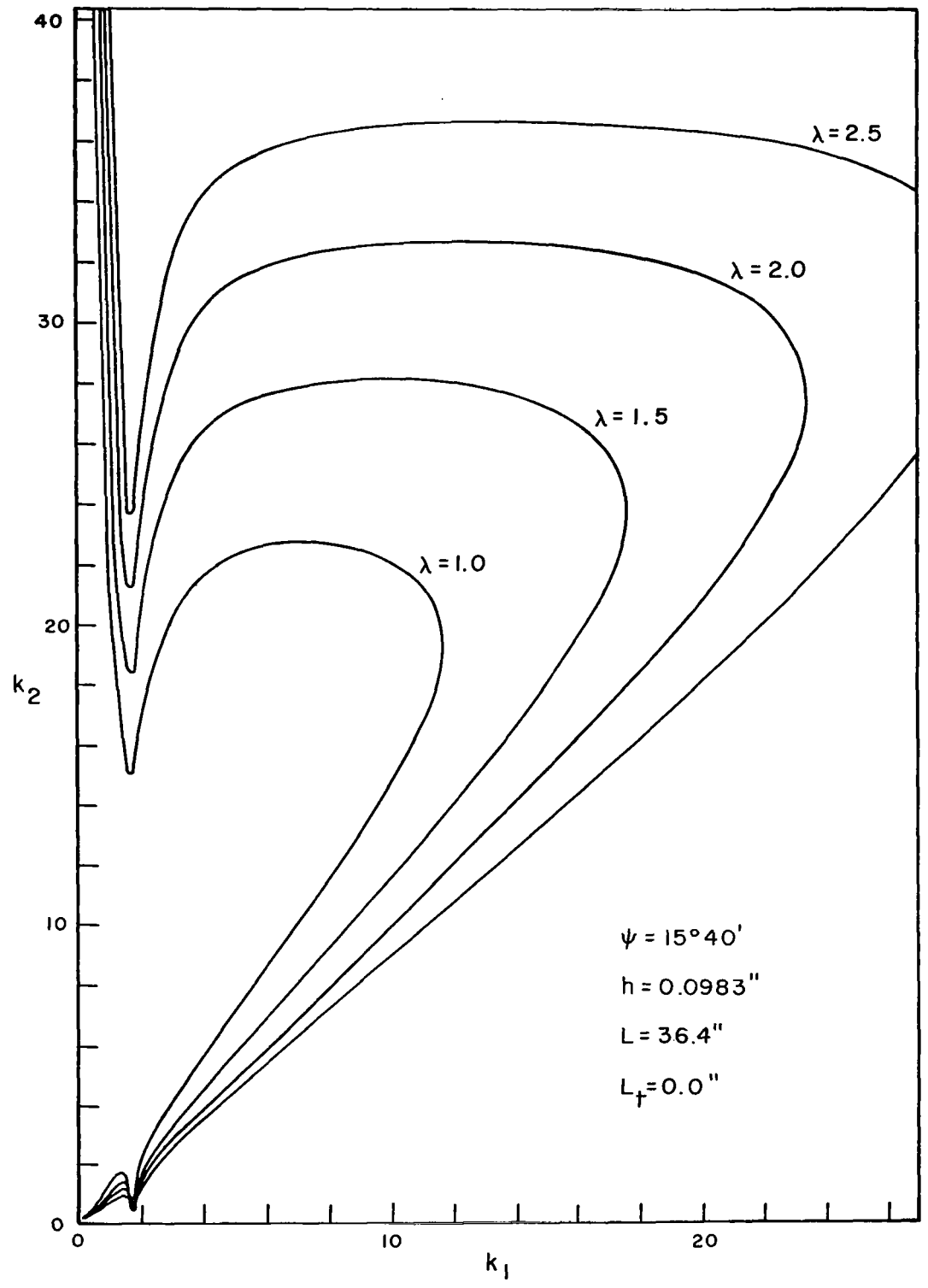

FIGURE 3.10 FREQUENCY EQUATION TWO K-SPACE FOR A CLOSED CONE

where

$$S = [-3(1-\alpha_1^2)/(1-\alpha_1^4)] - [4\lambda(1-\alpha_1^5)L\sqrt{3(1-\nu^2)}/5h\cot\psi\ (1-\alpha_1^4)]$$

$$T = 4\lambda(1-\alpha_1^3)L\sqrt{3(1-\nu^2)}\ /\ h\cot\psi\ (1-\alpha_1^4)$$

$$U = -6\lambda(1-\alpha_1)L\sqrt{3(1-\nu^2)}\ /\ h\cot\psi\ (1-\alpha_1^4)\ .$$

The solution of the cubic equation (3.24) yields three real roots in the case of the truncated cone (Figure 3.9), and one real root and two imaginary roots in the case of the closed cone (Figure 3.10). In the latter case the real part of the two imaginary roots corresponds to the value of k_1 where the upper and lower bounds are at a minimum.

3.3.2 Cumulative Number of Eigenvalues

Recalling equation (3.10) which was developed in section 3.1 as an expression for the number of eigenvalues, and substituting the appropriate values for Δk_1 (change in longitudinal wave number as n is incremented) and Δk_2 (change in circumferential wave number as m is incremented), the following expression for the number of eigenvalues is obtained:

$$N(\lambda)\ \frac{\pi}{\sin\psi\,(1-\alpha_1)}\ \approx\ \int_a^b\ ([k_2]_u - [k_2]_\ell)\,dk_1\ . \qquad (3.25)$$

The upper and lower bounds of the space $[k_2]_u$ and $[k_2]_\ell$ are given by equation (3.23). Therefore equation (3.25) may be expressed in the following form:

$$N(\lambda)\ \frac{\pi}{\sin\psi(1-\alpha_1)}\ \approx\ \int_a^b\ \sqrt[4]{\frac{-B+\sqrt{B^2-4AC}}{2A}}\ dk_1 - \int_a^b\ \sqrt[4]{\frac{-B-\sqrt{B^2-4AC}}{2A}}\ dk_1\ . \qquad (3.26)$$

The upper and lower limits of the space a and b are obtained from the solution of equation (3.24). For the truncated cone case the largest root of equation (3.24) is denoted as b, and the second largest root is denoted as a. In the case of the closed cone, the one real root obtained in the solution of equation (3.24) is used as b, and the real part of either of the imaginary roots is used as a. In this way the integral (3.26) is evaluated over the closed portion, or the nearly closed portion of the k-space.

The evaluation of equation (3.26) for the number of eigenvalues, and the solution of equation (3.24) for the upper and lower limits of the k-space is handled by numerical procedures on an IBM 360 model 75 digital computer. The program used is described in detail in Appendix 8.3. Values are obtained for a wide range of dimensionless frequencies and a range of different cone geometries. The results of these calculations appear in graphical form in Figures 3.11 through 3.13.

As in section 3.2, Figure 3.11 shows the effect of variations in cone angle, Figure 3.12 shows the effect of variations in thickness, and Figure 3.13 shows the effect of variations in truncation ratio.

It should be noted that below the lower ring frequency (3.12) the number of eigenvalue results shown in Figures 3.3 through 3.5 are in very close agreement with the results shown in Figures 3.11 through 3.13. This is to be expected since the only difference between the derivation of frequency equation one and frequency equation two is in the assumption regarding the bending contributions to the differential equations. In equation two it was assumed that the contribution to the differential equations due to longitudinal bending is small in

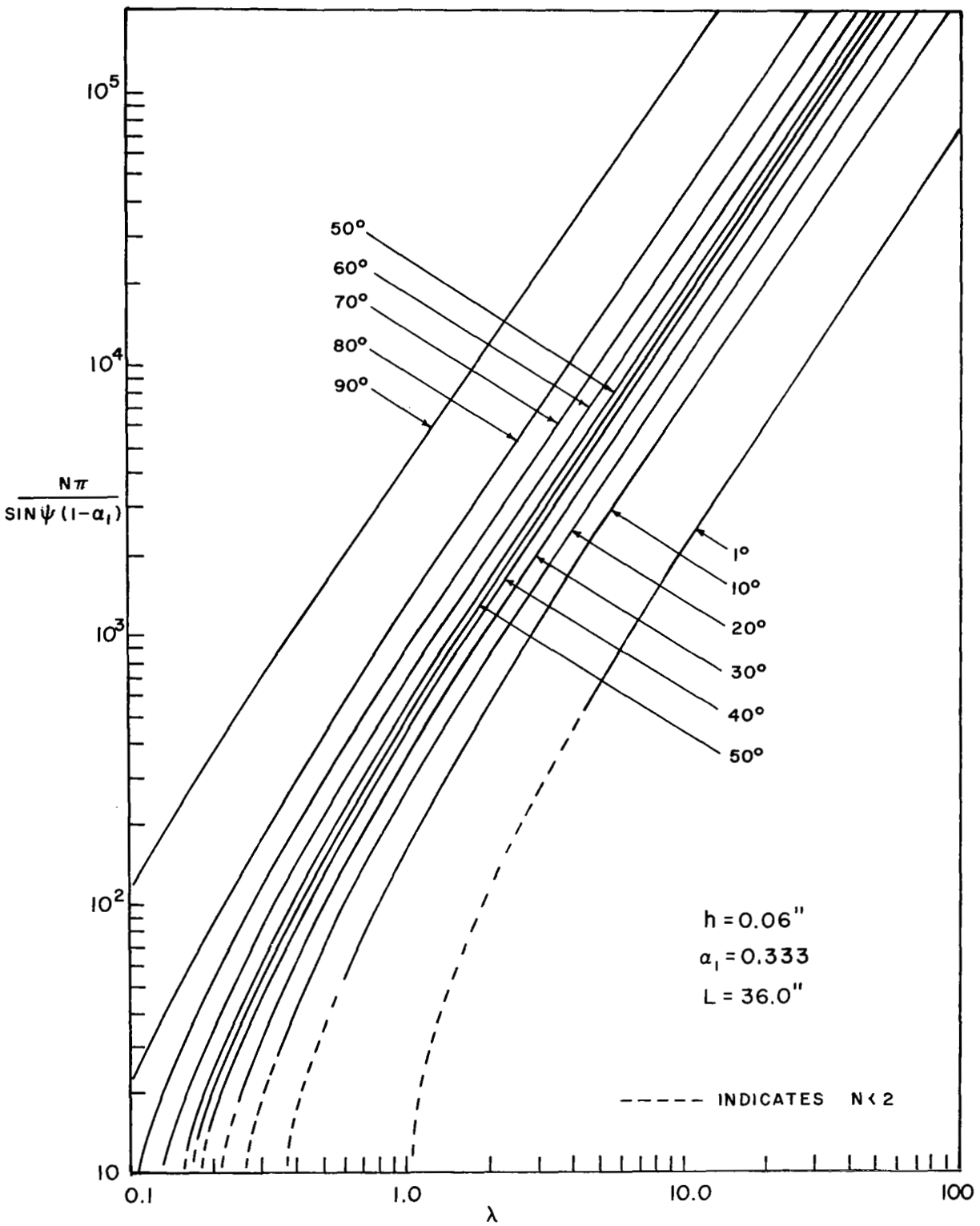

FIGURE 3.11 NUMBER OF MODES VERSUS λ WITH ψ AS THE PARAMETER FOR FREQUENCY EQUATION TWO

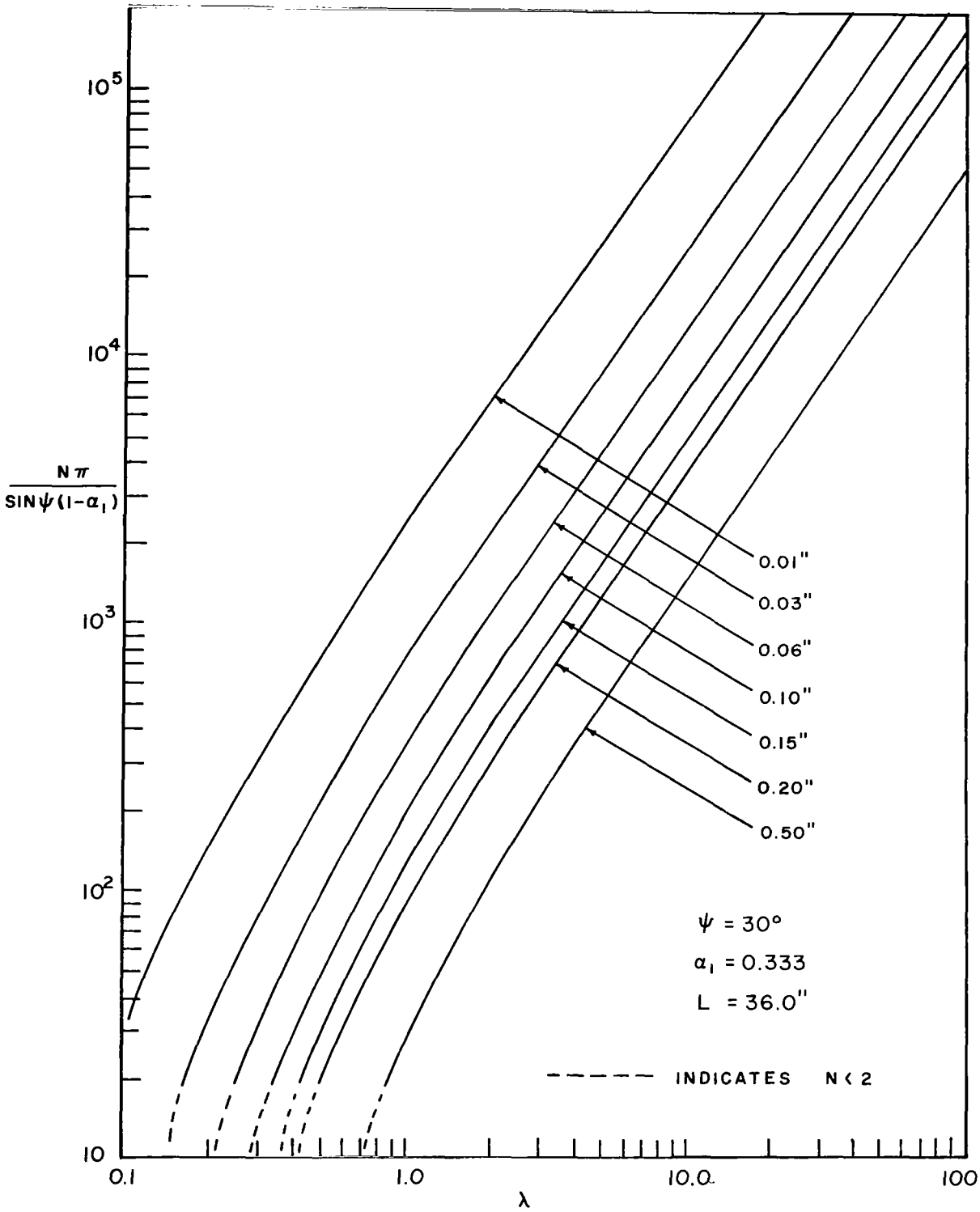

FIGURE 3.12 NUMBER OF MODES VERSUS λ WITH h AS THE PARAMETER FOR FREQUENCY EQUATION TWO

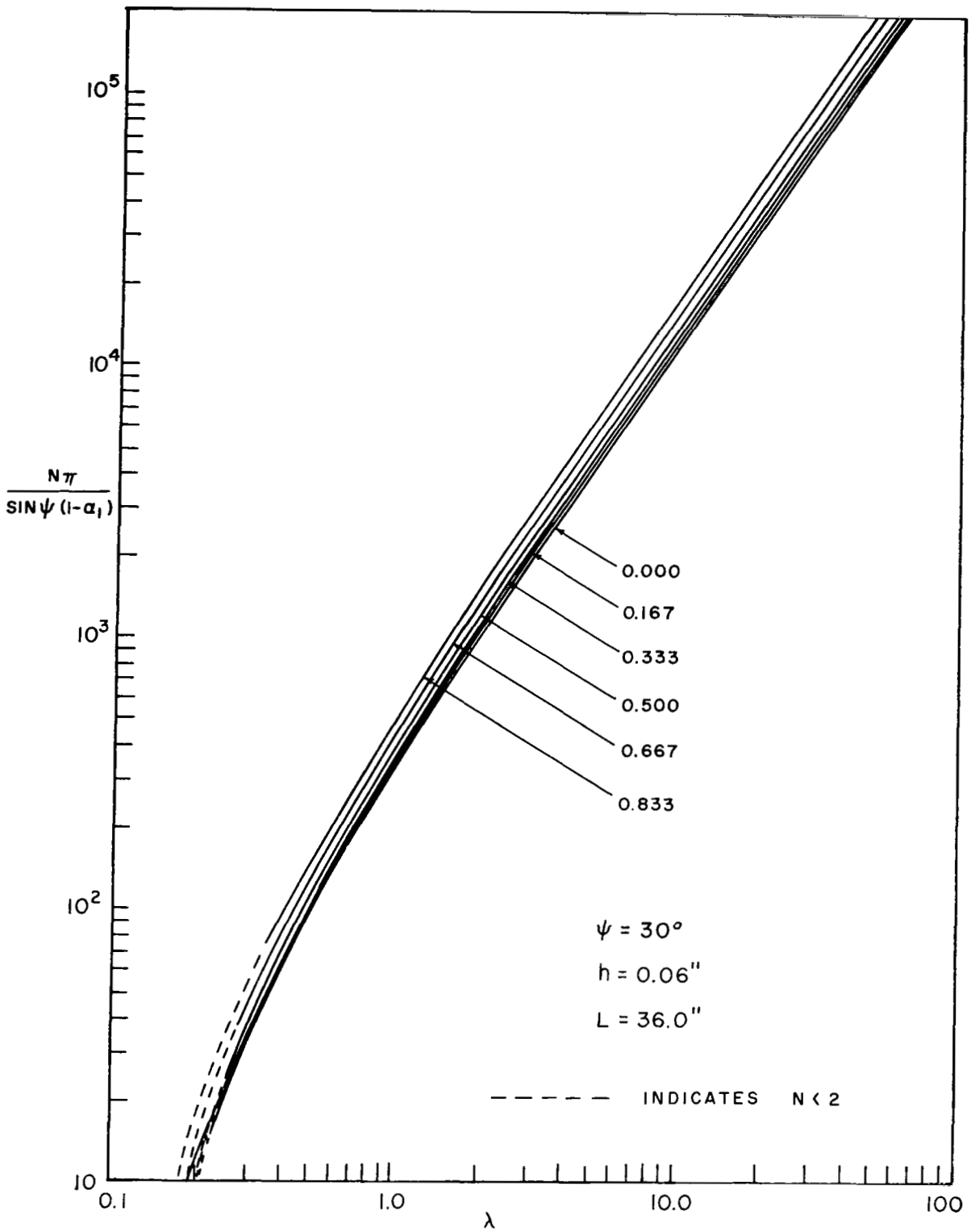

FIGURE 3.13 NUMBER OF MODES VERSUS λ WITH α_1 AS THE PARAMETER FOR FREQUENCY EQUATION TWO

comparison with the contribution due to circumferential bending. This assumption is equivalent to limiting frequency equation two to lower frequencies as the results point out. It may therefore be concluded that the results of the analysis based on frequency equation two are valid below the lower ring frequency.

Careful study of Figures 3.11 through 3.13 indicates that the dimensionless number of eigenvalues $\left(N(\lambda)\ \frac{\pi}{\sin\psi\,(1-\alpha_1)}\right)$ varies with changes in the cone angle directly as $(\tan^{\frac{1}{2}}\psi)$, with changes in the thickness inversely as (h/L), and with changes in the truncation ratio inversely as $((1-\alpha_1)^{1/4})$. Hence, the number of eigenvalues may be normalized in the following manner:

$$N(\lambda)\ \frac{\pi}{\sin\psi(1-\alpha_1)}\left[\frac{h}{L}\ \frac{(1-\alpha_1)^{1/4}}{(\tan\psi)^{1/2}}\right] \;=\; G(\lambda)\ . \qquad (3.27)$$

Figures 3.14 through 3.16 show graphically the results of this normalization process. Inspection of these figures, which correspond to normalized versions of Figures 3.11 through 3.13, indicates that with the exception of small variations near values of $G(\lambda)$ corresponding to the first few modes $(N(\lambda) \approx 1)$, $G(\lambda)$ is independent of the geometry of the conical shell and is a function of only the dimensionless frequency.

3.3.3 Eigenvalue Density

Using finite difference techniques on the numerical results of the k-space integration of equation (3.26) the density of eigenvalues with respect to dimensionless frequency is obtained $\left(n(\lambda) = \frac{dN(\lambda)}{d\lambda}\right)$. The results of these calculations are shown graphically in Figures 3.17 through 3.19 in the following form:

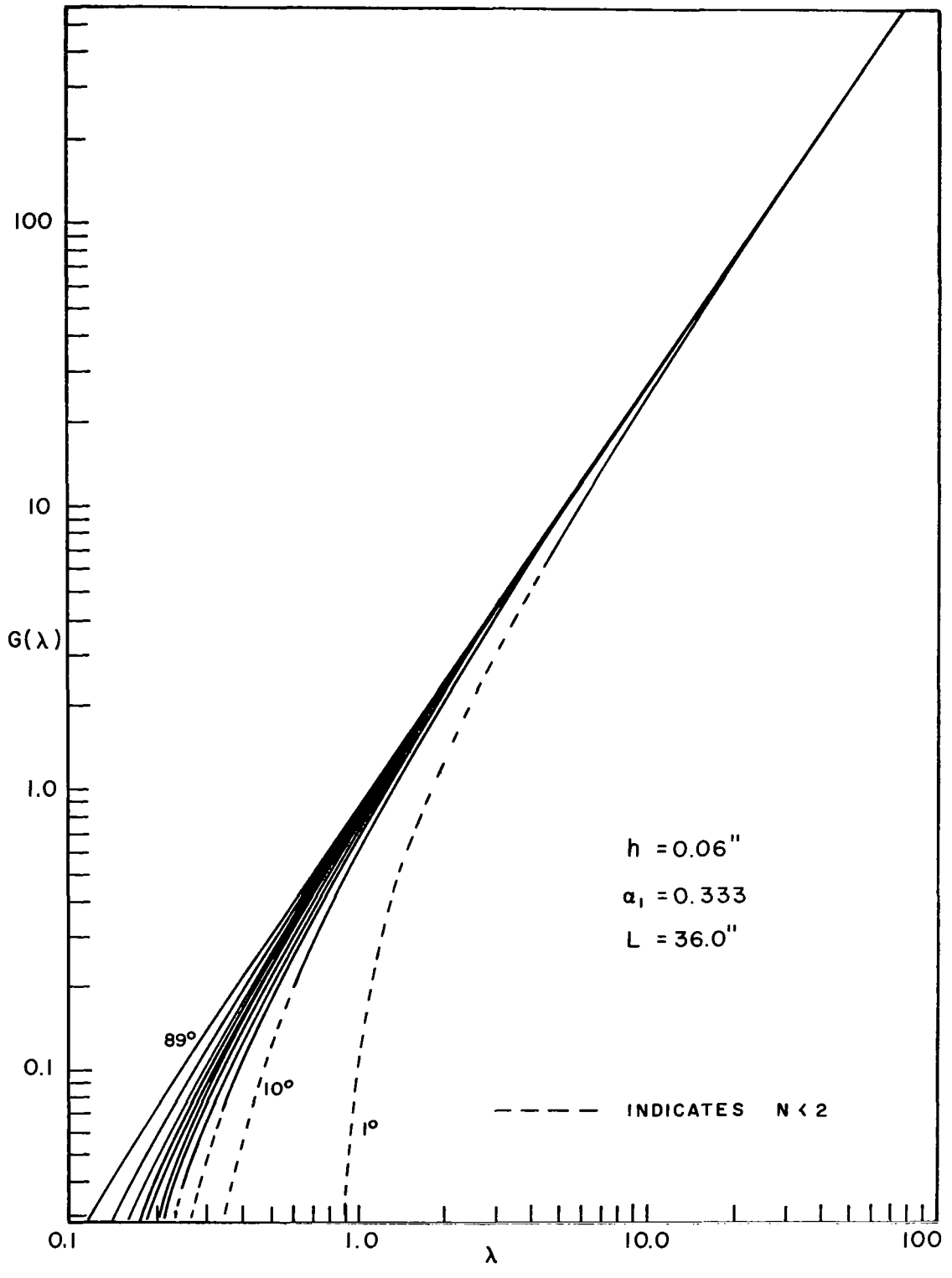

FIGURE 3.14 NORMALIZED NUMBER OF MODES VERSUS λ WITH ψ AS THE PARAMETER FOR EQUATION TWO

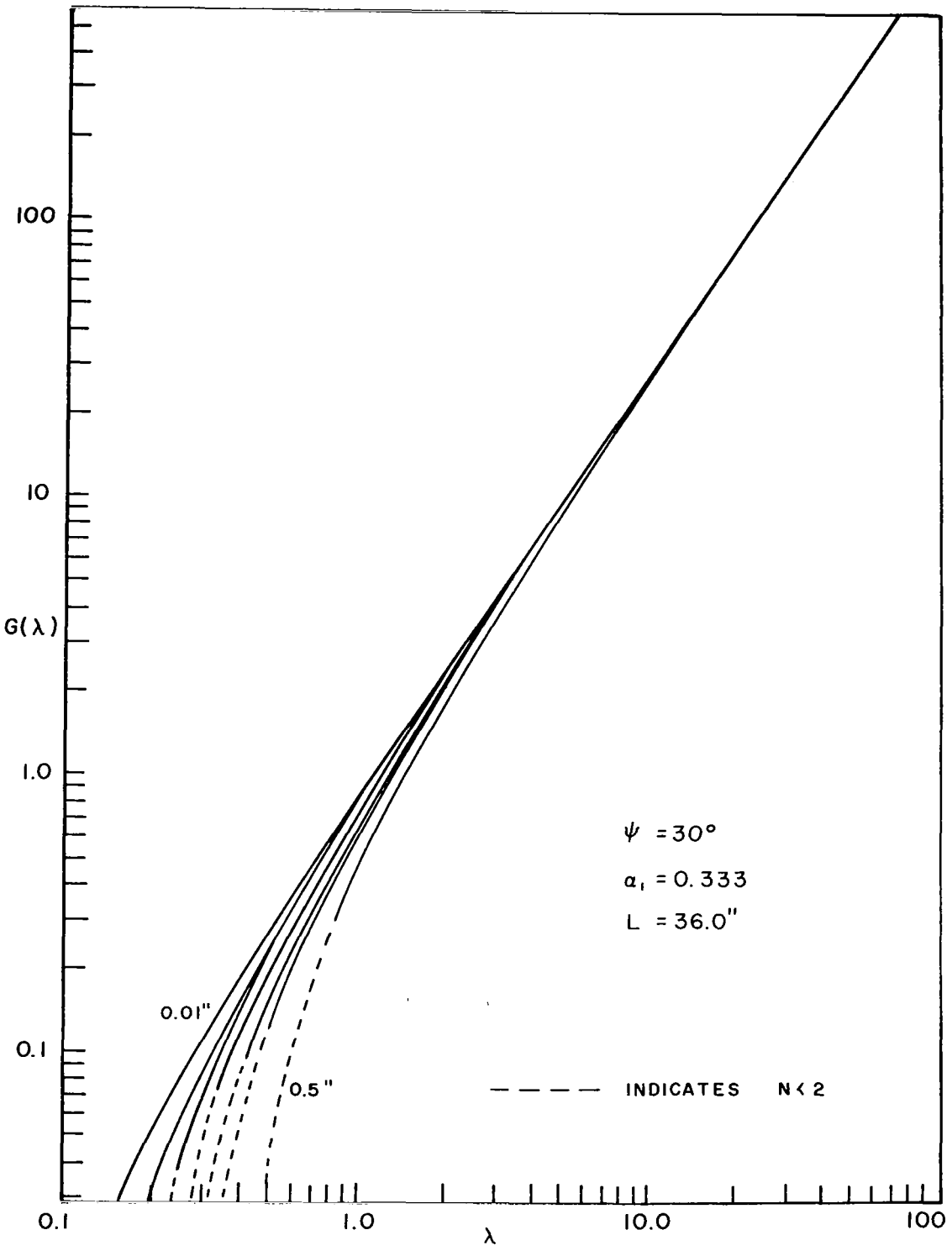

FIGURE 3.15 NORMALIZED NUMBER OF MODES VERSUS λ WITH h AS THE PARAMETER FOR EQUATION TWO

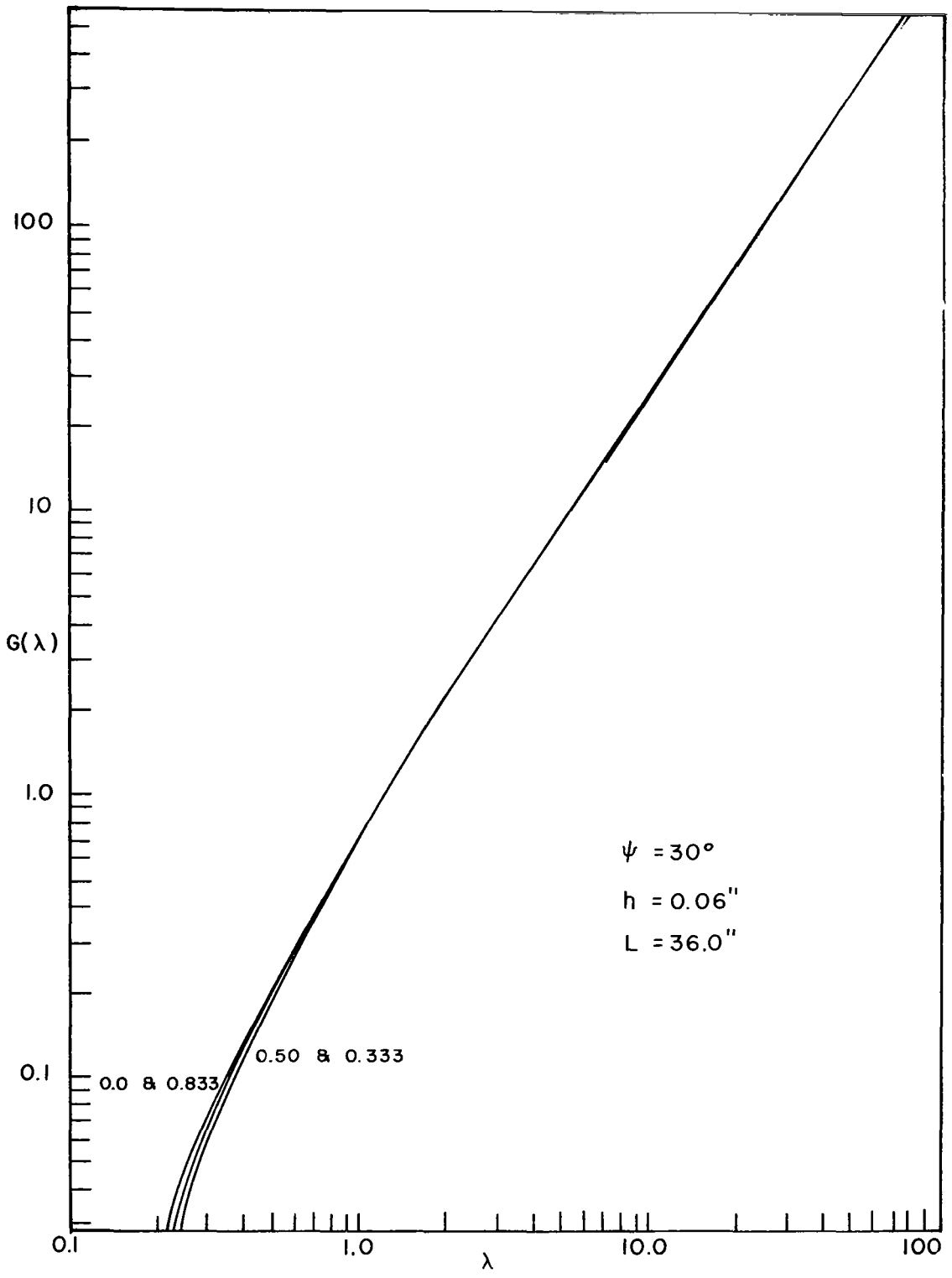

FIGURE 3.16 NORMALIZED NUMBER OF MODES VERSUS λ WITH α_1 AS THE PARAMETER FOR EQUATION TWO

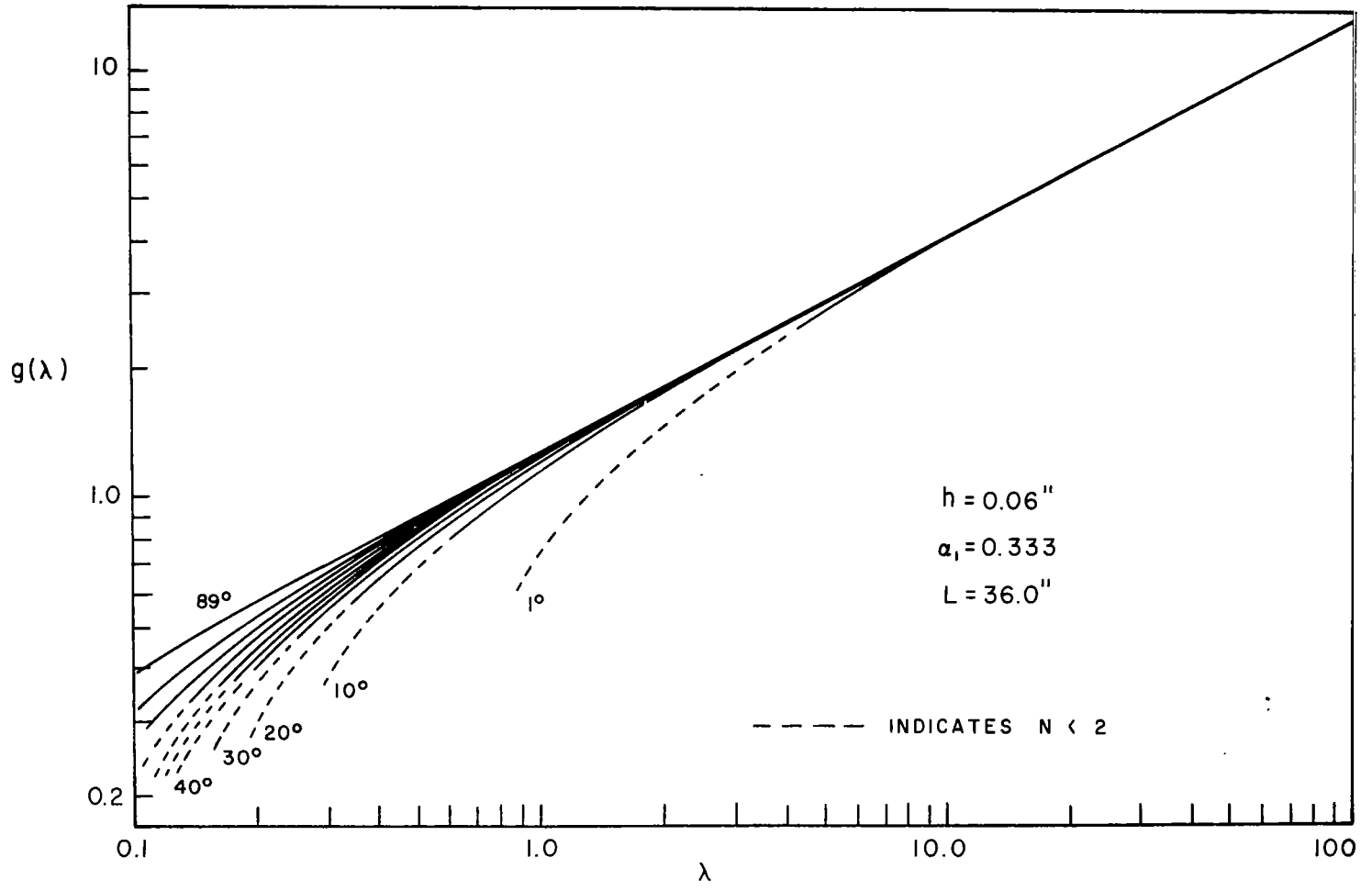

FIGURE 3.17 NORMALIZED EIGENVALUE DENSITY VERSUS λ WITH ψ AS THE PARAMETER FOR FREQUENCY EQUATION TWO

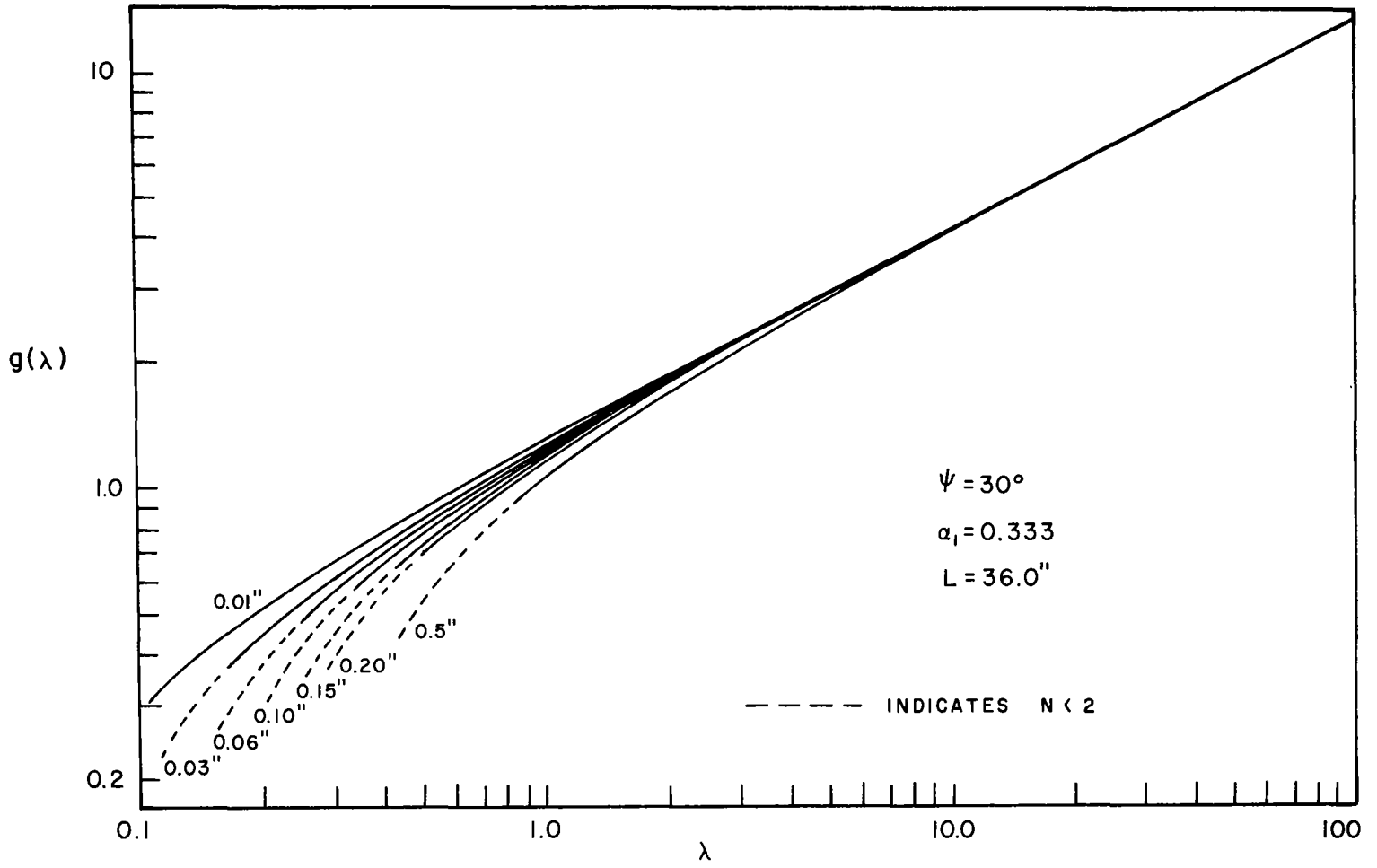

FIGURE 3.18 NORMALIZED EIGENVALUE DENSITY VERSUS λ WITH h AS THE PARAMETER FOR FREQUENCY EQUATION TWO

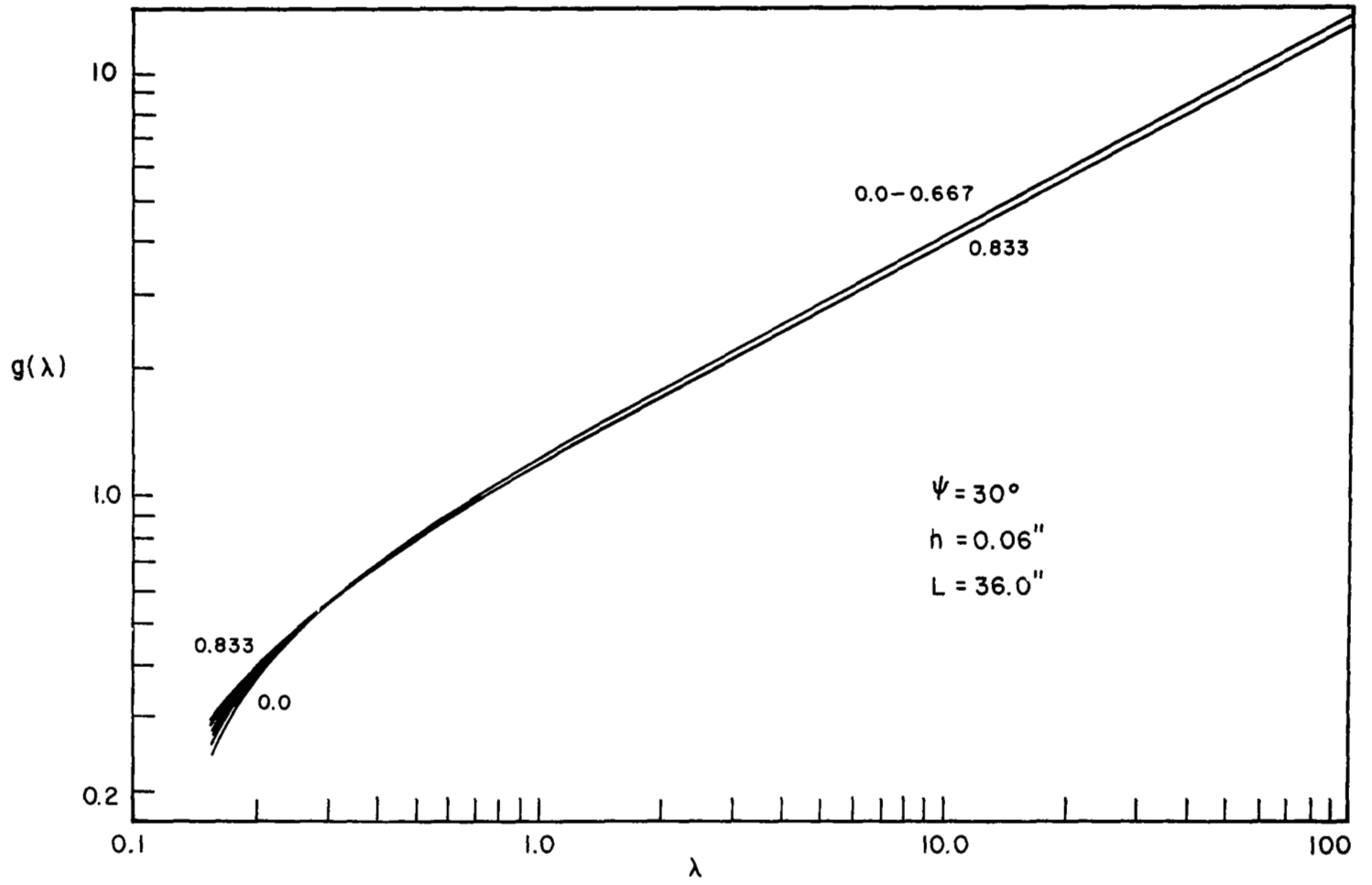

FIGURE 3.19 NORMALIZED EIGENVALUE DENSITY VERSUS λ WITH α_1 AS THE PARAMETER FOR FREQUENCY EQUATION TWO

$$n(\lambda) \frac{\pi}{\sin\psi\,(1-\alpha_1)} \left[\frac{h(1-\alpha_1)^{1/4}}{L(\tan\psi)^{1/2}}\right] = g(\lambda) \ . \qquad (3.28)$$

As before, Figure 3.17 illustrates variations in cone angle, Figure 3.18 illustrates variations in thickness, and Figure 3.19 illustrates variations in truncation ratio. Inspection of these figures reveals that $g(\lambda)$ is independent of the cone geometry with the exception values associated with the number of eigenvalues approximately equal to unity, as was the case with $G(\lambda)$.

Since the k-space integration presented in equation (3.26) avoids the portion of the k-space in the vicinity of $k_1 \approx 0$, there is some question as to the validity of the results. In order to provide a check of the results presented, a numerical procedure similar to that used in section 3.2 was used to obtain values of $N(\lambda)$. Using equation (3.22) as the frequency equation, and an IBM 360 model 75 digital computer, a very large number of frequencies were calculated and the number occurring below certain specific dimensionless frequencies was obtained. The result of this numerical counting procedure was then put in the form $N(\lambda) \frac{\pi}{\sin\psi\,(1-\alpha_1)}$. The number of circumferential and longitudinal number of waves was increased until the count in each interval terminated. A discussion of the computer program for this procedure appears in Appendix 8.4. The results of this procedure were in excellent agreement with the k-space integration results. Therefore the omission of a portion of the k-space in this case appears to be justified. It should be pointed out that the portion of the k-space which was omitted from the integration is unbounded.

3.3.4 Numerical Approximations

Careful examination of Figures 3.14 through 3.19 indicates the normalized number of eigenvalue and eigenvalue density curves are straight lines on log-log paper except near values associated with the first few resonant frequencies. In light of this, equations (3.27) and (3.28) may be approximated by the following expressions:

$$N(\lambda)\ \frac{\pi}{\sin\psi\,(1-\alpha_1)}\ \frac{h(1-\alpha_1)^{1/4}}{L(\tan\psi)^{1/2}} = 0.876\lambda^{3/2} \qquad (3.29)$$

$$n(\lambda)\ \frac{\pi}{\sin\psi\,(1-\alpha_1)}\ \frac{h(1-\alpha_1)^{1/4}}{L(\tan\psi)^{1/2}} = 1.31\lambda^{1/2}\ . \qquad (3.30)$$

It should be remembered that these equations only apply below the lower ring frequency due to the assumption made in the derivation of frequency equation two. The expressions also do not hold in the vicinity of the first few resonant frequencies ($N(\lambda) \approx 1$). This is to be expected since the concept of eigenvalue density has little or no meaning in this region. As a form of check, it should be noted that although expressions (3.29) and (3.30) were obtained independently of each other from the figures, equation (3.30) is indeed the derivative of equation (3.29) with respect to dimensionless frequency as it should be.

3.4 Summary of Analytical Results

The final analytic expressions for the cumulative number of eigenvalues $N(\lambda)$ and the eigenvalue density $n(\lambda)$ above the upper ring frequency and below the lower ring frequency have been collected in

Table 3.1 for easy reference. A graphical representation of the final equations is also given in Figures 3.20 and 3.21.

In preparing Figures 3.20 and 3.21 it was assumed that the $(1-\alpha_1)$ term in each equation was approximately equal. This was done in order to make it possible for the results to be presented graphically with only one parameter, that being the cone angle. The curves for the dimensionless frequency less than the lower ring frequency are shown up to the lower ring frequency for several cone angles. The lower ring frequency is shown as a vertical dotted line for each cone angle. The minimum upper ring frequency possible is also indicated by the same dotted line. This corresponds to the case for $\alpha_1 = 1$, or a completely truncated cone.

It would seem appropriate at this time to give some explanation as to how Figures 3.20 and 3.21 might be used in actual practice for the determination of the cumulative number of eigenvalue and eigenvalue density corresponding to a given frequency. First of all the dimensionless frequency corresponding to the frequency of interest would be calculated and located on the axis of Figures 3.20 and 3.21. Next the upper and lower ring frequencies corresponding to the cone geometry being investigated would be determined and noted on the graphs. There are now three possible cases, the dimensionless frequency of interest is either above the upper ring frequency, below the lower ring frequency, or between the two.

If the dimensionless frequency of interest is above the upper ring frequency the procedure is simple. The desired values are merely read off the curve corresponding to the solution above the upper ring frequency.

Table 3.1 Summary of the theoretical results for the number of eigenvalues and the eigenvalue density

---

Below the lower ring frequency: $\lambda < \frac{1}{\sin \psi}$

Cumulative number of eigenvalues

$$N(\lambda) \approx 0.876 \left[\frac{L \sin \psi (\tan \psi)^{1/2} (1-\alpha_1)^{3/4}}{\pi h}\right] \lambda^{3/2}$$

Eigenvalue density

$$n(\lambda) \approx 1.31 \left[\frac{L \sin \psi (\tan \psi)^{1/2} (1-\alpha_1)^{3/4}}{\pi h}\right] \lambda^{1/2}$$

Above the upper ring frequency: $\lambda > \frac{1}{\alpha_1 \sin \psi}$

Cumulative number of eigenvalues

$$N(\lambda) \approx 2.0 \left[\frac{L \sin \psi (1-\alpha_1)^{4/5}}{\pi h}\right] \lambda$$

Eigenvalue density

$$n(\lambda) \approx 2.0 \left[\frac{L \sin \psi (1-\alpha_1)^{4/5}}{\pi h}\right]$$

where:

$$\lambda^2 = \omega^2 \frac{\gamma L^2}{g_c E} \quad \text{or} \quad \lambda \approx \omega \frac{L}{C_L} \quad .$$

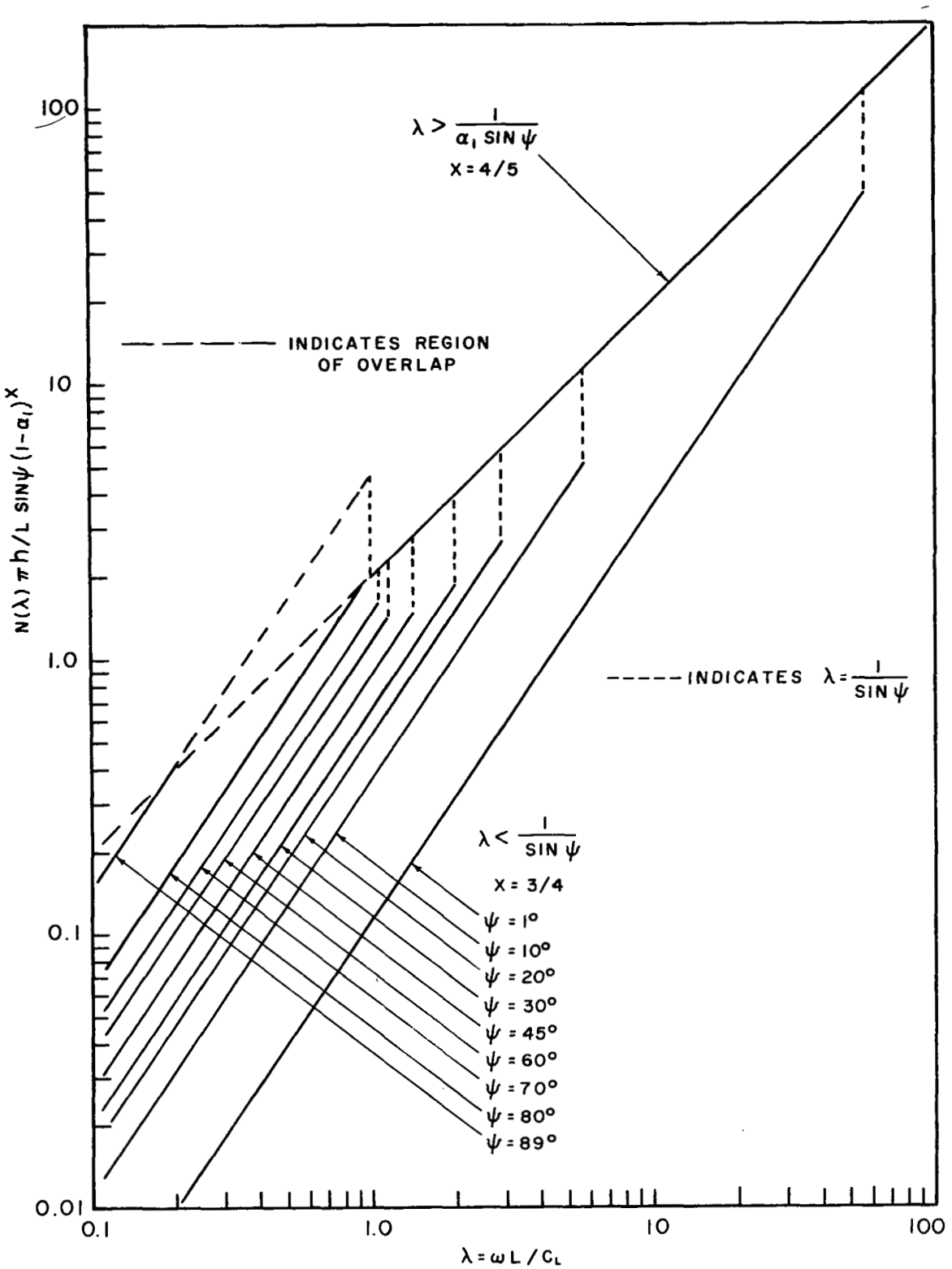

FIGURE 3.20 THEORETICAL NUMBER OF EIGENVALUE CURVES

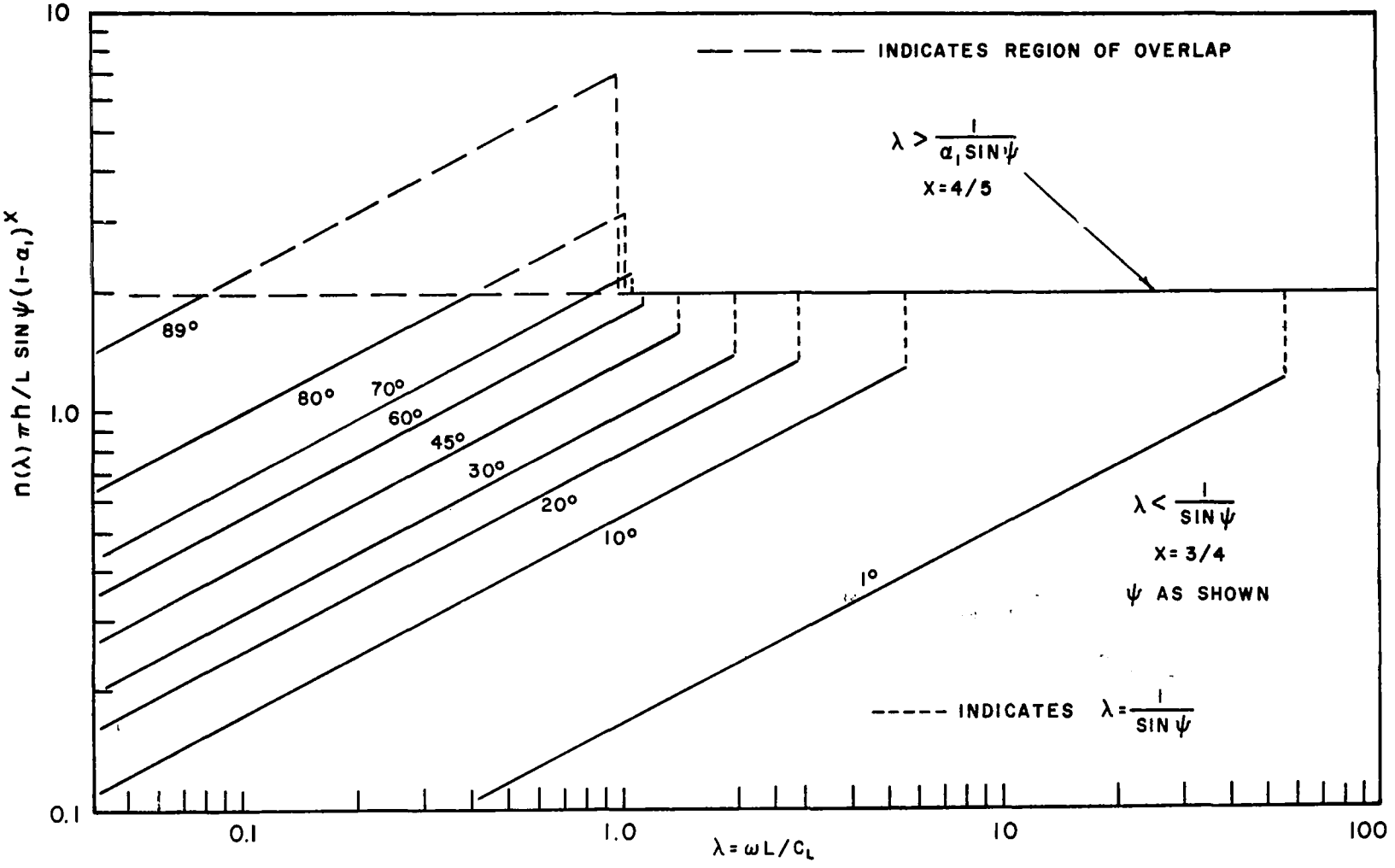

FIGURE 3.21 THEORETICAL EIGENVALUE DENSITY CURVES

If the dimensionless frequency of interest is below the lower ring frequency the procedure is again fairly simple. The desired values are read of the curve corresponding to the solution below the lower ring frequency having the appropriate cone angle. In this case the value of $N(\lambda)$ obtained should be checked to be sure it is not near unity or below since the results have little meaning in this region.

Finally, if the dimensionless frequency of interest is between the upper and lower ring frequencies the procedure is not quite as straightforward. If a good deal of accuracy is required it will be necessary to compute the desired values in the same manner as was used in section 3.2 to obtain the results shown in Figures 3.3 through 3.5. However, if only a reasonable estimate is needed the following approximation may be used. The value corresponding to the lower ring frequency should be located, and the value corresponding to the upper ring frequency should also be located. The value desired may then be read off a straight line drawn between these two points, as the resulting curve is a fair approximation of what happens in this transition region.

There are two major exceptions which should be indicated concerning the results presented in Table 3.1 and Figures 3.20 and 3.21. First of all, for cones with large cone angles the solution does not hold, up to the lower ring frequency. In fact the above upper ring frequency solution begins to apply even before the lower ring frequency is reached. As a general rule, when working with cones with large cone angles the values corresponding to both the solution above the upper ring frequency and the solution below the lower ring frequency

should be calculated and the minimum value used. This type of behavior is clearly indicated in Figure 3.6.

The second major exception applies to cones with little or no truncation. In this case the value of the upper ring frequency is infinite or very high, and the above upper ring frequency solution is reached long before the upper ring frequency. In this case a value for the upper ring frequency of no more than ten times the lower ring frequency should be used as a sort of artificial upper ring frequency. This type of behavior is clearly indicated in Figure 3.8.

4. EXPERIMENTAL PROGRAM

4.1 Objective

In order to provide a comparison with the analytical results of this paper, an experimental investigation of the cumulative number of eigenvalues was conducted. During this investigation two different conical shells were subjected to sinusoidal excitation over a wide range of frequencies, the object being to physically count the number of resonant modes contained within the frequency range covered. Once a count was obtained the results were nondimensionalized and compared with the analytical results obtained in section 3.

4.2 Experimental Apparatus

The two conical shells used in the investigation are fully described in Table 4.1. The cones used were formed of stainless steel sheet and butt welded at the seams. The instrumentation used in the investigation is shown schematically in Figure 4.1. The instrumentation consisted basically of a signal generator equipped with a sweep drive, a power amplifier, a preamplifier, a narrow band analyzer, and a level recorder.

The sinusoidal signal generated by the oscillator is fed to a power amplifier, and from there to the electromagnetic shaker. The shaker is attached rigidly to the cone and serves as the source of excitation. The transducers used to record the cone response to this excitation consisted of an accelerometer and a microphone which were used alternately. The signal from one of the transducers is then fed by way of a cathode follower type preamplifier to the narrow band

Table 4.1 Data on cones used in experimental investigations

	CONE 1	CONE 2
Cone Angle (ψ)	8.667°	12.385°
Thickness (h)	0.06 in.	0.06 in.
Length (L)	59.7 in.	40.45 in.
Truncation Ratio (α_1)	0.3886	0.3881
Material	304 Stainless	304 Stainless
Dimensionless Frequency Multiplier	524.04 Hz/λ	773.43 Hz/λ
Lower Dimensionless Ring Frequency	6.64	4.66
Upper Dimensionless Ring Frequency	17.08	12.01

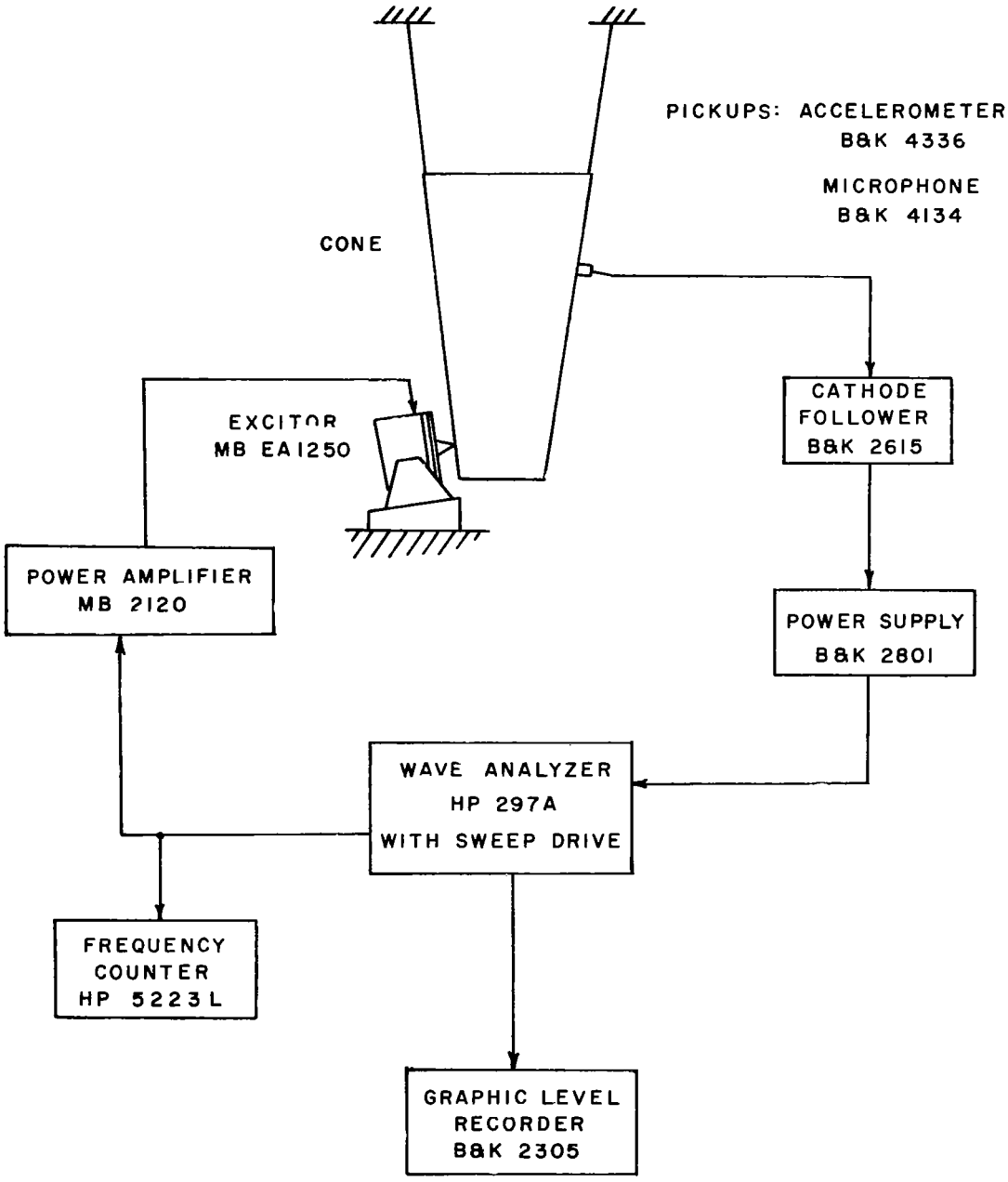

FIGURE 4.1 ARRANGEMENT OF TEST INSTRUMENTS

analyzer. The narrow band analyzer which, in the instrument used, is incorporated as part of the signal generator had the center band frequency of the continuously variable filter ($\pm$ 3 Hz of center) tuned to correspond to the signal being generated and used to excite the conical shell. In this manner only the component of the signal picked up by the transducer corresponding to the excitation frequency was retained and fed to the level recorder. In this way only the cone response to the generated frequency was recorded thus eliminating the effects of harmonics, reverberations, and stray noise. Photographs of various aspects of the experimental program are shown in Figures 4.2 through 4.6.

4.3 Collection of Data

The conical shell being excited is suspended vertically so that a free-free type boundary condition may be approximated. The exciter is then attached to the cone at a point near but not at the bottom edge of the cone. The cone was suspended with one end up, and then with the other end up so that it could be determined to what extent the end at which the cone was excited affected the experimental results. Data was taken with both cones in the two configurations referred to above. As mentioned previously two types of transducers are used: a two gram piezoelectric accelerometer, and a one-half inch capacitive type microphone. In the case of the accelerometer, attachment to the cone surface was accomplished with a hard wax so that no alterations were made on the surface of the shell. In the case of the microphone, it was placed as close to the shell surface as possible

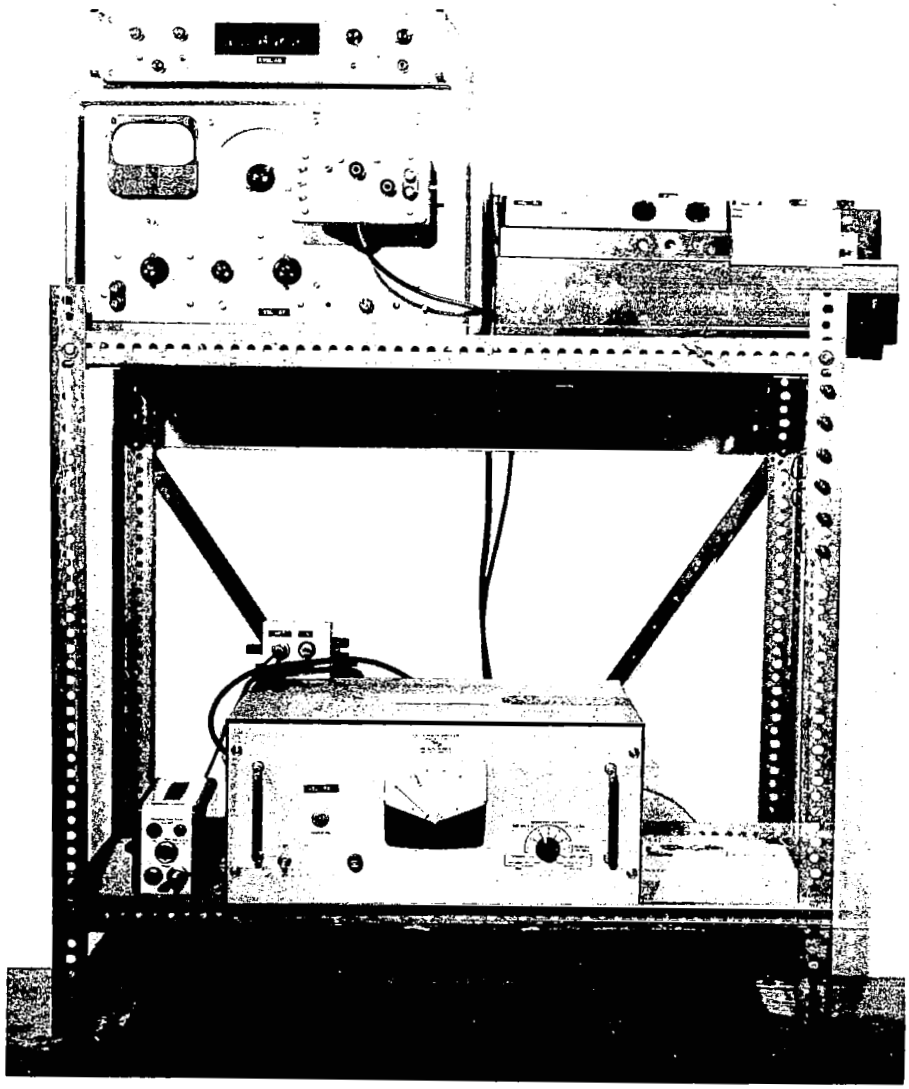

FIGURE 4.2 INSTRUMENTATION USED DURING THE EXPERIMENTAL INVESTIGATION

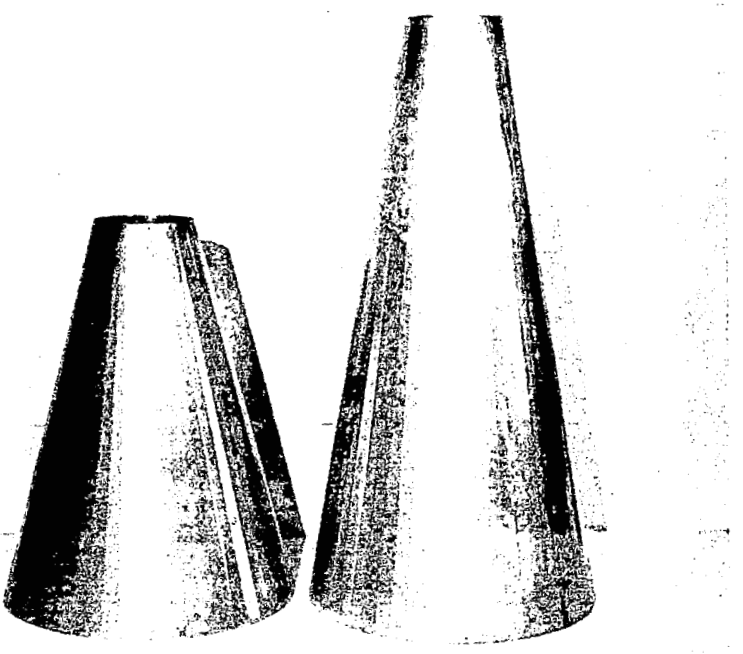

FIGURE 4.3 CONES ONE AND TWO USED IN EXPERIMENTS

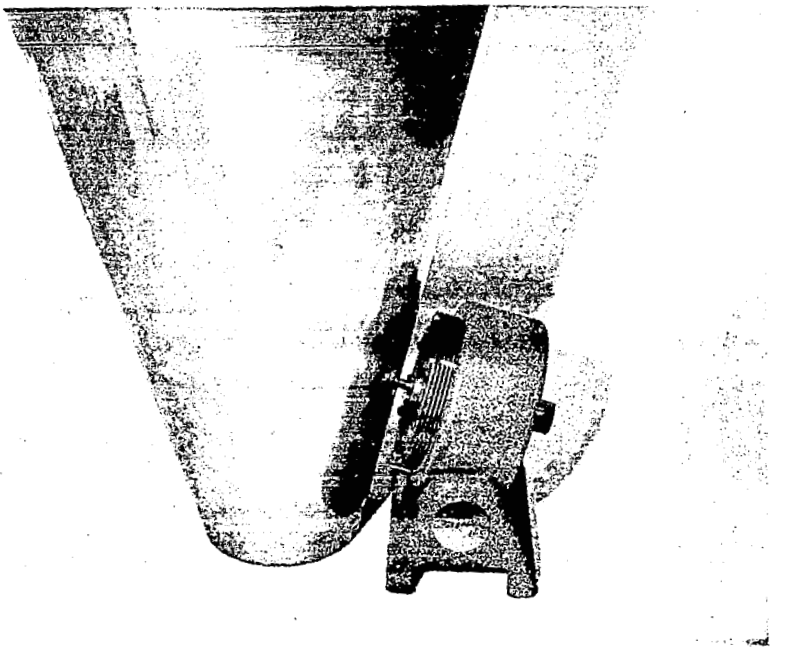

FIGURE 4.4 ELECTROMAGNETIC SHAKER TO CONE CONNECTION

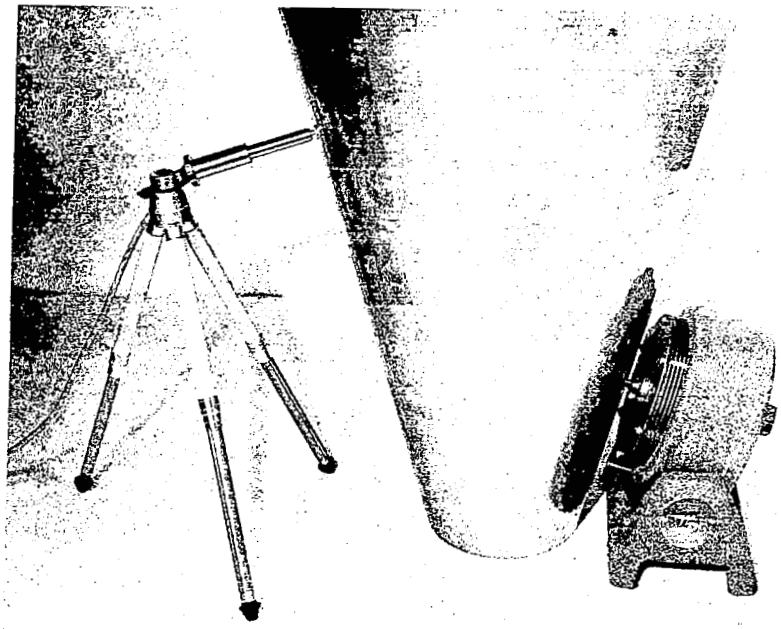

FIGURE 4.5 CONE IN APEX DOWN POSITION WITH MICROPHONE

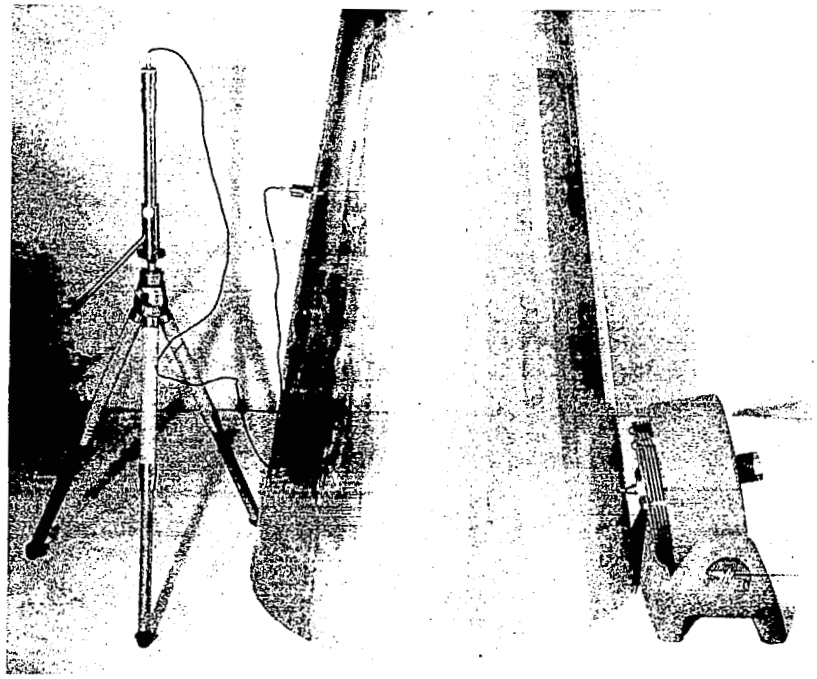

FIGURE 4.6 CONE IN APEX UP POSITION WITH ACCELEROMETER

without any possibility of the microphone touching the shell surface during a data run. A distance of approximately three sixteenths of an inch was found to be satisfactory for this purpose.

Data was taken using both transducers at three different positions on the cone surface. The recording points were picked in a fairly arbitrary manner with care being taken to avoid the edges of the cone, seams, and connection points for the exciter and the suspension system. Twelve runs were made in all for each cone using all the combinations mentioned above of transducer type, transducer location, and cone orientation. Each run consisted of a slow sweep of the frequency band from one hundred Hz (below the first resonance of either cone) to approximately six-thousand Hz. The magnitude of the response of the transducer was recorded continuously and the paper used was frequency calibrated. Samples of a portion of two of the chart records obtained are shown in Figures 4.7 and 4.8.

4.4 Analysis of Data

Once the chart records for all data runs were obtained they were broken up into bands corresponding to specific dimensionless frequency intervals. The number of peaks corresponding to resonant frequencies occurring in each band was counted and tabulated. The results of this process appear in absolute and in non-dimensional form in Tables 4.2 through 4.13. The results pertaining to each cone were then lumped together and the arithmetic average, as well as the absolute maximum and minimum for each dimensionless frequency band, is shown in Table 4.14. The final results for each cone are shown compared with the

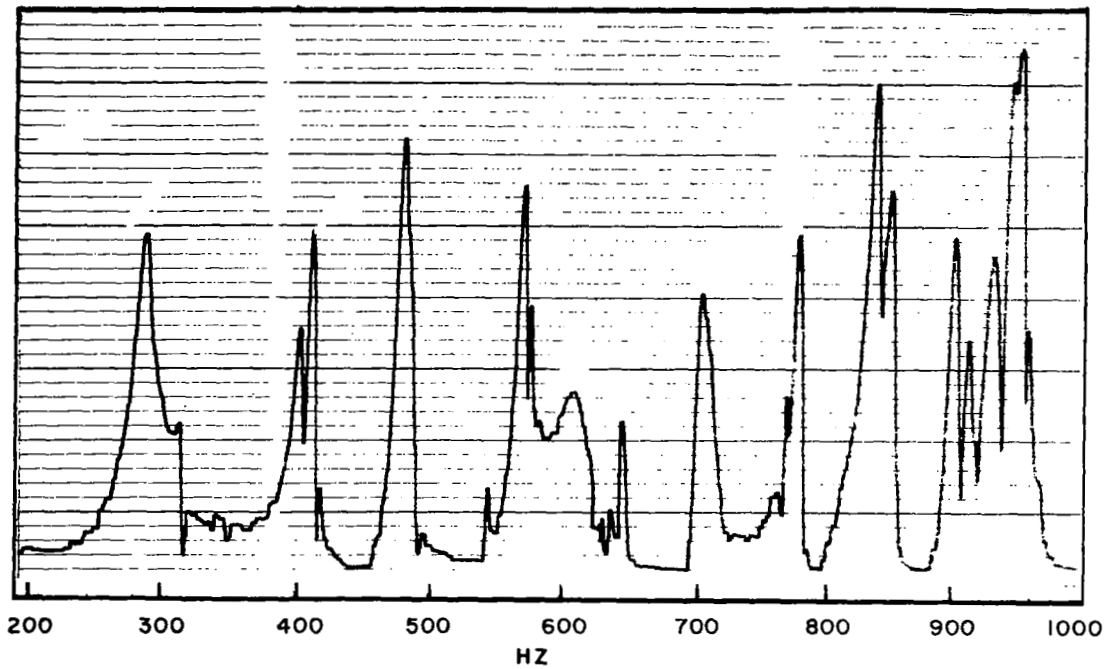

FIGURE 4.7 SAMPLE CHART RECORD FROM RUN 15

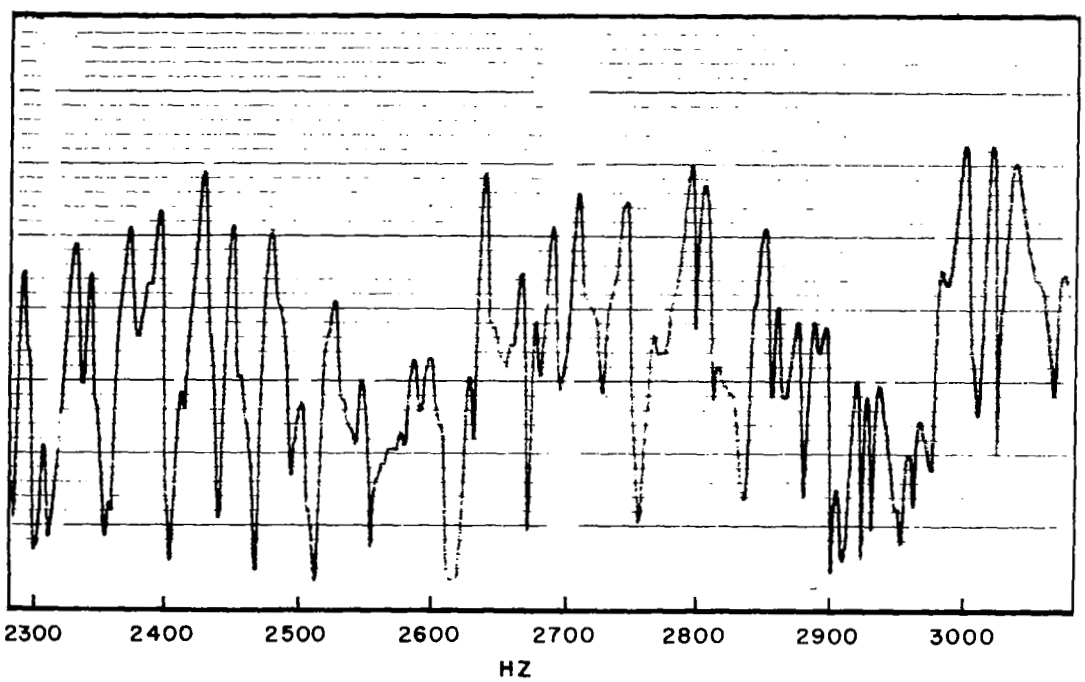

FIGURE 4.8 SAMPLE CHART RECORD FROM RUN 24

Table 4.2 Experimental data for runs 1 and 2

	Run No. 1			Run No. 2		
Cone No.	1			1		
Orientation	Apex Down			Apex Up		
Pickup	Microphone			Microphone		
Position No.	1			1		
λ	ΔN	N	$N \frac{\pi 10^{-2}}{\sin \psi (1-\alpha_1)}$	ΔN	N	$N \frac{\pi 10^{-2}}{\sin \psi (1-\alpha_1)}$
0.5	3	3	1.025	3	3	1.025
1.0	5	8	2.74	5	8	2.74
1.5	10	18	6.15	16	24	8.20
2.0	13	31	10.6	14	38	13.0
2.5	11	42	14.3	13	51	17.4
3.0	19	61	20.8	18	69	23.6
3.5	24	85	29.0	21	90	30.8
4.0	21	106	39.7	17	107	36.6
4.5	23	129	44.1	19	126	43.0
5.0	21	150	51.3	19	145	49.5
6.0	43	193	66.0	44	189	64.5
7.0	37	230	78.6	43	232	79.3
8.0	43	273	93.3	42	274	93.7
9.0	46	319	109.0	45	319	109.0
10.0	40	359	123.0	44	363	124.0

Table 4.3 Experimental data for runs 3 and 4

	Run No. 3			Run No. 4		
Cone No.	1			1		
Orientation	Apex Down			Apex Up		
Pickup	Accelerometer			Accelerometer		
Position No.	1			1		
λ	ΔN	N	$N \frac{\pi\ 10^{-2}}{\sin\psi\ (1-\alpha_1)}$	ΔN	N	$N \frac{\pi\ 10^{-2}}{\sin\psi\ (1-\alpha_1)}$
0.5	2	2	0.685	3	3	1.025
1.0	5	7	2.39	5	8	2.74
1.5	10	17	5.80	14	22	7.41
2.0	13	30	10.2	14	36	12.3
2.5	15	45	15.4	16	52	17.8
3.0	15	60	20.5	17	69	23.6
3.5	19	79	27.0	20	89	30.4
4.0	20	99	33.8	19	108	37.0
4.5	19	118	40.4	21	129	44.1
5.0	22	140	47.9	19	148	50.5
6.0	39	179	61.1	43	191	65.3
7.0	38	217	74.1	37	228	78.0
8.0	37	254	86.9	40	268	91.5
9.0	38	292	99.9	37	305	104.0
10.0	39	331	113.0	37	342	117.0

Table 4.4 Experimental data for runs 5 and 6

	Run No. 5			Run No. 6		
Cone No.	1			1		
Orientation	Apex Down			Apex Up		
Pickup	Microphone			Microphone		
Position No.	2			2		
λ	ΔN	N	$N \frac{\pi\ 10^{-2}}{\sin\psi\ (1-\alpha_1)}$	ΔN	N	$N \frac{\pi\ 10^{-2}}{\sin\psi\ (1-\alpha_1)}$
0.5	2	2	0.685	3	3	1.025
1.0	6	8	2.74	5	8	2.74
1.5	8	16	5.46	13	21	7.18
2.0	14	30	10.3	12	33	11.3
2.5	15	45	15.4	16	49	16.8
3.0	18	63	21.6	20	69	23.6
3.5	17	80	27.4	20	89	30.4
4.0	20	100	34.2	22	111	38.0
4.5	20	120	41.0	21	132	45.1
5.0	20	140	47.9	19	151	51.6
6.0	39	179	61.1	44	195	66.6
7.0	43	222	75.9	40	235	80.4
8.0	45	267	91.2	42	277	94.6
9.0	40	307	105.0	39	316	108.0
10.0	41	348	119.0	46	362	124.0

Table 4.5 Experimental data for runs 7 and 8

	Run No. 7			Run No. 8		
Cone No.	1			1		
Orientation	Apex Down			Apex Up		
Pickup	Accelerometer			Accelerometer		
Position No.	2			2		
λ	ΔN	N	$N \frac{\pi 10^{-2}}{\sin \psi (1-\alpha_1)}$	ΔN	N	$N \frac{\pi 10^{-2}}{\sin \psi (1-\alpha_1)}$
0.5	2	2	0.685	2	2	0.685
1.0	5	7	2.39	5	7	2.39
1.5	7	14	4.79	13	20	6.84
2.0	12	26	8.89	12	32	10.9
2.5	13	39	13.3	16	48	16.4
3.0	13	52	17.8	17	65	22.2
3.5	20	72	24.6	20	85	29.0
4.0	21	93	31.6	20	105	35.9
4.5	18	111	38.0	19	124	42.5
5.0	16	127	43.5	20	144	49.3
6.0	43	170	58.1	40	184	63.0
7.0	36	206	70.5	38	222	76.0
8.0	38	244	83.4	42	264	90.4
9.0	36	280	95.6	35	299	102.0
10.0	40	320	109.0	35	334	114.0

Table 4.6 Experimental data for runs 9 and 10

	Run No. 9			Run No. 10		
Cone No.	1			1		
Orientation	Apex Up			Apex Down		
Pickup	Microphone			Microphone		
Position No.	3			3		
λ	ΔN	N	$N \frac{\pi\ 10^{-2}}{\sin\psi\ (1-\alpha_1)}$	ΔN	N	$N \frac{\pi\ 10^{-2}}{\sin\psi\ (1-\alpha_1)}$
0.5	3	3	1.025	3	3	1.025
1.0	4	7	2.39	4	7	2.39
1.5	7	14	4.79	9	16	5.47
2.0	15	29	9.91	12	28	9.57
2.5	12	41	14.0	15	43	14.7
3.0	13	54	18.5	21	64	21.9
3.5	21	75	25.6	19	83	28.4
4.0	20	95	32.5	20	103	35.2
4.5	20	115	39.3	21	124	42.5
5.0	21	136	46.9	21	145	49.5
6.0	42	178	60.9	48	193	66.0
7.0	43	221	75.5	43	236	80.6
8.0	40	261	89.1	44	280	95.6
9.0	44	305	104.0	44	324	112.0
10.0	33	338	115.0	37	361	123.0

Table 4.7 Experimental data for runs 11 and 12

	Run No. 11			Run No. 12		
Cone No.	1			1		
Orientation	Apex Down			Apex Up		
Pickup	Accelerometer			Accelerometer		
Position No.	1			1		
λ	ΔN	N	$N \frac{\pi\ 10^{-2}}{\sin\psi\ (1-\alpha_1)}$	ΔN	N	$N \frac{\pi\ 10^{-2}}{\sin\psi\ (1-\alpha_1)}$
0.5	3	3	1.025	3	3	1.025
1.0	4	7	2.39	4	7	2.39
1.5	8	15	5.14	10	17	5.81
2.0	14	29	9.91	10	27	9.22
2.5	13	42	14.4	12	39	13.3
3.0	15	57	19.5	18	57	19.5
3.5	20	77	26.4	20	77	26.4
4.0	17	94	32.3	18	95	32.5
4.5	16	110	37.6	21	116	39.7
5.0	18	128	43.8	18	134	45.9
6.0	39	167	57.0	45	179	61.1
7.0	31	198	67.7	30	209	71.5
8.0	40	238	81.5	41	250	85.5
9.0	33	271	92.6	41	291	99.5
10.0	37	308	105.0	37	328	112.0

Table 4.8 Experimental data for runs 13 and 14

	Run No. 13			Run No. 14		
Cone No.	2			2		
Orientation	Apex Down			Apex Up		
Pickup	Microphone			Microphone		
Position No.	1			1		
λ	ΔN	N	$N \frac{\pi\ 10^{-2}}{\sin\psi\ (1-\alpha_1)}$	ΔN	N	$N \frac{\pi\ 10^{-2}}{\sin\psi\ (1-\alpha_1)}$
0.5	3	3	0.717	4	4	0.955
1.0	5	8	1.91	9	13	3.11
1.5	12	20	4.78	10	23	5.50
2.0	10	30	7.17	19	42	10.0
2.5	15	45	10.8	18	60	14.3
3.0	16	61	14.6	22	82	19.6
3.5	20	81	19.3	21	103	24.6
4.0	26	107	25.6	26	129	30.8
4.5	27	134	32.0	25	154	36.8
5.0	24	158	37.8	28	182	43.5
6.0	71	229	54.8	63	245	58.5
7.0	61	290	69.3	55	300	71.6
8.0	60	350	83.6	56	356	85.0
9.0	-	-	-	-	-	-
10.0	-	-	-	-	-	-

Table 4.9 Experimental data for runs 15 and 16

	Run No. 15			Run No. 16		
Cone No.	2			2		
Orientation	Apex Down			Apex Up		
Pickup	Accelerometer			Accelerometer		
Position No.	1			1		
λ	ΔN	N	$N \frac{\pi 10^{-2}}{\sin \psi (1-\alpha_1)}$	ΔN	N	$N \frac{\pi 10^{-2}}{\sin \psi (1-\alpha_1)}$
0.5	2	2	0.478	3	3	0.717
1.0	6	8	1.91	7	10	2.39
1.5	11	19	4.55	11	21	5.02
2.0	10	29	6.93	13	34	8.13
2.5	18	47	11.5	18	52	12.4
3.0	14	61	14.6	16	68	16.2
3.5	18	79	18.9	19	87	20.8
4.0	23	102	24.4	23	110	26.3
4.5	23	125	29.9	22	132	31.6
5.0	22	147	35.2	25	157	37.5
6.0	56	203	48.5	53	210	50.2
7.0	49	252	60.3	46	256	61.1
8.0	50	302	72.1	38	294	70.3
9.0	-	-	-	-	-	-
10.0	-	-	-	-	-	-

Table 4.10 Experimental data for runs 17 and 18

	Run No. 17			Run No. 18		
Cone No.	2			2		
Orientation	Apex Down			Apex Up		
Pickup	Microphone			Microphone		
Position No.	2			2		
λ	ΔN	N	$N \frac{\pi 10^{-2}}{\sin \psi (1-\alpha_1)}$	ΔN	N	$N \frac{\pi 10^{-2}}{\sin \psi (1-\alpha_1)}$
0.5	5	5	1.20	3	3	0.717
1.0	7	12	2.87	7	10	2.39
1.5	10	22	5.26	9	19	4.54
2.0	18	40	9.56	16	35	8.36
2.5	18	58	13.9	18	53	12.7
3.0	17	75	17.9	22	75	17.9
3.5	14	89	21.2	23	98	23.4
4.0	25	114	27.2	26	124	29.6
4.5	16	130	31.1	22	146	34.9
5.0	30	160	38.2	23	169	40.4
6.0	69	229	54.8	62	231	55.3
7.0	67	296	70.8	63	294	70.3
8.0	66	362	86.5	66	360	86.0
9.0	-	-	-	-	-	-
10.0	-	-	-	-	-	-

Table 4.11 Experimental data for runs 19 and 20

	Run No. 19			Run No. 20		
Cone No.	2			2		
Orientation	Apex Down			Apex Up		
Pickup	Accelerometer			Accelerometer		
Position No.	2			2		
λ	ΔN	N	$N \frac{\pi\ 10^{-2}}{\sin\psi\ (1-\alpha_1)}$	ΔN	N	$N \frac{\pi\ 10^{-2}}{\sin\psi\ (1-\alpha_1)}$
0.5	4	4	0.955	3	3	0.717
1.0	8	12	2.87	6	9	2.15
1.5	10	22	5.25	10	19	4.55
2.0	9	31	7.41	16	35	8.36
2.5	17	48	11.5	17	52	12.4
3.0	16	64	15.3	20	72	17.2
3.5	18	82	19.6	20	92	22.0
4.0	22	104	24.9	23	115	27.5
4.5	16	120	28.7	22	137	32.8
5.0	25	145	34.7	26	163	39.0
6.0	51	196	46.9	51	214	51.1
7.0	53	249	59.5	53	267	63.9
8.0	55	304	72.6	43	310	74.0
9.0	-	-	-	-	-	-
10.0	-	-	-	-	-	-

Table 4.12 Experimental data for runs 21 and 22

	Run No. 21			Run No. 22		
Cone No.	2			2		
Orientation	Apex Down			Apex Up		
Pickup	Microphone			Microphone		
Position No.	3			3		
λ	ΔN	N	$N \frac{\pi\ 10^{-2}}{\sin\psi\ (1-\alpha_1)}$	ΔN	N	$N \frac{\pi\ 10^{-2}}{\sin\psi\ (1-\alpha_1)}$
0.5	3	3	0.717	3	3	0.717
1.0	5	8	1.91	5	8	1.91
1.5	13	21	5.01	10	18	4.30
2.0	14	35	8.36	20	38	9.08
2.5	18	53	12.7	22	60	14.3
3.0	19	72	17.2	23	83	19.9
3.5	22	94	22.5	24	107	25.6
4.0	25	119	28.4	25	132	31.6
4.5	20	139	33.2	24	156	37.3
5.0	27	166	39.7	32	188	45.0
6.0	63	229	54.7	63	251	60.0
7.0	65	294	70.3	61	312	74.5
8.0	58	352	84.0	52	364	87.0
9.0	-	-	-	-	-	-
10.0	-	-	-	-	-	-

Table 4.13 Experimental data for runs 23 and 24

	Run No. 23			Run No. 24		
Cone No.	2			2		
Orientation	Apex Down			Apex Up		
Pickup	Accelerometer			Accelerometer		
Position No.	3			3		
λ	ΔN	N	$N \frac{\pi\ 10^{-2}}{\sin\Psi\ (1-\alpha_1)}$	ΔN	N	$N \frac{\pi\ 10^{-2}}{\sin\Psi\ (1-\alpha_1)}$
0.5	3	3	0.717	3	3	0.717
1.0	5	8	1.91	5	8	1.91
1.5	11	19	4.54	11	19	4.54
2.0	11	30	7.17	15	34	8.13
2.5	22	52	12.4	21	55	13.1
3.0	16	68	16.2	18	73	17.5
3.5	18	86	20.6	21	94	22.4
4.0	22	108	25.8	23	117	28.0
4.5	21	129	30.8	19	136	32.5
5.0	25	154	36.8	26	162	38.8
6.0	55	209	50.0	55	217	51.9
7.0	54	263	62.9	41	258	61.6
8.0	43	306	73.1	42	300	71.7
9.0	-	-	-	-	-	-
10.0	-	-	-	-	-	-

Table 4.14 Tabulation of experimental data in reduced form

$$N(\lambda) \frac{\pi}{\sin \psi (1-\alpha_1)} \times 10^{-2}$$

λ	CONE 1			CONE 2		
	min.	average	max.	min.	average	max.
0.5	0.685	0.912	1.03	0.478	0.777	1.20
1.0	2.39	2.54	2.74	1.91	2.27	3.11
1.5	4.79	6.09	8.20	4.30	4.82	5.50
2.0	8.89	10.5	13.0	7.17	8.23	10.0
2.5	13.3	15.3	17.8	10.8	12.7	14.3
3.0	17.8	21.1	23.6	14.6	17.0	19.9
3.5	24.6	27.9	30.8	18.9	21.7	25.6
4.0	31.6	34.9	39.7	24.4	27.5	31.6
4.5	38.0	41.4	45.1	28.7	32.6	37.3
5.0	43.5	48.1	51.6	34.7	39.0	45.3
6.0	57.0	62.6	66.6	46.9	53.1	60.0
7.0	67.7	75.7	80.6	59.5	66.3	74.5
8.0	81.5	89.7	95.6	70.3	78.8	87.0
9.0	92.6	103.0	112.0			
10.0	105.0	117.0	124.0			

analytical results in Figures 4.9 and 4.10. Analytical results corresponding to both frequency equations are shown.

Agreement between the analytical and the experimental results appears to be very good. Data was not taken beyond six thousand Hz. because beyond this point a good deal of overlap between modes appeared to be present. This caused the resonant peaks to become less pronounced on the chart record as the frequency was increased. This overlapping made it difficult to count the number of resonant peaks in the last two or three frequency bands analyzed in the case of each cone, and probably caused the values obtained experimentally in these bands to be somewhat lower than would otherwise be the case.

It should be mentioned that the data runs taken using the accelerometer as a pickup were consistently lower overall than those obtained using the microphone as the transducer. This is as would be expected, since the accelerometer picks up only the response of the cone at the point at which it is attached, whereas the microphone would tend to pick up the response of the cone over a broader area. This would tend to make the microphone slightly less sensitive to position, and would decrease the possibility of missing a mode if the transducer were located on or near a nodal line for some of the modes present in the conical shell.

The position of the transducer on the shell surface, and the orientation of the cone seemed to have very little effect on the overall count of resonant frequencies obtained. However, some differences were noted in the shape and magnitude of specific resonant peaks recorded. Also, the first few modes seemed to be affected to

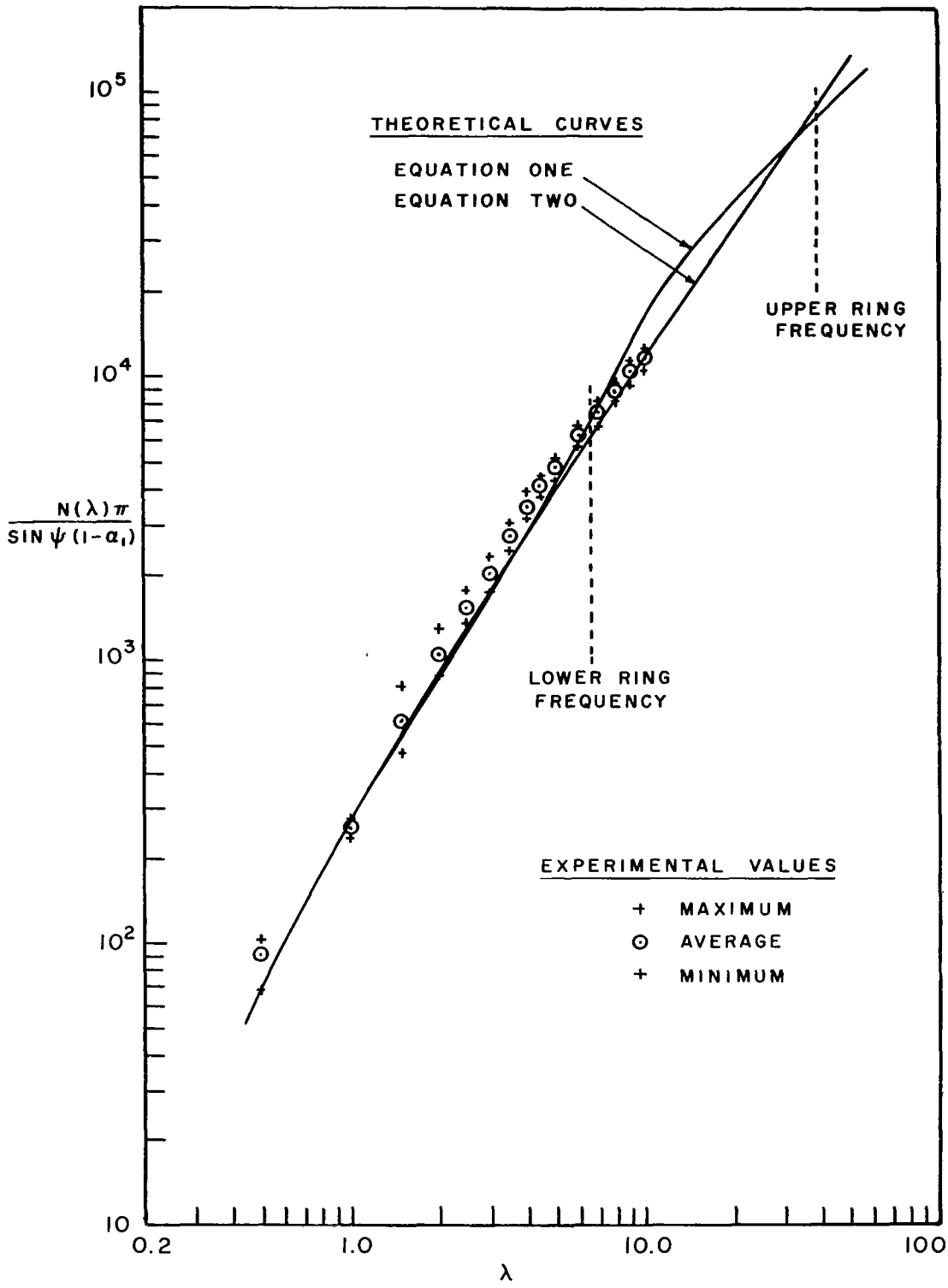

FIGURE 4.9 EXPERIMENTAL RESULTS FOR CONE ONE

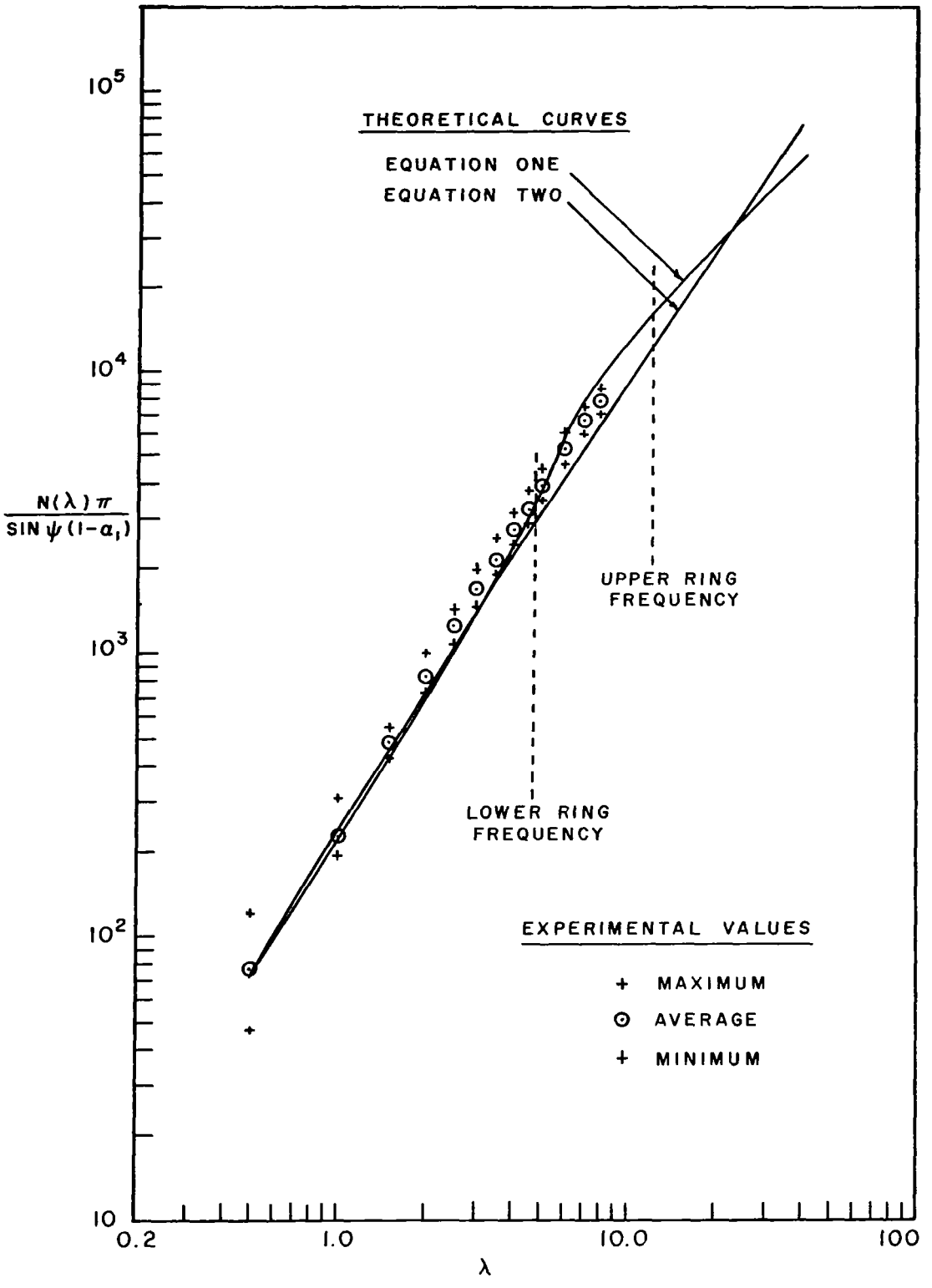

FIGURE 4.10 EXPERIMENTAL RESULTS FOR CONE TWO

some extent with respect to the frequency at which they occurred. This would be expected since changes in the orientation of the cone would affect the boundary conditions slightly. It has already been noted in section 2 that changes in boundary condition will effect the first few resonant modes slightly, but will have little effect on higher modes.

5. SUMMARY AND CONCLUSIONS

The results of the analytical determination of expressions for the cumulative number of eigenvalues up to a given dimensionless frequency, and the modal or eigenvalue density with respect to dimensionless frequency are given in Table 3.1. The results have also been presented in graphical form in Figures 3.20 and 3.21. There are certain limitations regarding the results obtained which should be noted before any attempt is made to use them to predice actual values.

First of all the curves and equations are invalid for cones with large cone angles in that the shell goes into a so called plate mode (above upper ring frequency solution) even before the lower ring frequency is reached. Secondly the results are invalid for cones with little or no truncation in that the shell goes into the plate mode long before the upper ring frequency is reached (but not before the lower ring frequency except as noted above). Finally it should be remembered that the expressions obtained do not give explicit information regarding the frequency band between the upper and lower ring frequencies, although fair approximations for the values in this region may be obtained using the techniques described in section 3.4.

Aside from the exceptions noted above, the desired expressions for the cumulative number of eigenvalues and the eigenvalue density of a thin conical shell have been obtained. The expressions presented in Table 3.1 have been normalized in such a way as to make them independent of the cone geometry. Figures 3.20 and 3.21 have been handled in a similar manner except for the fact that the cone angle

appears as a parameter for the results below the lower ring frequency. The upper ring frequency has not been indicated in the figures since it is a function of the truncation ratio of the cone and may vary anywhere from the lower ring frequency for a completely truncated cone to infinity for a closed cone.

The results of the companion experimental investigation which was undertaken are presented in Figures 4.9 and 4.10. Besides the experimental values for the cumulative number of eigenvalues, the two analytical curves based on the two frequency equations are also shown in these figures. Very good agreement is obtained between the experimental results and the analytical curves, although the experimental values appear to drop off for the higher frequencies investigated. This is due to an overlapping of resonant modes rather than an actual drop off in the number of eigenvalues. This is also the reason data was not obtained for frequencies higher than those given.

The values for the upper and lower ring frequencies are also noted in the figures corresponding to each cone. It is seen that the data taken only extended a short way into the region between the two ring frequencies. Therefore the experimental investigation served only as a check of the analytical results below the lower ring frequency. Due to the overlapping of modes in this frequency domain it was not possible to obtain data above the upper ring frequency, hence the transition of the conical shell into a plate mode was not detected experimentally. However it would seem reasonable that this would be the case, as indicated by the results based on frequency equation one.

It is concluded that the experimental results correlate with the results of the two analytical solutions in the region where the two approaches predict essentially the same values for the cumulative number of eigenvalues, that is below the lower ring frequency. Above the upper ring frequency data was not obtained, but since frequency equation two is known to be invalid in this range, and since it is expected that at high frequencies the shell would exhibit a plate mode, the results in this range based on frequency equation one are assumed to be valid.

In conclusion, it may be stated that expressions have been obtained for the cumulative number of modes, and for the modal density above the upper ring frequency and below the lower ring frequency. The results are in agreement with experimental results below the lower ring frequency and behave as would be expected above the upper ring frequency. Between the upper and lower ring frequencies a procedure by which the desired values may be approximated in an accurate manner has also been given.

6. RECOMMENDATIONS

Based on the frequency equations presented in this paper, expressions for the cumulative number of eigenvalues and the eigenvalue density of thin conical shell have been obtained for the frequency ranges discussed. However, there are still several areas in which further work on this subject could be done.

First of all, the k-space integration technique could still theoretically be used to compute results based on the first frequency equation. This technique was not used as it was not necessary to use it in order to obtain the desired results, and because of the difficulties mentioned in obtaining the appropriate k-space limits. However, this method would provide a good check of the work presented here, and would also offer a much faster way, with respect to computer time, of obtaining the cumulative number of eigenvalues and eigenvalue curves versus dimensionless frequency. This would be particularly helpful if more exact information regarding the region between the two ring frequencies was required for specific cones.

A second area of possible analytic interest would be a more exact method of handling the expressions in the frequency range between the upper and lower ring frequencies. It would probably be necessary to use the k-space integration discussed above to perform a more complete parameter study of cone geometries in this region. The information which has been obtained indicates that the cone parameters do not affect the curves in an independent manner in this region. It appears that the relevant combination of parameters would have to be

isolated, if indeed this is possible, before expressions in this region could be formulated.

Finally, there is still a need, although of less importance for more experimental work in the area of cones. The data presented does not extend into the region above the upper ring frequency. In order to obtain data in this area it would be necessary to either improve the sensitivity of the instrumentation used or to choose a cone geometry where mode overlap does not become a problem until well into the region of interest. The latter procedure would probably be the easier of the two, as it is felt that the instrumentation used performed in a very satisfactory manner.

It might also be added that since this paper is based on a single frequency equation derivation which is approximate, the possibility is open for a similar type of analysis on a less approximate equation. However, unless an exact frequency equation were obtained, it is felt that there would be little value in this procedure as the results obtained appear to be of sufficient accuracy for engineering work.

7. LIST OF REFERENCES

Bolotin, V. V. 1963. On the density of the distribution of natural frequencies of thin elastic shells. PMM., Moscow 27(2):362-364.

Bolotin, V. V. 1965. The density of eigenvalues in vibrational problems of elastic plates and shells. Proc. Vibr. Probl., Warsaw 6(5):342-351.

Chao-tsien, T. 1964. The vibration and eigenfrequencies of circular conical (and cylindrical) shells. Scientia Sinica 13(8):1189-1210.

Courant, R. and Hilbert, D. 1953. Methods of Mathematical Physics, Vol. I. Interscience Publishers, Inc., New York.

Federhofer in Graz, K. 1962. Natural vibrations of the conical shell. National Aeronautics and Space Administration, Washington, D. C., NASA-TT-F-8261.

Flugge, W. 1966. Stresses in Shells. Springer-Verlag, Inc., New York, New York.

Godzevich, V. G. 1962. Free vibrations of circular conic shells, pp. 339-343. In S. M. Durgar'yan (ed.), Theory of Plates and Shells. Israel Program for Scientific Translations, Jerusalem, National Aeronautics and Space Administration, Washington, D. C., NASA-TT-F-341.

Hu, W. C. L. 1965. Free vibrations of conical shells. National Aeronautics and Space Administration, Washington, D. C., NASA TN D-2666.

Hu, W. C. L., Gormley, J. F. and Lindholm, U. S. 1967. An experimental study and inextensional analysis of vibrations of free-free conical shells. Int. J. Mech. Sci. 9:123-135.

Hu, W. C. L. and Lindholm, U. S. 1966. Non-symmetric transverse vibrations of truncated conical shells. Int. J. Mech. Sci. 8:561-579.

Kogawa, Y. 1965. On the axisymmetrical vibration of conical shells. Air Force Office of Scientific Research, Washington, D. C., AFOSR 65-1422.

Kol'man, E. R. 1965. Axisymmetric vibration modes of thin conical shells. Rasch. na Prochn. i Zhestk., Mashiz., Moscow, pp. 49-60.

Kol'man, E. R. 1966. Influence of the boundary conditions on the free vibration frequency and modes of a conical shell. Izv. VUZ, Mashinostr., No. 3, pp. 178-183.

Meyerovich, I. I. 1966. Approximate method for the determination of the natural oscillation frequencies of cylindrical, conic, and toroidal shells. National Aeronautics and Space Administration, Washington, D. C., NASA-TT-F-10377.

Mikhlin, S. G. 1964. Variational Methods in Mathematical Physics. The Macmillan Company, New York, New York.

Miller, D. K. and Hart, F. D. 1967. Modal density of thin circular cylinders. National Aeronautics and Space Administration, Washington, D. C., NASA CR-897.

Mixon, J. S. 1967. On the modes of vibration of conical frustrum shells with free ends. J. of Spacecraft and Rockets 4:414-416.

Platus, D. H. 1965. Conical shell vibrations. National Aeronautics and Space Administration, Washington, D. C., NASA TN D-2767.

Seide, P. 1964. On the free vibration of simply supported truncated conical shells. Space Systems Division, United States Air Force, Inglewood, Calif., SSD TDR-64-15.

Smith, B. W. and Lyon, R. H. 1965. Sound and structural vibration. National Aeronautics and Space Administration, Washington, D. C., NASA CR-160.

Sokolnikoff, I. S. 1956. Mathematical Theory of Elasticity. McGraw-Hill Book Company, Inc., New York, New York.

Tang, C. and Hong, Z. 1966. The vibration behavior of circular conical shells. National Aeronautics and Space Administration, Washington, D. C., NASA-TT-F-10393.

Ungar, E. E. 1966. Fundamentals of statistical energy analysis of vibrating systems. Air Force Flight Dynamics Laboratory Research and Technology Division, Air Force Systems Command, Wright-Patterson Air Force Base, Ohio, AFFDL TR-66-52.

Vlasov, V. Z. 1949. General theory of shells and its applications in engineering. National Aeronautics and Space Administration, Washington, D. C., NASA-TT-F-99

Wang, C. 1953. Applied Elasticity. McGraw-Hill Book Company, Inc., New York.

Watkins, J. D. and Clary, R. R. 1964. Vibrational characteristics of thin-walled conical frustrum shells. AIAA Journal 2:1815-1816.

Weingarten, V. I. 1965. Free vibrations of conical shells. ASCE Engineering Mechanics Division. Journal of Engineering Mechanics 91:69-87.

8. APPENDICES

8.1 Development of Differential Equations and Frequency Equation

8.1.1 Equilibrium Equations

Starting with the equilibrium conditions on a typical conical shell element, the differential equation of motion will be obtained. Figure 8.1 shows the basic geometry of a conical shell and of a typical element on the surface of the shell. In the figure, ψ is one-half the apex angle of the cone, r is the radius of the cone measured in the plane perpendicular to the axis of the cone, x is the coordinate along the cone surface measured from the apex, and θ is the angular coordinate measured in the plane perpendicular to the cone axis. Also, L is the slant length from the apex to the base of the cone, L_t is the slant length from the apex to the top of the cone, and h is the thickness of the cone.

Figure 8.2 shows a typical element of the cone with the various stress resultants indicated in their positive directions along with the three body forces X, Y, and Z. In Figure 8.2 the normal stress resultants are indicated by N_x and N_θ, the shear stress resultants are indicated by $N_{x\theta}$ and $N_{\theta x}$, and the transverse shear stresses by Q_x and Q_θ.

Assuming that the shell is of constant thickness (h) the resultant forces acting in the x, y, and z directions may be determined, where z is the coordinate perpendicular to the shell surface and y is the coordinate perpendicular to the x-z plane. Summing the forces acting in each coordinate direction and neglecting second order and

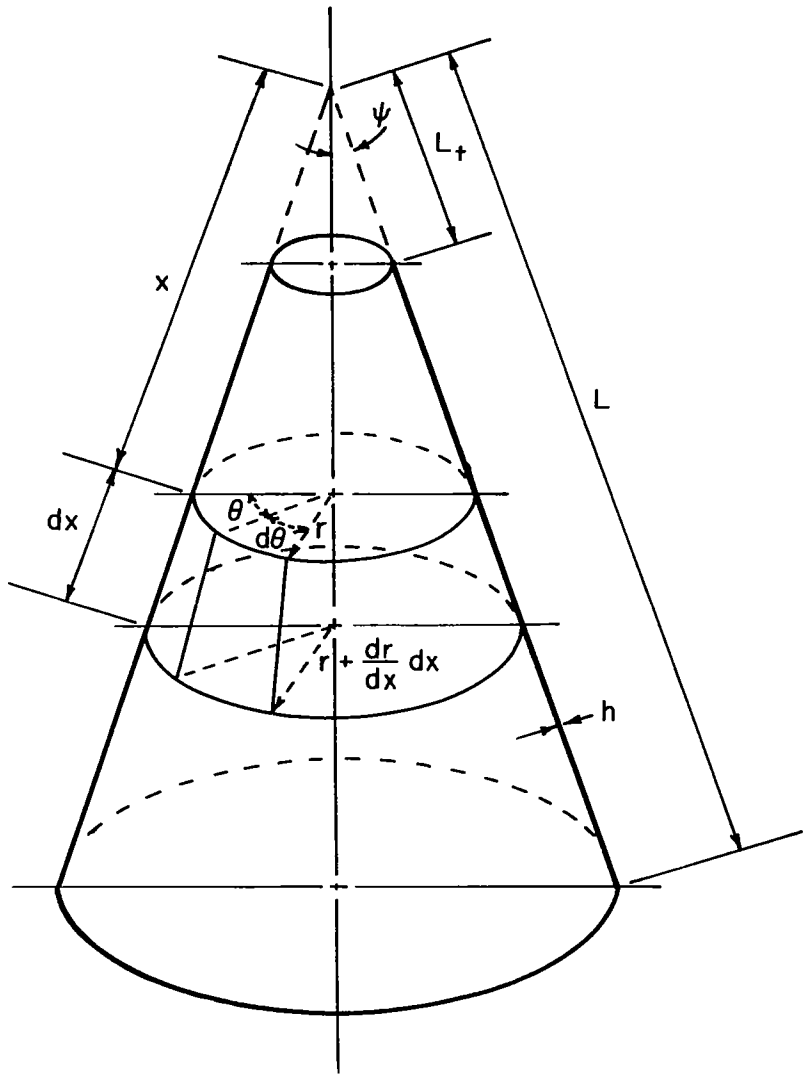

FIGURE 8.1 CONICAL SHELL AND ELEMENT GEOMETRY

higher terms the three force equilibrium equations for a conical shell are obtained:

$$\frac{\partial}{\partial x}(rN_x) - N_\theta \sin\psi + \frac{\partial}{\partial\theta}(N_{\theta x}) + rX = 0 \tag{8.1}$$

$$\frac{\partial}{\partial\theta}(N_\theta) + \frac{\partial}{\partial x}(rN_{x\theta}) + N_{\theta x}\sin\psi - Q_\theta \cos\psi + rY = 0 \tag{8.2}$$

$$-\frac{\cos\psi}{r}N_\theta - \frac{1}{r}\left[\frac{\partial}{\partial x}(rQ_x) + \frac{\partial}{\partial\theta}(Q_\theta)\right] = -Z\ . \tag{8.3}$$

Figure 8.3 shows a typical shell element with the six moment resultants necessary for equilibrium acting, again along with the three body forces. The moment resultants are shown in the figure in their positive directions. Under the assumption that the thickness of the shell is constant, remembering moment contributions due to the stress resultants in Figure 8.2, and neglecting second order and higher terms which appear, the three moment equilibrium equations may be written in the following form:

$$\frac{\partial}{\partial x}(rM_{x\theta}) + M_{\theta x}\sin\psi + \frac{\partial}{\partial\theta}(M_\theta) = Q_\theta r \tag{8.4}$$

$$-\frac{\partial}{\partial x}(rM_x) - \frac{\partial}{\partial\theta}(M_{\theta x}) + M_\theta \sin\psi = -Q_x r \tag{8.5}$$

$$M_{\theta x}\cos\psi + rN_{x\theta} - rN_{\theta x} = 0\ . \tag{8.6}$$

8.1.2 Differential Equations

It is now necessary to obtain the strain relationships for the shell element in terms of the three displacements of the shell. The displacement in the x direction is given the symbol u, the displacement in the θ direction has the symbol v, and the displacement in the

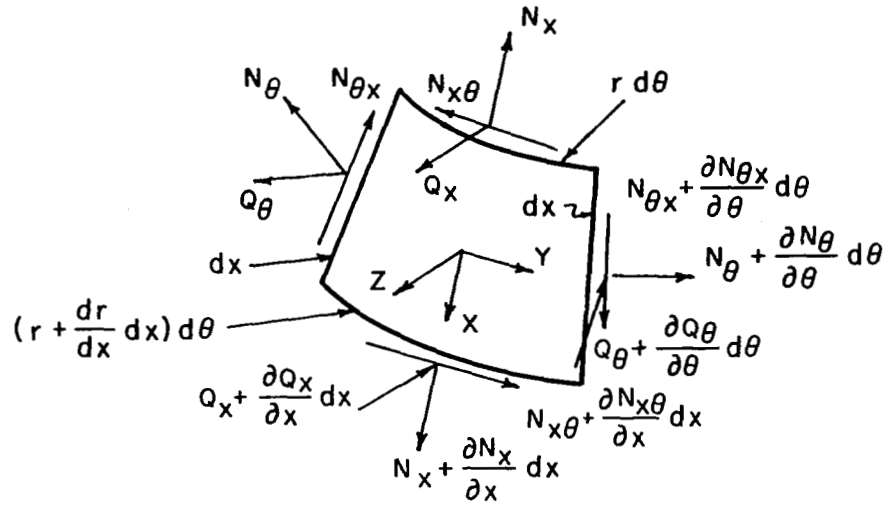

FIGURE 8.2 STRESS RESULTANT DIRECTIONS

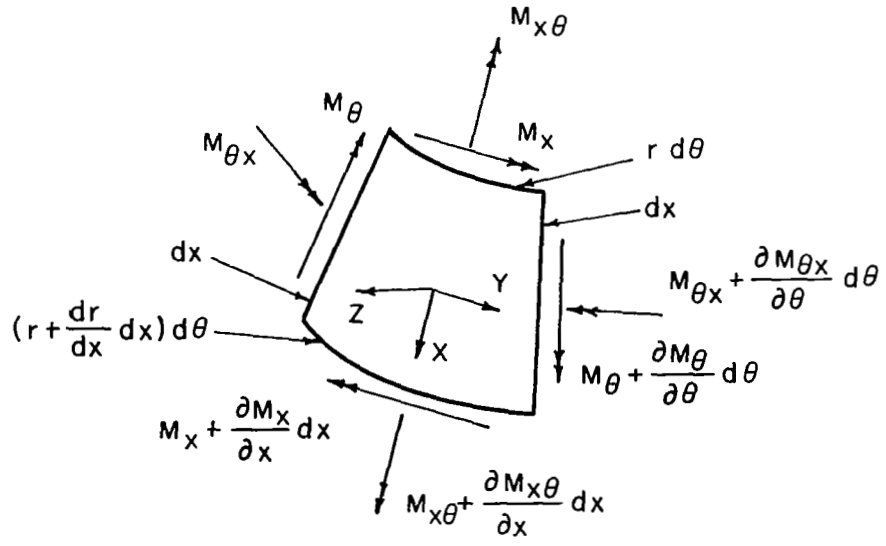

FIGURE 8.3 MOMENT RESULTANT DIRECTIONS

z direction the symbol w. Also defining the three strains due to extensions of the middle surface as follows. The change in length in the x direction over the length of the element in the x direction is given the symbol ϵ_x, the change in length in the θ direction over the length of the element in the θ direction the symbol ϵ_θ, and the change in angle between the x and θ directions the symbol $\gamma_{\theta x}$. The three extensional strains may be written in terms of the displacements as follows:

$$\epsilon_x = \frac{\partial u}{\partial x} \tag{8.7}$$

$$\epsilon_\theta = \frac{1}{r} u \sin\psi + \frac{1}{r} w \cos\psi + \frac{1}{r}\frac{\partial v}{\partial \theta} \tag{8.8}$$

$$\gamma_{\theta x} = \frac{1}{r}\frac{\partial u}{\partial \theta} + r\frac{\partial}{\partial x}\left(\frac{v}{r}\right) . \tag{8.9}$$

These then are the strains in the middle surface associated with the extension of the middle surface in terms of the displacements of the middle surface u, v, and w. There are also three strains associated with the bending of the middle surface which are given the symbols χ_x, χ_θ, and τ. Assuming that the strain in the z-direction is approximately zero, and that the u and v displacements do not affect the bending strains significantly, and that the displacement in the z direction is much smaller than the radius of the cone (r), the bending strains may be written in terms of the displacement in the z direction (w) in the following manner:

$$\chi_x = -\frac{\partial^2 w}{\partial x^2} \tag{8.10}$$

$$\chi_\theta = -\frac{1}{r}\frac{\partial w}{\partial x}\sin\psi - \frac{1}{r}\frac{\partial}{\partial\theta}\left(\frac{1}{r}\frac{\partial w}{\partial\theta}\right) \tag{8.11}$$

$$\tau = -\frac{1}{r}\frac{\partial^2 w}{\partial x\partial\theta} + \frac{1}{r^2}\frac{\partial w}{\partial\theta}\sin\psi \ . \tag{8.12}$$

Equations (8.7) through (8.12) have been derived by Flugge (1966) and Wang (1953).

The stress resultants and moments used in the equilibrium equations and shown in Figures 8.2 and 8.3 are defined in terms of the normal and shear stress in the following conventional manner, where h is the thickness of the shell:

$$N_x = \int_{-h/2}^{h/2} \sigma_x \left(1 - \frac{z\cos\psi}{r}\right) dz \tag{8.13}$$

$$N_\theta = \int_{-h/2}^{h/2} \sigma_\theta \, dz \tag{8.14}$$

$$N_{x\theta} = \int_{-h/2}^{h/2} \tau_{x\theta} \left(1 - \frac{z\cos\psi}{r}\right) dz \tag{8.15}$$

$$N_{\theta x} = \int_{-h/2}^{h/2} \tau_{\theta x} \, dz \tag{8.16}$$

$$M_x = \int_{-h/2}^{h/2} \sigma_x \left(1 - \frac{z\cos\psi}{r}\right) z\,dz \tag{8.17}$$

$$M_\theta = \int_{-h/2}^{h/2} \sigma_\theta \, z\,dz \tag{8.18}$$

$$M_{x\theta} = -\int_{-h/2}^{h/2} \tau_{x\theta} \left(1 - \frac{z \cos \psi}{r}\right) z\,dz \tag{8.19}$$

$$M_{\theta x} = -\int_{-h/2}^{h/2} \tau_{\theta x}\, z\,dz \ . \tag{8.20}$$

The normal stresses σ_x and σ_θ and the shear stress $\tau_{x\theta}$ are related for an elastic shell to the strains in the shell by the theory of elasticity in the following manner, where ν is Poisson's Ratio:

$$\sigma_x = \frac{E}{1-\nu^2} (\bar{\epsilon}_x + \nu\, \bar{\epsilon}_\theta) \tag{8.21}$$

$$\sigma_\theta = \frac{E}{1-\nu^2} (\bar{\epsilon}_\theta + \nu\, \bar{\epsilon}_x) \tag{8.22}$$

$$\tau_{x\theta} = \tau_{\theta x} = \frac{E}{2(1+\nu)} \bar{\gamma}_{\theta x} \ , \tag{8.23}$$

where $\bar{\epsilon}_x$, $\bar{\epsilon}_\theta$, and $\bar{\gamma}_{\theta x}$ are the total strains in the shell surface. The total strains are related to the extensional strains and the bending strains given in equations (8.7) through (8.12) by the following relationships:

$$\bar{\epsilon}_x = \epsilon_x + z\, \chi_x \tag{8.24}$$

$$\bar{\epsilon}_\theta = \epsilon_\theta + z\, \chi_\theta \tag{8.25}$$

$$\bar{\gamma}_{\theta x} = \gamma_{\theta x} + 2z\tau \ . \tag{8.26}$$

Using equations (8.24) through (8.26) along with equations (8.21) through (8.23) to express the stresses in terms of the bending and extensional strains and then using this result together with equations

(8.13) through (8.20) expressions for the stress resultants in terms of the extensional and bending strains are obtained. In so doing it is assumed that the h cos ψ/r term occurring in several of the stress resultant definitions is small compared to unity and may be neglected. This assumption has the added effect of satisfying equilibrium equation (8.6) identically, which therefore needs no further consideration. The stress resultants may be written as follows:

$$N_x = \frac{Eh}{1-\nu^2} (\epsilon_x + \nu \epsilon_\theta) \tag{8.27}$$

$$N_\theta = \frac{Eh}{1-\nu^2} (\epsilon_\theta + \nu \epsilon_x) \tag{8.28}$$

$$N_{x\theta} = N_{\theta x} = \frac{Eh}{2(1+\nu)} \gamma_{\theta x} \tag{8.29}$$

$$M_x = \frac{-Eh^3}{12(1-\nu^2)} (\chi_x - \nu \chi_\theta) \tag{8.30}$$

$$M_\theta = \frac{-Eh^3}{12(1-\nu^2)} (\chi_\theta - \nu \chi_x) \tag{8.31}$$

$$M_{\theta x} = M_{x\theta} = - \frac{Eh^3}{12(1+\nu)} \tau \quad . \tag{8.32}$$

For the remaining equilibrium equations (8.1) through (8.5), the following assumptions are made. The X and Y body forces are assumed to be unimportant in the vibration problem, and are neglected. It is also assumed that the transverse shear may be neglected in the second equilibrium equation (8.2). This assumption is based on the supposition that the radius of curvature of the shell is large. The equilibrium equations may therefore be written as:

$$\frac{\partial}{\partial x}(rN_x) - N_\theta + \frac{\partial}{\partial \theta}(N_{\theta x}) = 0 \tag{8.33}$$

$$\frac{\partial}{\partial \theta}(N_\theta) + \frac{\partial}{\partial x}(rN_{\theta x}) + N_{\theta x}\sin\psi = 0 \tag{8.34}$$

$$-\frac{\cos\psi}{r}N_\theta - \frac{1}{r}\left[\frac{\partial}{\partial x}(rQ_x) + \frac{\partial}{\partial \theta}(Q_\theta)\right] + Z = 0 \tag{8.35}$$

$$-\frac{\partial}{\partial x}(rM_{\theta x}) - M_{\theta x}\sin\psi - \frac{\partial}{\partial \theta}(M_\theta) + rQ_\theta = 0 \tag{8.36}$$

$$-\frac{\partial}{\partial x}(rM_x) - \frac{\partial}{\partial x}(M_{\theta x}) + M_\theta \sin\psi + rQ_x = 0 \ . \tag{8.37}$$

The stress function (ϕ) which is a function of the coordinates x and θ is now introduced. The stress function is defined in the following manner:

$$N_x = \frac{1}{r^2}\frac{\partial^2\phi}{\partial\theta^2} + \frac{\sin\psi}{r}\frac{\partial\phi}{\partial x} \tag{8.38}$$

$$N_\theta = \frac{\partial^2\phi}{\partial x^2} \tag{8.39}$$

$$N_{\theta x} = -\frac{1}{r}\left(\frac{\partial^2\phi}{\partial x\partial\theta} - \frac{\sin\psi}{r}\frac{\partial\phi}{\partial\theta}\right) \ . \tag{8.40}$$

By defining the stress function in the above manner, the first two equilibrium equations (8.33) and (8.34) are satisfied identically. This may be shown to be true merely by substituting equations (8.38) through (8.40) into the two equilibrium equations mentioned.

Examination of the relationships cited previously for the bending strains (8.10) through (8.12) reveals the following. The functional dependence between the displacement normal to the shell surface $w(x,\theta)$

and the three bending strains, χ_x, χ_θ, and τ is identical to that between the stress function $\phi(x,\theta)$ and the stress resultants N_x, N_θ, and N_x as given by equations (8.38) through (8.40). Therefore since equations (8.38) through (8.40) satisfy equations (8.33) and (8.34) identically, a similar result would be expected regarding χ_x, χ_θ, and τ. This analogy produces the following identities:

$$\frac{\partial}{\partial x}(r\chi_\theta) - \chi_x \sin\psi - \frac{\partial}{\partial\theta}(\tau) = 0 \tag{8.41}$$

$$\frac{\partial}{\partial\theta}(\chi_x) + \frac{\partial}{\partial x}(r\tau) - \tau \sin\psi = 0 \ . \tag{8.42}$$

Using the first two moment equilibrium equations (8.36) and (8.37) explicit expressions for the transverse shears Q_x and Q_θ may be obtained. If this result is used in conjunction with the expressions for the moments in terms of the bending strains (8.30) through (8.32) and the identities obtained above (8.41) and (8.42) the following expressions may be written for the transverse shear components:

$$-Q_x = \frac{Eh^3}{12(1-\nu^2)} \frac{\partial}{\partial x}[\chi_x + \chi_\theta] \tag{8.43}$$

$$-Q_\theta = \frac{Eh^3}{12(1-\nu^2)} \frac{1}{r} \frac{\partial}{\partial\theta}[\chi_x + \chi_\theta] \ . \tag{8.44}$$

Introducing the expressions for the bending strains in terms of the normal displacement (8.10) and (8.11) and the ∇^2 operator the expressions for the transverse shear components become:

$$Q_x = \frac{Eh^3}{12(1-\nu^2)} \frac{\partial}{\partial x} (\nabla^2 w) , \tag{8.45}$$

$$Q_\theta = \frac{Eh^3}{12(1-\nu^2)} \frac{1}{r} \frac{\partial}{\partial \theta} (\nabla^2 w) , \tag{8.46}$$

where

$$\nabla^2 = \frac{1}{r} [\frac{\partial}{\partial x} (r \frac{\partial}{\partial x}) + \frac{\partial}{\partial \theta} (\frac{1}{r} \frac{\partial}{\partial \theta})] .$$

Returning to the final equilibrium equation (8.35) and using the expressions (8.45) and (8.46) to eliminate the transverse shear terms, the z equilibrium equation may be expressed with the aid of the definition of the ∇^2 operator as

$$- \frac{\cos \psi}{r} N_\theta - \frac{Eh^3}{12(1-\nu^2)} \nabla^2 \nabla^2 w + Z = 0 . \tag{8.47}$$

Equation (8.47) may be rewritten in a simpler form by using the definition of the stress function (8.39) to eliminate the stress resultant N_θ:

$$\frac{\cos \psi}{r} \frac{\partial^2 \phi}{\partial x^2} + \frac{Eh^3}{12(1-\nu^2)} \nabla^2 \nabla^2 w - Z = 0 . \tag{8.48}$$

This then is the first differential equation for the motion of a conical shell. The equation is expressed in terms of two dependent variables ϕ and w which are both functions of the two independent variables x and θ. In order to obtain a second differential equation so that the system of equations may be solved, a form of the continuity equation involving the volume deformation θ is introduced. The volume

deformation is defined as the sum of the two extensional strains ϵ_x and ϵ_θ. Therefore from continuity considerations the following equation is written:

$$\nabla^2 \theta - (1-\nu) \frac{1}{r} \left[\frac{\partial}{\partial x} \left(\cos \psi \frac{\partial w}{\partial x}\right)\right] = 0 \tag{8.49}$$

Using this equation together with the above definition of volume deformation, the expressions for the stress resultants in terms of extensional strains (8.27) and (8.28), the definition of the stress function (8.38) and (8.39), and the definition of the ∇^2 operator the following relationship may be written:

$$\frac{1}{Eh} \nabla^2 \nabla^2 \phi - \frac{\cos \psi}{r} \frac{\partial^2 w}{\partial x^2} = 0 . \tag{8.50}$$

Equations (8.48) and (8.50) are therefore the differential equations governing the motion of a thin conical shell. These equations have been derived in a more general form by Vlasov (1949) and have been used in approximately the form given by Godzevich (1962) applied to a conical shell.

The differential equations derived above are based on several assumptions which although noted in the derivation will be restated here in a collected form. It was assumed that the shell thickness (h) remained constant over the shell, that the shell material obeyed Hooke's elastic law, that the compressive strain of the shell element in the z-direction was approximately zero, that the u and v displacements of the shell element did not appreciably affect the bending strain relations, and that the X and Y body forces could be neglecting in the

formulation of the vibration problem. All of these assumptions appear to be such that no further explanation is needed. It was also assumed that the radius of curvature of the shell was large, in other words $\frac{r}{h \cos \psi}$ is much greater than zero. This assumption is obviously true for cones with large cone angles, and for points well away from the cone apex; however, for small cone angles, and points near the cone apex the assumption is only approximate.

8.1.3 Frequency Equation

Before proceeding with the solution of the differential equations for the conical shell the results thusfar will be grouped and put in the following form:

$$\frac{1}{Eh} \nabla^2 \nabla^2 \phi - \frac{\cos \psi}{r} \frac{\partial^2 w}{\partial x^2} = 0 \tag{8.51}$$

$$\frac{\cos \psi}{r} \frac{\partial^2 \phi}{\partial x^2} + D \nabla^2 \nabla^2 w - \frac{\gamma h \omega^2}{g_c} w = 0 \tag{8.52}$$

where

$$\nabla^2 = \frac{\partial^2}{\partial x^2} + \frac{\sin \psi}{r} \frac{\partial}{\partial x} + \frac{1}{r^2} \frac{\partial^2}{\partial \theta^2} .$$

The only difference between these equations and the ones given previously is that the $Eh^3/12(1-\nu^2)$ term has been replaced by D, the plate stiffness, and that the Z body force has been replaced by the inertia force of the shell, where γ is the shell density and ω is the frequency of vibration.

Since the main problem of interest is to obtain an expression for the resonant frequencies of a vibrating cone, the solutions for the

stress function and the normal displacement will be confined to expressions of the form:

$$w(x,\theta) = W(x) \cos m\theta \qquad m = 2,3,\ldots \tag{8.53}$$

$$\phi(x,\theta) = \Phi(x) \cos m\theta \qquad m = 2,3,\ldots \tag{8.54}$$

It is therefore assumed that the circumferential modes are independent of the longitudinal modes, and that the mode shapes in the circumferential direction are sinusoidal and uniform over the length of the cone. In other words for a given mode number there are the same number of circumferential waves all the way up and down the cone surface. Substituting equations (8.53) and (8.54) into equations (8.51) and (8.52) and noting that r and x are related ($r = x \sin\psi$) the differential equations may be expanded to the following form. In so doing, the independent variable x has been nondimensionalized by making the substitution $\dot{x} = \alpha L$, where L is the slant length of the cone, and α is the new dimensionless variable:

$$\frac{1}{Eh}\left\{\frac{d^4\Phi}{d\alpha^4} + \frac{2}{\alpha}\frac{d^3\Phi}{d\alpha^3} - \frac{1}{\alpha^2}\left(1 + \frac{2m^2}{\sin^2\psi}\right)\frac{d^2\Phi}{d\alpha^2} + \frac{1}{\alpha^3}\left(1 + \frac{2m^2}{\sin^2\psi}\right)\frac{d\Phi}{d\alpha}\right.$$

$$\left. + \frac{1}{\alpha^4}\left(\frac{m^4}{\sin^4\psi} - \frac{4m^2}{\sin^2\psi}\right)\Phi\right\} - \frac{L}{\alpha\tan\psi}\frac{d^2w}{d\alpha^2} = 0 \tag{8.55}$$

$$\frac{L}{\alpha\tan\psi}\frac{d^2\Phi}{d\alpha^2} + D\left\{\frac{d^4w}{d\alpha^4} + \frac{2}{\alpha}\frac{d^3w}{d\alpha^3} - \frac{1}{\alpha^2}\left(1 + \frac{2m^2}{\sin^2\psi}\right)\frac{d^2w}{d\alpha^2}\right.$$

$$\left. + \frac{1}{\alpha^3}\left(1 + \frac{2m^2}{\sin^2\psi}\right)\frac{dw}{d\alpha} + \frac{1}{\alpha^4}\left(\frac{m^4}{\sin^4\psi} - \frac{4m^2}{\sin^2\psi}\right)w\right\} - \frac{\gamma h L^4\omega^2}{g_c}W = 0 . \tag{8.56}$$

Equations (8.55) and (8.56) are now two simultaneous differential equations in the two dependent variables Φ and W which are functions of the independent variable α. The equation may be solved by the Galerkin Method, as has been pointed out by Godzevich (1962). In order to use this method it is first necessary to assume a series type solution for the unknown functions $\Phi(\alpha)$ and $W(\alpha)$. The assumed solutions to be used in this case are of the following form:

$$\Phi(\alpha) = \sum_{n=1}^{\infty} A_n \sin a_n (\alpha-\alpha_1) \tag{8.57}$$

$$W(\alpha) = \sum_{n=1}^{\infty} B_n \sin a_n (\alpha-\alpha_1) \tag{8.58}$$

where $a_n = \frac{n\pi}{1-\alpha_1}$ and α_1 is the ratio of the slant length of the truncated portion of the cone L_t to the slant length of the entire cone L. The integer n represents the number of half waves in the longitudinal direction along the cone. The constants A_n and B_n are unknowns which are to be determined as part of the solution.

The Galerkin method as explained in some detail by Mikhlin (1964) essentially imposed an orthogonality condition between the differential equations with the assumed solutions substituted into them, and the assumed solutions themselves. It is this orthogonality requirement which is used to obtain the constants A_n and B_n, or in this case is used to obtain the eigenvalue expression (frequency equation).

Substituting equations (8.57) and (8.58) into the differential equations (8.55) and (8.56) and insisting that the resulting expressions are orthogonal to the assumed solution form (sin $a_n (\alpha-\alpha_1)$) two simultaneous equations in A_n and B_n are obtained. Instead of

solving the system of equations for the unknowns A_n and B_n the determinant of the coefficient matrix is set equal to zero. This is the condition which will lead to an expression for the eigenvalues of the conical shell. The expression may be written in the following form:

$$\omega^2 = \frac{B_1^2 + \frac{1}{DEh} B_2^2}{B_1 B_3} , \tag{8.59}$$

where B_1, B_2, and B_3 are the integral portions of the coefficient matrix which occurred due to the orthogonality condition which was imposed. The integral expressions are evaluated over the length of the cone, or from $\alpha = 0$ and $\alpha = 1$. Evaluating the integral expressions which occur and substituting them into equation (8.59) results in the desired expression for the eigenvalues of a conical shell. This expression is given as

$$\omega^2 = \left[\frac{g_c E}{\gamma L^2}\right] \frac{\frac{D}{EL^2h}\left\{\frac{a_n^4}{10}(1-\alpha_1^5) + a_n\left(1 + \frac{2m^2}{\sin^2\psi}\right)\left[\frac{a_n}{6}(1-\alpha_1^3) - \frac{1}{2a_n}(1-\alpha_1)\right] + \right.}{\left\{\frac{a_n^4}{10}(1-\alpha_1^5) + a_n\left(1 + \frac{2m^2}{\sin^2\psi}\right)\left[\frac{a_n}{6}(1-\alpha_1^3) - \frac{1}{2a_n}(1-\alpha_1)\right] + \right.}$$

$$\frac{\left. + \left(\frac{m^4}{\sin^4\psi} - \frac{4m^2}{\sin^2\psi}\right)\left(\frac{1-\alpha_1}{2}\right)^2 + \frac{a_n^4}{\tan^2\psi}\left\{\frac{1}{8}(1-\alpha_1^4) - \frac{3}{8a_n^2}(1-\alpha_1^2)\right\}^2 \right.}{\left. + \left(\frac{m^4}{\sin^4\psi} - \frac{4m^2}{\sin^2\psi}\right)\left(\frac{1-\alpha_1}{2}\right)\left\{\frac{1}{10}(1-\alpha_1^5) - \frac{1}{2a_n^2}(1-\alpha_1^3) + \frac{3}{4a_n^2}(1-\alpha_1)\right\}\right.} \tag{8.60}$$

It should be remembered that aside from the assumptions made in the development of the differential equations, this equation is also dependent on the assumptions which were made in obtaining a solution of the differential equations. It was assumed that the circumferential modes were sinusoidal in nature and the mode shape in the circumferential direction was consistent over the length of the cone, and that the circumferential modes were independent of the longitudinal modes. It was also assumed that the longitudinal mode shape could be approximated by a single term series of the form given in equations (8.57) and (8.58). These assumptions all appear reasonable, however experimental evidence regarding the mode shapes indicates that they are only approximations. Equation (8.60) will be referred to as frequency equation one throughout this paper.

8.2 Comparison of Frequency Equation One with Experimental Results in the Literature

In order to provide some form of check for the frequency equation derived in section 8.1, since it is an approximate equation, frequencies predicted by this equation (8.60) are compared with experimentally obtained frequencies available in the literature. The results of studies conducted by Weingarten (1965) and Lindholm and Hu (1966) are used as sources of experimental data for this comparison.

The data obtained by Weingarten (1965) is presented in tabular form in Tables 8.1 and 8.2, and the data obtained by Lindholm and Hu (1966) is presented in Tables 8.3 and 8.4. Relevant data concerning the cones used in the investigation is also given in the respective table with the corresponding data.

Table 8.1 Experimental data in literature (1)[a]

Cone Angle (ψ): 20^{o}

Length (L): 14.14 inches

Truncation (L_t): 6.14 inches

Thickness (h): 0.04 inches

Material: 1020 steel, rolled and butt welded

m	f(Hz) for n=1	f(Hz) for n=2	f(Hz) for n=3
2	1850	5116	6388
3	1451/1453	-	-
4	1206	2831	4417
5	1151	2374	-
6	1304	2277	-
7	1535	2449	3262
8	1831	2710	3453
9	2169	3007	3751
10	2555	-	4264/4219
11	-	3775	4732
12	-	-	5291
13	-	-	5871

[a]Weingarten (1965); taken from tables.

Table 8.2 Experimental data in literature (2)[a]

Cone Angle (ψ): 20^{o}

Length (L): 14.14 inches

Truncation (L_t): 6.14 inches

Thickness (h): 0.02 inches

Material: 1020 steel, rolled and butt welded

m	f(Hz) for n=1	f(Hz) for n=2	f(Hz) for n=3
2	1551	-	-
3	1468	3045/3049	-
4	1182	2407	3980
5	1001	2215/2175	3472
6	964	1858/1867	2989/2949
7	1032	1747/1734	2647/2623
8	1160	1781	2514
9	1317	1915	2542/2544
10	-	2090/2082	2694
11	-	2293	2796/2785
12	-	2419/2428	3070/2085

[a]Weingarten (1960); taken from tables.

Table 8.3 Experimental data in literature (3)[a]

Cone Angle (ψ): 30.2^{o}

Length (L): 15.7 inches

Truncation (L_t): 6.94 inches

Thickness (h): 0.01 inches

Material: Shim stock, rolled and butt welded

n	f(Hz) for n=1	f(Hz) for n=2	f(Hz) for n=3
5	670	-	-
6	510	-	-
7	410	-	-
8	395	980	-
9	390	875	-
10	400	800	-
11	420	760	-
12	480	-	-
13	500	800	1100
14	555	850	1125
15	600	895	1175
16	650	950	1210
17	705	1000	1260
18	780	1050	1315
19	820	-	1400
20	900	1195	1470

[a]Lindholm and Hu (1966); taken from graphs.

Table 8.4 Experimental data in literature (4)[a]

Cone Angle (ψ): 45.1°

Length (L): 12.7 inches

Truncation (L_t): 5.61 inches

Thickness (h): 0.01 inches

Material: Shim stock, rolled and butt welded

n	f(Hz) for n=1	f(Hz) for n=2	f(Hz) for n=3
6	610	-	-
7	510	-	-
8	455	-	-
9	415	970	-
10	405	885	-
11	410	805	-
12	440	795	1300
13	480	805	1200
14	505	855	1160
15	545	895	1170
16	590	-	1210
17	610	975	1270
18	670	1005	1315
19	705	1060	1375
20	770	1105	1410

[a]Lindholm and Hu (1966); taken from graphs.

Using the information presented in each table concerning the cone geometry and the cone material in conjunction with the frequency equation for the conical shell (8.60) the resonant frequencies corresponding to various mode numbers are obtained. Figures 8.4 through 8.7 show the results of these calculations in graphical form. The resonant frequency is shown plotted as a function of the number of circumferential waves (m), and the number of one-half longitudinal waves (n) is shown as the parameter. The experimental values presented in Tables 8.1 through 8.4 are shown in the respective figure pertaining to each cone studied. Hence Figures 8.4 through 8.7 offer a quick comparison between the experimental results and the analytical results based on equation (8.60).

A study of Figures 8.4 through 8.7 indicates that the frequency equation developed in section 8.1 is by no means exact, but does reflect trends of frequency variation with changing wave numbers. Since the purpose of the investigation undertaken in this paper is not to obtain discrete frequency values, but rather to study the overall variation of frequency with respect to mode number, it is felt that the agreement obtained is sufficient for the purpose at hand.

8.3 Computer Program for Numerical k-Space Integration

8.3.1 Description of Program

The general equation (3.25) used in the evaluation of the k-space integral has already been discussed in some detail. In this section a general outline of the program used to accomplish the integration numerically will be presented.

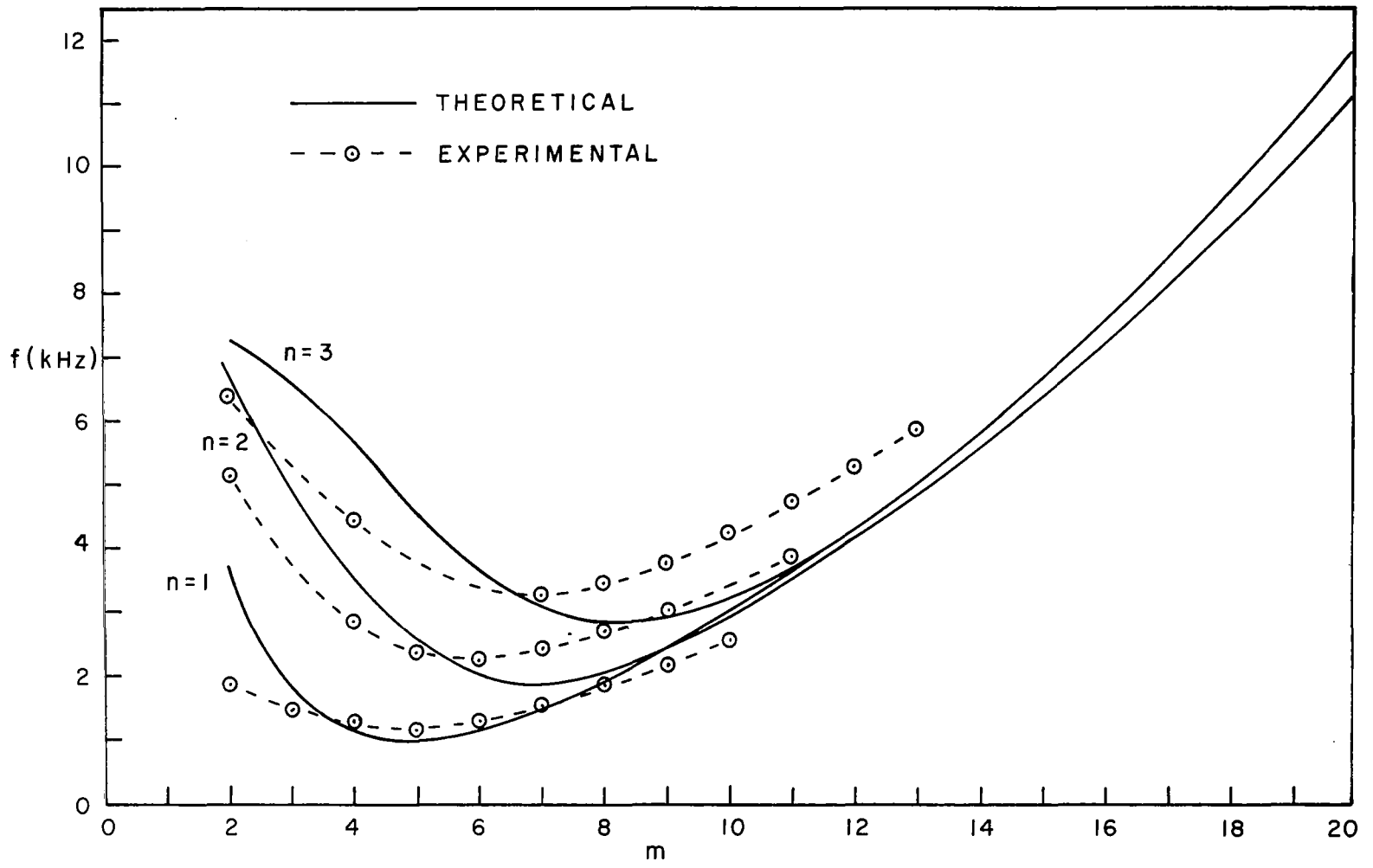

FIGURE 8.4 COMPARISON OF FREQUENCY EQUATION ONE WITH VALUES IN TABLE 8.1

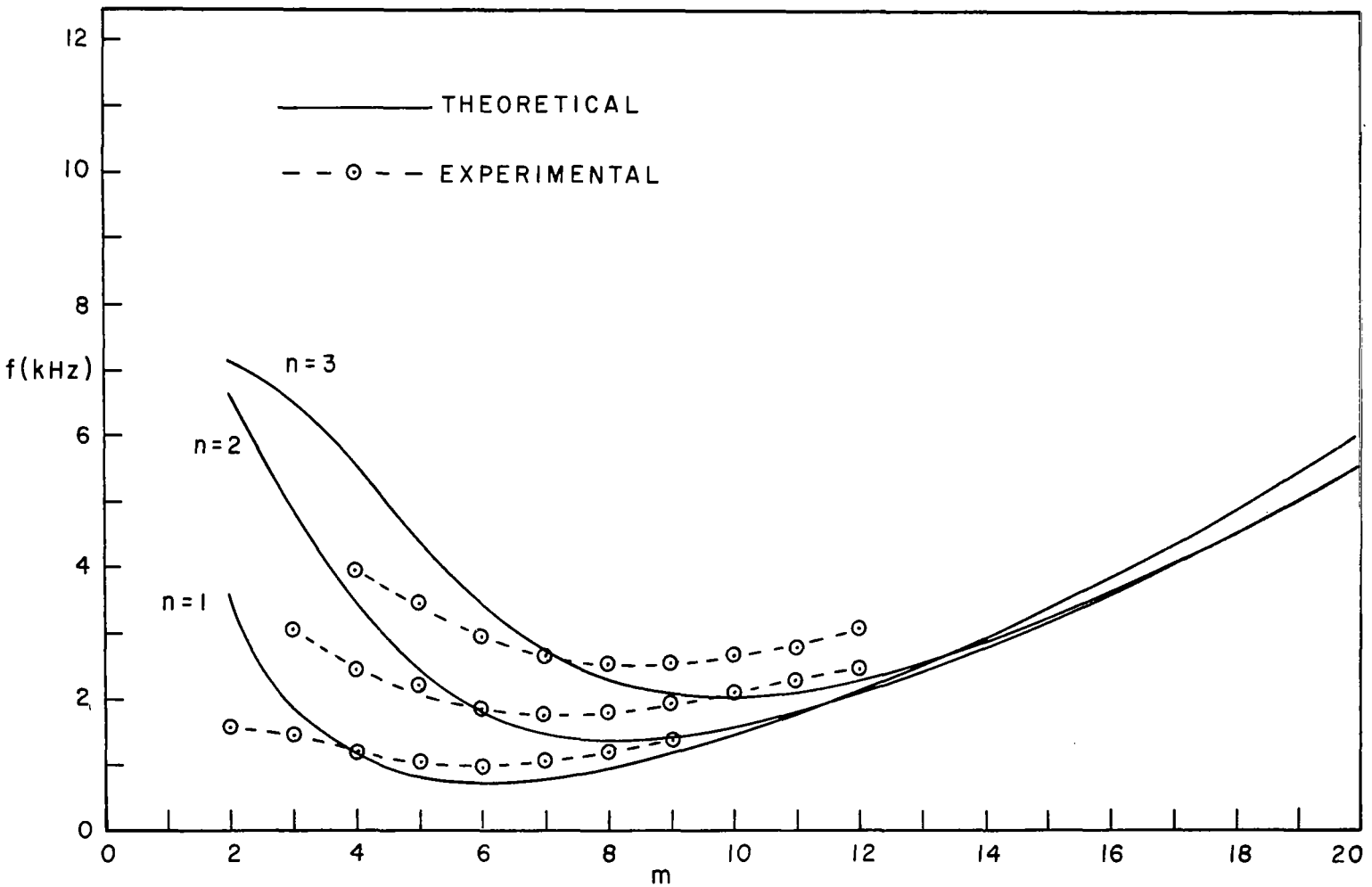

FIGURE 8.5 COMPARISON OF FREQUENCY EQUATION ONE WITH VALUES IN TABLE 8.2

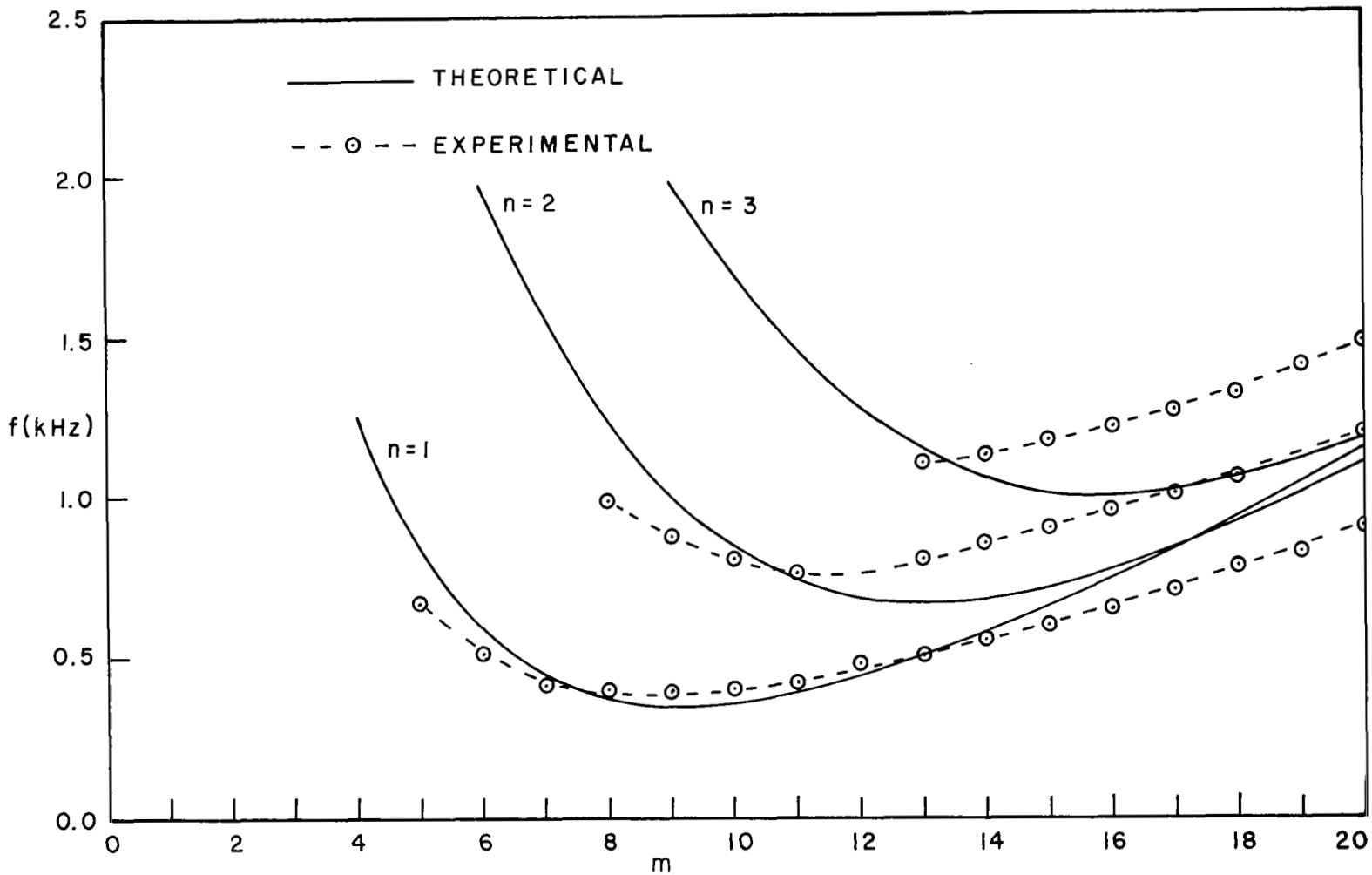

FIGURE 8.6 COMPARISON OF FREQUENCY EQUATION ONE WITH VALUES IN TABLE 8.3

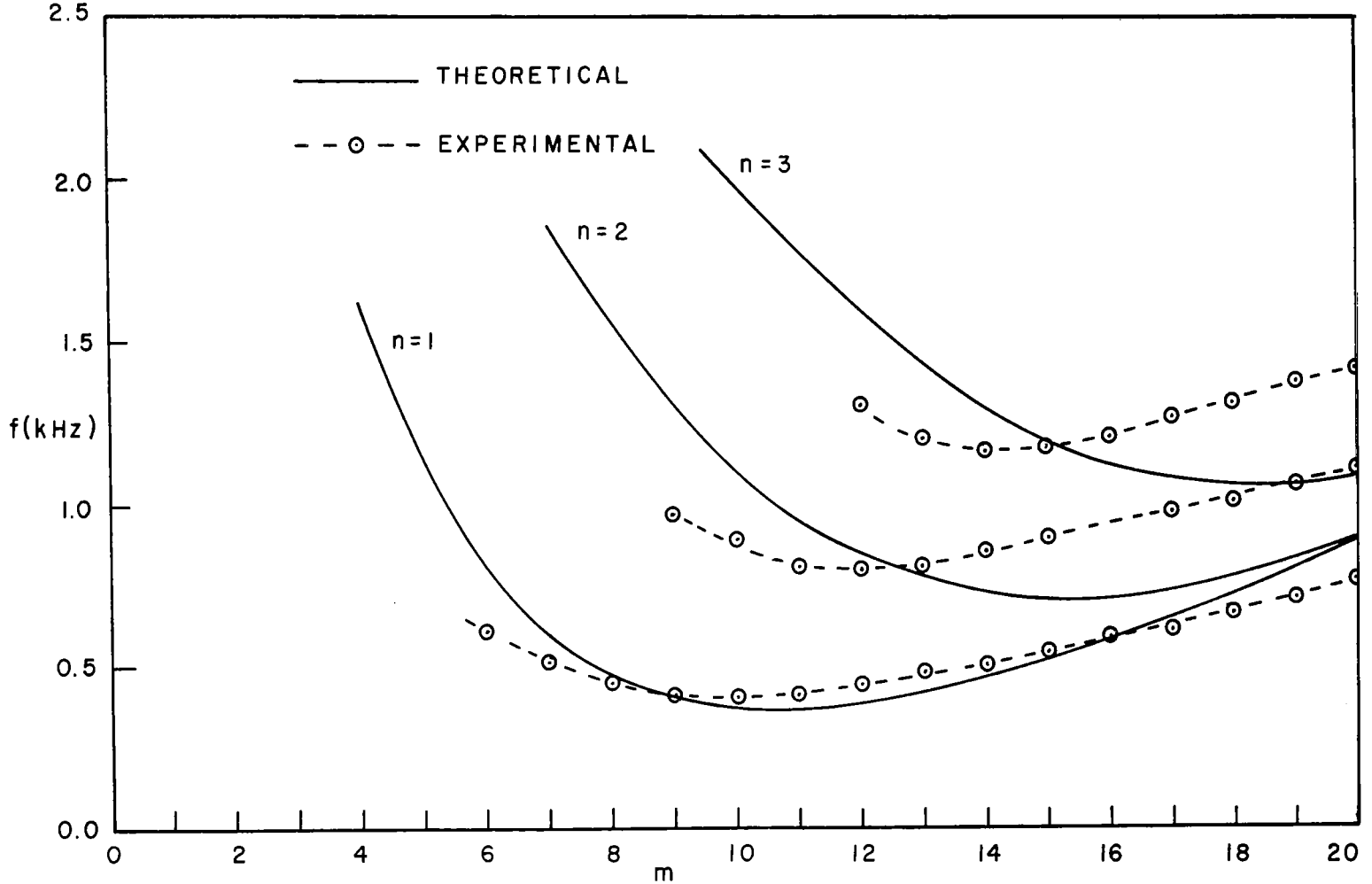

FIGURE 8.7 COMPARISON OF FREQUENCY EQUATION ONE WITH VALUES IN TABLE 8.4

This program may be broken down into five separate parts; the main program or control section, two function subprograms, and two subroutines, plus data on the cone geometries studied. The two function subprograms define the upper and lower boundaries of the space as functions as given by equation (3.23). The first of the subroutines is a standard library subprogram used to find the real and imaginary roots of a polynomial by Newton Raphson iteration techniques. This subprogram is used to solve the cubic polynomial (3.24) which yields the upper and lower limits of the k-space. The second subroutine is also a standard library subroutine used to evaluate integrals by Simpson's Rule. This subprogram is used to evaluate the integral over the upper and lower bounds of the space (3.26). The main program provides for input and output of information and serves to coordinate the various subprograms and subroutines.

The basic sequence of events is indicated in Figure 8.8. The program begins by inputting the data concerning the cone to be analyzed. Each data card contains the data for one cone in the following sequence; cone angle, length, truncation length, thickness, Young's modulus, Poisson's ratio, and the density. This data is then used to generate several constants which are needed in the equations to be solved. Then, an initial dimensionless frequency value is calculated and several more constants dependent on this parameter are determined. The first subroutine is then called and provided with the required information. The subroutine solves the cubic equation given it, and returns the roots to the main program. The main program then picks the appropriate roots to be the limits of the k-space integral. The second

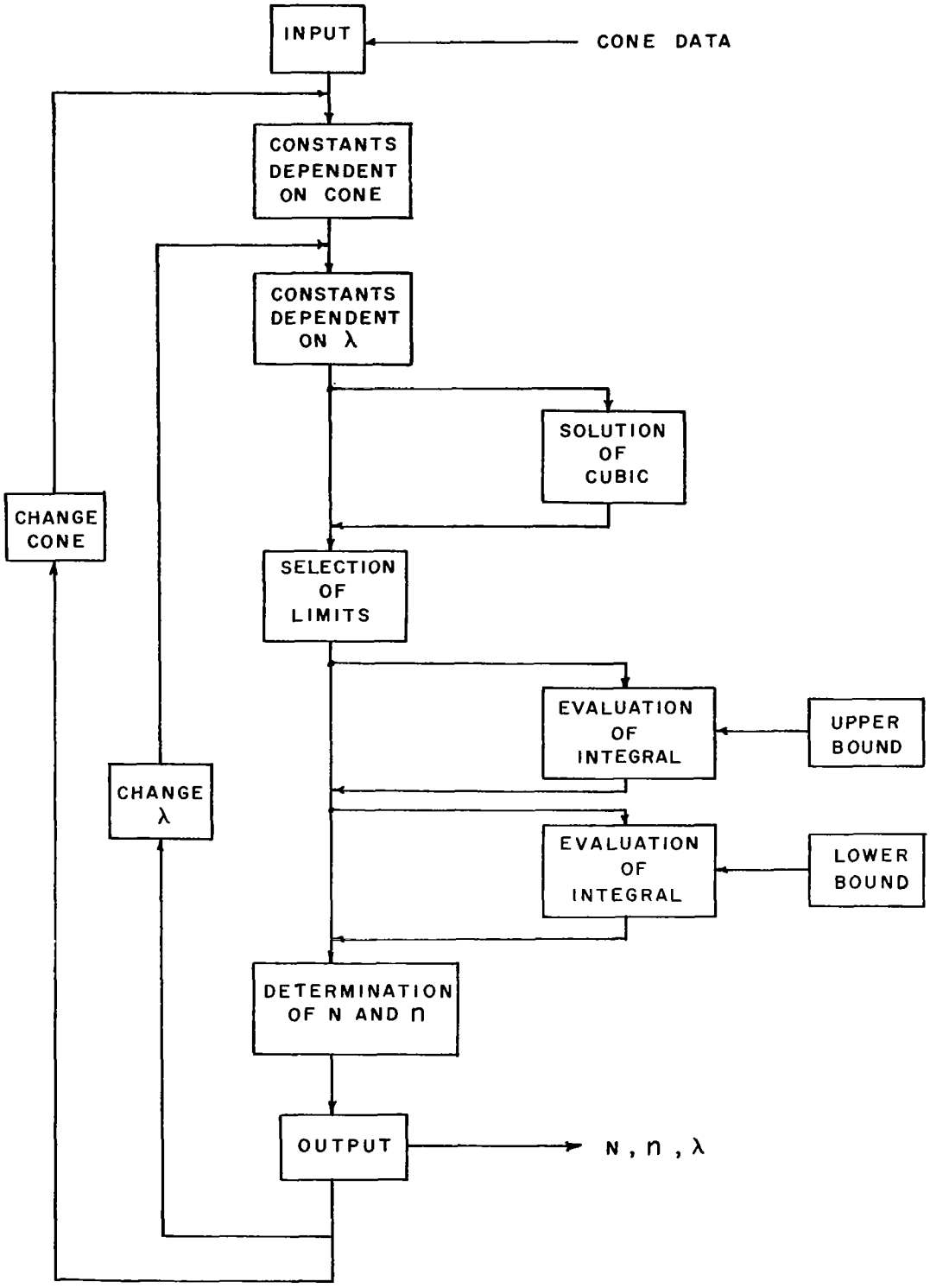

FIGURE 8.8 DIAGRAM OF NUMERICAL K-SPACE INTEGRATION PROGRAM

subroutine is then called and provided with the appropriate information such as the limits and the upper bound function subprogram. The subroutine calculates the value of the integral and returns it. The subroutine is called a second time and given the same information except that the lower bound function subprogram is used. This value is returned and subtracted from the value obtained previously; the final value for the cumulative number of eigenvalues is then printed out along with the corresponding dimensionless frequency. The dimensionless frequency value is then increased and the above procedure repeated until a sufficient range of dimensionless frequency values have been covered.

Between each successive calculation of the cumulative number of eigenvalues, the eigenvalue density is obtained by dividing the change in number of eigenvalues by the change in dimensionless frequency. This information is also printed out along with a corresponding value of dimensionless frequency equal to the value half way between the values corresponding to the number of eigenvalues used in the determination of the eigenvalue density. After a sufficient number of dimensionless frequencies have been used the data for a new cone is selected and used in the same manner as above. All the results obtained may be printed either in normalized form or merely in the form given in equation (3.26).

A copy of the actual program used on an IBM 360 model 75 computer written in G level Fortran appears in the next subsection.

8.3.2 Main Program

```
001       DOUBLE PRECISION CONE (22,7)
002       DOUBLE PRECISION XCOF(4),COF(4),ROOTR(3),ROOTI(3)
003       DOUBLE PRECISION A,DEG,ANGL,RL,XI,AL,H,E,RATO,DEN,G,C1,C2,AL1,
         *AL2,AL3,AL4,AL5,SDFR,DFRE,S,T,U,B,SU,SL,DN,DELDN,DNO,DELDF,
         *DFREM,DM,DFREQ
004       COMMON AL1,AL2,AL3,AL4,AL5,C1,C2,SDFR
005       EXTERNAL UPPER,LOWER
006   100 FORMAT('1','INTEGRATION OF K-SPACE FROM 2ND FREQUENCY EQUATION
         *TO GET D-NUMBER OF MODES'//'0','ANGLE=',F7.4,3X,'LENGTH RATIO
         *=',F6.4,3X,'THICKNESS=',F6.4,3X,'LENGTH=',F8.4//)
007   200 FORMAT(7F10.0)
008   300 FORMAT('0','D-FREQUENCY  D-NUMBER MODES          D-FREQUENCY
         *D-MODAL DENSITY'//)
009   400 FORMAT(' ',F10.3,D15.5,F20.3,D15.5,3I3,2I6)
    C
    C        INPUT OF CONE DATA
    C
010       READ(1,200)((CONE(I,J),J=1,7),I=1,22)
011       DO 1 K=1,22
012       DEG=CONE(K,1)
013       ANGL=DEG/57.295779531
014       RL=CONE(K,2)
015       XI=CONE (K,3)
016       AL=XI/RL
017       H=CONE(K,4)
018       E=CONE(K,5)*1.D2
019       RATO=CONE(K,6)
020       DEN=CONE(K,7)
021       G=3.864D2
022       C1=(H**2)/(1.2D1*(RL**2)*(1.DO-(RATO**2)))
023       C2=DCOTAN(ANGL)**2
024       AL1=1.DO-AL
025       AL2=1.DO-AL**2
026       AL3=1.DO-AL**3
027       AL4=1.DO-AL**4
028       AL5=1.DO-AL**5
    C
    C        IDENTIFICATION OF CONE
    C
029       WRITE(3,100) DEG,AL,H,RL
030       WRITE(3,300)
031       DFRE=0.0925DO
032       DNO=0.DO
033       DFREQ=0.DO
    C
    C        LOOP ON DIMENSIONLESS FREQUENCY
    C
034       DO 2 L=1,100
035       DFRE=DFRE*1.0715DO
```

```
036       SDFR=DFRE**2
037       S=-(3.DO*AL2/AL4+2.DO*SDFR*AL5/(5.DO*AL4*DSQRT(C1*C2)))
038       T=2.DO*SDFR*AL3/(AL4*DSQRT(C1*C2))
039       U=-3.DO*SDFR*AL1/(AL4*DSQRT(C1*C2))
040       XCOF(1)=U
041       XCOF(2)=T
042       XCOF(3)=S
043       XCOF(4)=1.0DO
      C
      C         SOLUTION OF CUBIC TO OBTAIN UPPER LIMIT OF CK1
      C
044       CALL ROOTS(XCOF,COF,3,ROOTR,ROOTI,IC)
045       A=DSQRT(ROOTR(2))
046       B=DSQRT(ROOTR(3))
      C
      C         SIMPSON INTEGRATION OF UPPER BOUNDRY
      C
047       CALL BOBYJO(UPPER,A,B,1.D-3,10,S1U,SU,NU,IERU)
      C
      C         SIMPSON INTEGRATION OF LOWER BOUNDRY
      C
048       CALL BOBYJO(LOWER,A,B,1.D-3,10,S1L,SL,NL,IERL)
      C
      C         CALCULATION OF AREA OF K-SPACE
049       DN=SU-SL
050       DN=DN*H/(DSQRT(DTAN(ANGL)))*DSQRT(DSQRT(AL1))/RL
051       DELDN=DN-DNO
052       DELDF=DFRE-DFREQ
053       DFREM=DELDF/2.DO+DFREQ
054       DM=DELDN/DELDF
055       WRITE(3,400) DFRE,DN,DFREM,DM,IC,IERU,IERL,NU,NL
056       DFREQ=DFRE
057       DNO=DN
058     2 CONTINUE
059     1 CONTINUE
060       STOP
061       END
```

8.3.3 Upper Bound Function Subprogram

```
001       DOUBLE PRECISION FUNCTION UPPER(X)
002       DOUBLE PRECISION AL1,AL2,AL3,AL4,AL5,C1,C2,CK1,T,U,V,W,SDER
003       COMMON AL1,AL2,AL3,AL4,AL5,C1,C2,SDFR
004       CK1=X
005       T=AL1/2.DO
006       U=C2*((AL4*(CK1**4)/8.DO)-(3.DO*AL2*(CK1**2)/8.DO))**2
007       V=(AL5*(CK1**4)/1.D1)-(AL3*(CK1**2)/2.DO)+(3.DO*AL1/4.DO)
008       W=C1*(CK1**4)
009       IF (V*SDFR/(2.DO*W*T)) 1,2,2
010     1 UPPER=0.0
```

```
011       GO TO 3
012     2 CONTINUE
013       UPPER=DSQRT(DSQRT((V*SDFR/(2.DO*W*T))*(1.DO+DSQRT(DMAX1(1.D-
         *25,(1.DO-(4.DO*U*W/((V*SDFR)**2)))))))))
014     3 CONTINUE
015       RETURN
016       END
```

8.3.4 Lower Bound Function Subprogram

```
001       DOUBLE PRECISION FUNCTION LOWER(X)
002       DOUBLE PRECISION AL1,AL2,AL3,AL4,AL5,C1,C2,CK1,T,U,V,W,SDFR
003       COMMON AL1,AL2,AL3,AL4,AL5,C1,C2,SDFR
004       CK1=X
005       T=AL1/2.DO
006       U=C2*((AL4*(CK1**4)/8.DO)-(3.DO*AL2*(CK1**2)/8.DO))**2
007       V=(AL5*(CK1**4)/1.D1)-(AL3*(CK1**2)/2.DO)+(3.DO*AL1/4.DO)
008       W=C1*(CK1**4)
009       IF (V*SDFR/(2.DO*W*T)) 1,2,2
010     1 LOWER=0.0
011       GO TO 3
012     2 CONTINUE
013       LOWER=DSQRT(DSQRT((V*SDFR/(2.DO*W*T))*(1.DO-DSQRT(DMAX1(1.D-
         *25,(1.DO-(4.DO*L*W/((V*SDFR)**2)))))))))
014     3 CONTINUE
015       RETURN
016       END
```

8.3.5 Subroutine to Solve Cubic

```
001       SUBROUTINE ROOTS(XCOF,COF,M,ROOTR,ROOTI,IER)
002       DIMENSION XCOF(1),COF(1),ROOTR(1),ROOTI(1)
003       DOUBLE PRECISION XO,YO,X,Y,XPR,YPR,UX,UY,V,YT,XT,U,XT2,YT2,
         *SUMSQ,DX,DY,TEMP,ALPHA
004       DOUBLE PRECISION XCOF,COF,ROOTR,ROOTI
005       IFIT=0
006       N=M
007       IER=0
008       IF (XCOF(N+1)) 10,25,10
009    10 IF (N) 15,15,32
010    15 IER=1
011    20 RETURN
012       GO TO 20
014    30 IER=2
015       GO TO 20
016    32 IF (N-36) 35,35,30
017    35 NX=N
018       NXX=N+1
019       N2=1
```

```
020       KJ1=N+1
021       DO 40 I=1,KJ1
022       MT=KJ1-L+1
023    40 COF(MT)=XCOF(L)
024    45 XO=.00500101
025       YO=0.01000101
026       IN=0
027    50 X=XO
028       XO=-10.0*YO
029       YO=-10.0*X
030       X=XO
031       Y=YO
032       IN=IN+1
033       GO TO 59
034    55 IFIT=1
035       XPR=X
036       YPR=Y
037    59 ICT=0
038    60 UX=0.0
039       UY=0.0
040       V=0.0
041       YT=0.0
042       XT=1.0
043       U=COF(N+1)
044       IF (U) 65,130,65
045    65 DO 70 I=1,N
046       L=N-I+1
047       TEMP=COF(L)
048       XT2=X*XT-Y*YT
049       YT2=X*YT+Y*XT
050       U=U+TEMP*XT2
051       V=V+TEMP*YT2
052       FI=I
053       UX=UX+FI*XT*TEMP
054       UY=UY-FI*YT*TEMP
055       XT=XT2
056    70 YT=YT2
057       SUMSQ=UX*UX+UY*UY
058       IF (SUMSQ) 75,110,75
059    75 DX=(V*UY-U*UX)/SUMSQ
060       X=X+DX
061       DY=-(U*UY+V*UX)/SUMSQ
062       Y=Y+DY
063    78 IF (DABS(DY)+DABS(DX)-1.0D-05) 100,80,80
064    80 ICT=ICT+1
065       IF (ICT-500) 60,85,85
066    85 IF (IFIT) 100,90,100
067    90 IF (IN-5) 50,95,95
068    95 IFR=3
069       GO TO 20
070   100 DO 105 L=1,NXX
```

```
071       MT=KJ1-L+1
072       TEMP=XCOF(MT)
073       XCOF(MT)=COF(L)
074   105 COF(L)=TEMP
075       ITEMP=N
076       N=NX
077       NX=ITEMP
078       IF (IFIT) 120,55,120
079   110 IF (IFIT) 115,50,115
080   115 X=XPR
081       Y=YPR
082   120 IFIT=0
083   122 IF (DABS(Y/X)-1.0D-04) 135,125,125
084   125 ALPHA=X+X
085       SUMSQ=X*X+Y*Y
086       N=N-2
087       GO TO 140
088   130 X=0.0
089       NX=NX-1
090       NXX=NXX-1
091   135 Y=0.0
092       SUMSQ=0.0
093       ALPHA=X
094       N=N-1
095   140 COF(2)=COF(2)+ALPHA*COF(1)
096   145 DO 150 L=2,N
097   150 COF(L+1)=COF(L+1)+ALPHA*COF(L)-SUMSQ*COF(L-1)
098   155 ROOTI(N2)=Y
099       ROOTR(N2)=X
100       N2=N2+1
101       IF (SUMSQ) 160,165,160
102   160 Y=-Y
103       SUMSQ=0.0
104       GO TO 155
105   165 IF (N) 20,20,45
106       END
```

8.3.6 Subroutine for Numerical Integration

```
001       SUBROUTINE BOBYJO (F,A,B,DEL,IMAX,SI1,S,N,IER)
002       DOUBLE PRECISION A,B,DEL,SI1,S,BA,X,SUMK,FRSTX,XK,FINC,F
003       SI1=0.DO
004       D=0.0DO
005       N=0
006       BA=B-A
007       IF (BA) 20,19,20
008    19 IER=1
009       RETURN
010    20 IF(DEL) 22,22,23
011    22 IER=2
```

```
012        RETURN
013     23 IF(IMAX-1) 24,24,25
014     24 IER=3
015        RETURN
016     25 X=BA/2.0DO+A
017        NHALF=1
018        SUMK=F(X)*BA*2.0DO/3.0DO
019        S=SUMK+(F(A)+F(B))*BA/6.0DO
020        DO 28 I=2,IMAX
021        SI1=S
022        S=(S-SUMK/2.0DO)/2.0DO
023        NHALF=NHALF*2
024        ANHLF=NHALF
025        FRSTX=A+(BA/ANHLF)/2.0DO
026        SUMK=F(FRSTX)
027        XK=FRSTX
028        KLAST=NHALF-1
029        FINC=BA/ANHLF
030        DO 26 K=1,KLAST
031        XK=XK+FINC
032     26 SUMK=SUMK+F(XK)
033        SUMK=SUMK*2=0DO*BA/(3.0DO*ANHLF)
034        S=S+SUMK
035     27 IF(DABS(S-SI1)-DABS(DEL*S)) 29,28,28
036     28 CONTINUE
037        IER=4
038        GO TO 30
039     29 IER=0
040     30 N=2*NHALF
041        RETURN
042        END
```

8.4 Computer Program for Numerical Count of Eigenvalues

8.4.1 Description of Program

This section contains a computer program which will determine the cumulative number of eigenvalues by counting them numerically from the frequency equation. The program used to accomplish the counting procedure is fairly simple and is described in block form in Figure 8.9. A copy of the program used on an IBM 360 model 75 computer written in G level Fortran may be found in the following subsection.

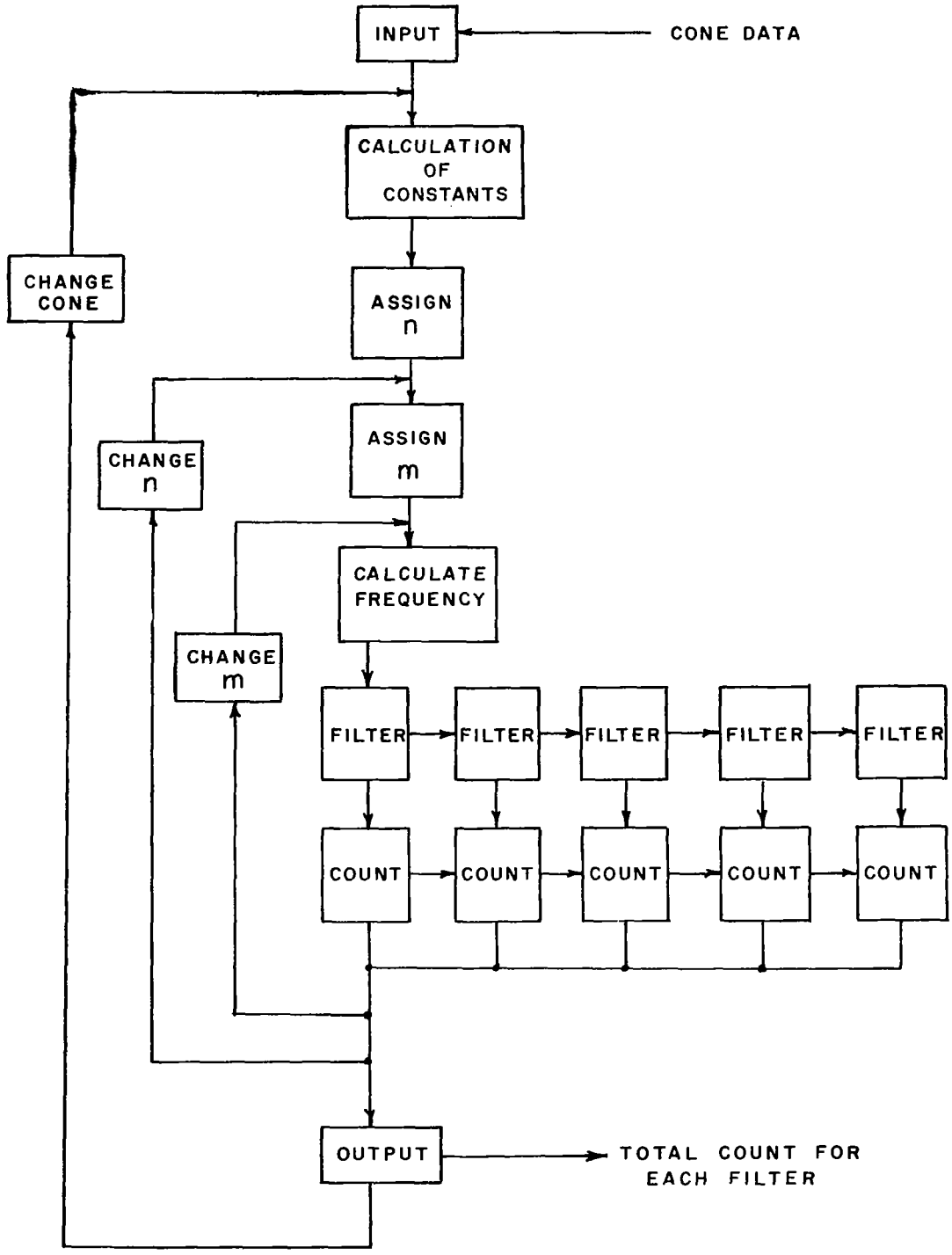

FIGURE 8.9 DIAGRAM OF NUMERICAL EIGENVALUE COUNT PROGRAM

The program begins by inputting data on the cones to be analyzed. The data cards used are the same as for the program described in section 8.3. Several necessary constants for the cone geometry are calculated and then initial values for the number of circumferential waves (m=2) and the number of one half longitudinal waves (n=1) are set. The corresponding frequency for these wave numbers is calculated and put in dimensionless form. This frequency is then fed into a series of IF statements which act as frequency filters. Once the calculated frequency becomes less than one of the filter frequencies it is counted as being contained under that frequency and all succeeding frequencies. This process is repeated until the designated range of m and n values have been covered whereupon the number of modes contained under each filter value is printed out. The count under each filter is considered to be complete when a further increase in m and n produces no change in the results. The program then moves on to the next cone, and the entire process is repeated.

The program has one major drawback, and that is it is very time consuming. Using the computer cited above run times of approximately two minutes per cone were needed for the count to be complete for values of dimensionless frequencies up to forty. This corresponds to around a hundred thousand frequency calculations per cone. Careful selection of final and initial m and n values could greatly decrease the time needed, however, this would be difficult to do without first making some frequency calculations.

8.4.2 Main Program

```
001       DOUBLE PRECISION CONE(12,7),DN(20),DM(20),DF(1,20)
002       DIMENSION M(21),N(21)
003       INTEGER O,P
004       DOUBLE PRECISION ANGL,DEG,RL,XI,H,E,RATO,DEN,G,C1,C2,C3,AL,
         *AL1,AL2,AL3,AL4,AL5,FN,A2,A3,FM1,FM2,FM3,A1,SFR1,DFR1,SFR2,
         *DFR2,C4,FNOR
005    99 FORMAT(7F10.0)
006   100 FORMAT('1','NUMBER TO EIGENVALUES FOR A CONICAL SHELL UP TO
         *THE GI VEN DIMENSIONLESS FREQUENCY'/'0','ANGLE=',F6.3,4X,
         *'LENGTH RATIO=',F6.4,4X,'THICKNESS =',F6.4,4X,'LENGTH =',
         *F6.3/'0','DIMENSIONLESS FREQUENCY MULTIPLIER=',F10.4)
007   500 FORMAT('0','LOWER DIMENSIONLESS RING FREQUENCY=',F10.4/'0',
         *'UPPER DIMENSIONLESS RING FREQUENCY=',F10.4/)
008   600 FORMAT('0','LOWER DIMENSIONLESS RING FREQUENCY=',F10.4/'0',
         *'UPPER DIMENSIONLESS RING FREQUENCY IS INFINITE'/)
009   200 FORMAT(20F4.0)
010   300 FORMAT('0','D-FREQUENCY',9X,'D-MODES ONE',9X,'D-MODES TWO
         *MODES ONE   MODES TWO'//)
011   900 FORMAT(' ',F11.2,2D20.5,2I12)
    C
    C        INPUT OF CONE DATA
    C
012       READ(1,99)((CONE(I,J),J=1,7),I=1,12)
013       READ(1,200)(DF(1,JL),JL=1,20)
014       KONT=210
    C
    C        LOOP ON DIFFERENT CONES
    C
015       DO 1 K=1,12
    C
    C        INITIALIZE TOTAL COUNTS AT ZERO
    C
016       DO 700 L=1,21
017       M(L)=0
018       N(L)=0
019   700 CONTINUE
020       DEG=CONE(K,1)
021       ANGL=DEG/57.295779531
022       RL=CONE(K,2)
023       XI=CONE(K,3)
024       H=CONE(K,4)
025       E=CONE(K,5)*1.D2
026       RATO=CONE(K,6)
027       DEN=CONE(K,7)
028       G=3.864D2
029       C1=(G*E)/(DEN*(RL**2))
030       C2=(H**2)/(1.2D1*(RL**2)*(1.DO-(RATO**2)))
031       C3=(DCOTAN(ANGL)**2)
032       C4=DSQRT(E*G/DEN)/(2.DO*3.1415926536*RL)
```

```
033       AL=XI/RL
    C
    C         IDENTIFICATION OF CONE
    C
034       WRITE(3,100) DEG,AL,H,RL,C4
035       AL1=1.DO-AL
036       AL2=1.DO-AL**2
037       AL3=1.DO-AL**3
038       AL4=1.DO-AL**4
039       AL5=1.DO-AL**5
    C
    C         LOOP ON LONGITUDINAL NUMBER OF WAVES
    C
040       DO 2 P=1,KONT
041       FN=P*3.1415926356
042       A2=((AL4*(FN**2))/(8.DO*(AL1**2)))-((3.DO*AL2)/(8.DO))
043       A3=((AL5)/(1.D1))-((AL3*(AL1**2))/(2.DO*(FN**2)))+((3.DO*(AL1
         ***5))/(4.DO*(FN**4)))
    C
    C         LOOP ON CIRCUMFERENTIAL NUMBER OF WAVES
    C
044       DO 3 0=2,KONT
045       FM1=(1=DO)+((2.DO*(0**2))/(DSIN(ANGL)**2))
046       FM2=((0**4)/(DSIN(ANGL)**4))-((4.DO*(0**2))/(DSIN(ANGL)**2))
047       FM3=(AL1*(0**4))/(2.DO*(DSIN(ANGL)**4))
048       A1=((FN**4)*AL5)/(1.D1*(AL1**4))+(FM1)*((AL3*(FN**2))/(6.0D1*
         *(AL1**2))-(AL1)/(2.DO))=(FM2*AL1)/(2.DO)
    C
    C         CALCULATION OF DIMENSIONLESS FREQUENCY FROM EQUATION ONE
    C
049       SFR1=((C2*(A1**2))+(C3*(A2**2)))/(A1*A3)
050       DFR1=DSQRT(SFR1)
    C
    C         CALCULATION OF DIMENSIONLESS FREQUENCY FROM EQUATION TWO
    C
051       SFR2=((C2*(FM3**2))+(C3*(A2**2)))/(FM3*A3)
052       DFR2=DSQRT(SFR2)
    C
    C         EQUATION ONE FILTERS
    C
053       IF (DFR1-5.OD-1) 5,5,6
054     6 IF (DFR1-1.0DO) 7,7,8
055     8 IF (DFR1-1.5DO) 9,9,10
056    10 IF (DFR1-2.0DO) 11,11,12
057    12 IF (DFR1-2.5OD) 13,13,14
058    14 IF (DFR1-3.0DO) 15,15,16
059    16 IF (DFR1-3.5DO) 17,17,18
060    18 IF (DFR1-4.0DO) 19,19,20
061    20 IF (DFR1-4.5DO) 21,21,22
062    22 IF (DFR1-5.0DO) 23,23,24
063    24 IF (DFR1-6.0DO) 25,25,26
```

```
064    26 IF (DFR1-7.0DO) 27,27,28
065    28 IF (DFR1-8.0DO) 29,29,30
066    30 IF (DFR1-9.0DO) 31,31,32
067    32 IF (DFR1-1.0D1) 33,33,34
068    34 IF (DFR1-1.5D1) 35,35,36
069    36 IF (DFR1-2.0DL) 37,37,38
070    38 IF (DFR1-2.5D1) 39,39,40
071    40 IF (DFR1-3.0D1) 41,41,42
072    42 IF (DFR1-4.0D1) 83,83,84
     C
     C          EQUATION ONE COUNTERS
     C
073     5 N(1)=N(1)+1
074     7 N(2)=N(2)+1
075     9 N(3)=N(3)+1
076    11 N(4)=N(4)+1
077    13 N(5)=N(5)+1
078    15 N(6)=N(6)+1
079    17 N(7)=N(7)+1
080    19 N(8)=N(8)+1
081    21 N(9)=N(9)+1
082    23 N(10)=N(10)+1
083    25 N(11)=N(11)+1
084    27 N(12)=N(12)+1
085    29 N(13)=N(13)+1
086    31 N(14)=N(14)+1
087    33 N(15)=N(15)+1
088    35 N(16)=N(16)+1
089    37 N(17)=N(17)+1
090    39 N(18)=N(18)+1
091    41 N(19)=N(19)+1
092    83 N(20)=N(20)+1
093    84 N(21)=N(21)+1
     C
     C          EQUATION TWO FILTERS
     C
094       IF (DFR2-5.D-1) 43,43,44
095    44 IF (DFR2-1.0DO) 45,45,46
096    46 IF (DFR2-1.5DO) 47,47,48
097    48 IF (DFR2-2.0DO) 49,49,50
098    50 IF (DFR2-2.5DO) 51,51,52
099    52 IF (DFR2-3.0DO) 53,53,54
100    54 IF (DFR2-3.5DO) 55,55,56
101    56 IF (DFR2-4.0DO) 57,57,58
102    58 IF (DFR2-4.5DO) 59,59,60
103    60 IF (DFR2-5.0DO) 61,61,62
104    62 IF (DFR2-6.0DO) 63,63,64
105    64 IF (DFR2-7.0DO) 65,65,66
106    66 IF (DFR2-8.0DO) 67,67,68
107    68 IF (DFR2-9.0DO) 69,69,70
108    70 IF (DFR2-1.0D1) 71,71,72
```

```
109    72 IF (DFR2-1.5D1) 73,73,74
110    74 IF (DFR2-2.0D1) 75,75,76
111    76 IF (DFR2-2.5D1) 77,77,78
112    78 IF (DFR2-3.0D1) 79,79,80
113    80 IF (DFR2-4.0D1) 81,81,82
   C
   C         EQUATION TWO COUNTERS
   C
114    43 M(1)=M(1)+1
115    45 M(2)=M(2)+1
116    47 M(3)=M(3)+1
117    49 M(4)=M(4)+1
118    51 M(5)=M(5)+1
119    53 M(6)=M(6)+1
120    55 M(7)=M(7)+1
121    57 M(8)=M(8)+1
122    59 M(9)=M(9)+1
123    61 M(10)=M(10)+1
124    63 M(11)=M(11)+1
125    65 M(12)=M(12)+1
126    67 M(13)=M(13)+1
127    69 M(14)=M(14)+1
128    71 M(15)=M(15)+1
129    73 M(16)=M(16)+1
130    75 M(17)=M(17)+1
131    77 M(18)=M(18)+1
132    79 M(19)=M(19)+1
133    81 M(20)=M(20)+1
134    82 M(21)=M(21)+1
135     3 CONTINUE
136     2 CONTINUE
   C
   C         CALCULATION OF RING FREQUENCIES
   C
137       DFRL=1.DO/DSIN(ANGL)
138       IF (AL) 95,96,95
139    95 DFRU=1.DO/(DSIN(ANGL)*AL)
140       WRITE(3,500) DFRL,DFRU
141       GO TO 1000
142    96 WRITE(3,600) DFRL
143  1000 FNOR=AL1*DSIN(ANGL)/(3.14151926356)
144       WRITE(3,300)
145       DO 800 KL=1,20
   C
   C         NORMALIZATION OF RESULTS OF COUNT
   C
146       DN(KL)=N(KL)/FNOR
147       DM(KL)=M(KL)/FNOR
   C
   C         PRINT OUT OF RESULTS IN NORMALIZED AND ACTUAL FORM
   C
148       WRITE(3,900) DF(1,KL),DN(KL),DM(KL),N(KL),M(KL)
```

```
149   800 CONTINUE
150     1 CONTINUE
151       STOP
152       END
```

8.5 List of Symbols

a_n	$n\pi/(1-\alpha_1)$
C_L	velocity of longitudinal wave in shell material $\approx\sqrt{\frac{Eg_c}{\gamma}}$
D	stiffness of shell $= Eh^3/12(1-\nu^2)$
E	modulus of elasticity of shell material
g_c	gravitational constant (32.2 lbm ft/lbf sec^2)
h	thickness of shell
k_1	longitudinal wave number $= a_n$
k_2	circumferential wave number $= m/\sin\psi$
L	length of cone, apex to base slant length
L_t	length of cone truncation, apex to top slant length
$M_x, M_\theta, M_{x\theta}, M_{\theta x}$	bending moment resultants on shell element
m	number of circumferential waves m = 2,3,4,...
$N(\lambda)$	cumulative number of eigenvalues up to frequency λ
N_x, N_θ	normal stress resultants on shell element
$N_{x\theta}, N_{\theta x}$	shear stress resultants on shell element
n	number of one-half longitudinal waves n = 1,2,3,...
$n(\lambda)$	modal or eigenvalue density with respect to λ
Q_x, Q_θ	transverse shear stress resultants on shell element
R	radius of a circular plate
r	radius of cone perpendicular to cone axis
u	displacement in x-direction
v	displacement in θ-direction

w	displacement in z-direction, normal to shell surface
X	body force in x-direction
x	coordinate along shell surface
Y	body force perpendicular to the x-z plane
Z	body force in the z-direction
z	coordinate normal to shell surface
α	normalized coordinate in x-direction = x/L
α_1	truncation ratio = L_t/L
γ	density of shell material
$\gamma_{x\theta}$	shear strain due to extension of middle surface
$\bar{\gamma}_{x\theta}$	total shear strain
Δk_1	change in longitudinal wave number $\cong \pi/(1-\alpha_1)$
Δk_2	change in circumferential wave number $\cong 1/\sin\psi$
$\epsilon_x, \epsilon_\theta$	normal strains due to extension of middle surface
$\bar{\epsilon}_x, \bar{\epsilon}_\theta$	total normal strains
θ	coordinate around surface of shell perpendicular to axis
λ	dimensionless frequency, $\lambda^2 = \omega^2 L^2 \gamma / g_c E$
ν	Poisson's ratio for shell material
σ_x, σ_θ	normal stresses
τ	shear strain due to bending
$\tau_{x\theta}, \tau_{\theta x}$	shear stresses
χ_x, χ_θ	normal strain due to bending
ϕ	stress function
ψ	one-half cone angle at apex
ω	angular frequency, $\omega = 2\pi f$
~~θ~~	volume deformation

NASA-Langley, 1970 —— 32 CR-1497